VARIABILITY OF SEA ICE DRIFT THROUGH NARES STRAIT, NUNAVUT, CANADA

ASHLEY O'BRIEN

A THESIS SUBMITTED TO THE FACULTY OF GRADUATE STUDIES IN PARTIAL FULFILLMENT OF THE REQUIREMENTS FOR THE DEGREE OF MASTER OF SCIENCE

GRADUATE PROGRAM IN GEOGRAPHY
YORK UNIVERSITY
TORONTO, ONTARIO

January 2019

Abstract

One of the greatest indicators of climate change is the state of the Arctic sea ice cover, whose extent is declining at an unprecedented rate due to both melt of sea ice and advection out of the Arctic Ocean. Nares Strait is an important conduit for the export of sea ice from the Arctic Ocean to sub-Arctic seas. Buoy trajectories for 2009, 2010, 2011 and 2014 were analyzed to evaluate the drift of sea ice through Nares Strait. Wind and ice concentration data were correlated with drift speeds to evaluate their influence on sea ice drift in this region which showed generally weak to moderate correlation coefficients. Drift speeds were highly variable spatially, seasonally and interannually. Smith Sound had the most spatial variability and the fastest drift speed (45 km/d). Drift through late summer showed high variability. It is believed that internal ice stress and ocean stress must play an integral role in ice dynamics in the strait but could not be quantified here. Further observations are required to more comprehensively understand sea ice dynamics in Nares Strait.

Dedication

I dedicate this thesis work to my friends and family who have unconditionally supported me throughout this entire process. I love you.

Acknowledgments

I would like to thank my supervisor Dr. Christian Haas for his guidance, support and immense knowledge. It has been a pleasure to work and learn from you over the past years. I also want to thank my committee Dr. Kathy Young and Dr. Rick Bello. A special thank you goes to Dr. John Alec Casey and Dr. Anne Irvin for their invaluable guidance throughout this process. To the Arctic Antarctic Sea Ice Lab, which includes Marzena Marosz-Wantuch and Mojtaba Daneshvar for support.

A sincere thank you to my friends and family who have unconditionally loved and supported me through this rollercoaster ride. I would not have stuck through it all without your words of tough love and support. The biggest thank you to my Mom and Dad for allowing me to peruse graduate studies and for sticking by my side through it all as well as all of your endless support throughout whatever endeavor I embark on. Finally, to Ernon for your endless love, support and patience with me.

Table of Contents

List of Tables

List of Figures

List of Abbreviations

AMAP	Arctic Monitoring and Assessment Program
AO	Arctic Ocean
BC	Baffin Current
CAA	Canadian Arctic Archipelago
CIS	Canadian Ice Service
CALIB	Compact Air-Launched Ice Beacon
EC	Environment Canada
ECCC	Environment and Climate Change Canada
IABP	International Arctic Buoy Program
IBCAO	International Bathymetric Chart of the Arctic Ocean
IPCC	Intergovernmental Panel on Climate Change
iSVP	Surface Velocity Profile
FYI	First-Year Ice
GIS	Geographical Information System
LOTI	Land-Ocean Temperature Index
MANICE	Manual of Standard Procedures for Observing and Reporting Ice Conditions
MYI	Multi-Year Ice
NASA	National Aeronautics and Space Administration
NOAA	National Oceans and Atmospheric Administration
NSIDC	National Snow and Ice Data Centre
PDF	Probability Density Function
SAMS	Scottish Association for Marine Science
WGC	West Greenland Current
WMO	World Meteorological Organization

Chapter 1
Introduction

1.0 Study Context

The Arctic environment is rapidly changing; sea ice is one of the most observable characteristics of this change. The Intergovernmental Panel on Climate Change's fifth assessment report states that "Arctic sea ice has continued to decrease in extent (high confidence) … It is very likely that Arctic sea ice cover will continue to shrink and thin… during the 21st century as global mean surface temperatures rise" (IPCC, 2013). Arctic sea ice is one of the most prominent indicators of global climate change for several reasons. 1) Climate change is amplified in the Arctic. 2) While there are many observable factors that are shifting due to climate change, the Arctic sea ice regime is one of the things that could eventually cross a threshold of "existing" to "non-existing" (Notz, 2017). The Arctic sea ice system has experienced great changes within recent decades. Sea ice extent in the Arctic continues to decrease and is expected to continue this trajectory. The result of this decline is thinner, weaker and younger ice cover (Stroeve, et al., 2012).

Arctic sea ice is an integral part of the global climate system; changes to the Arctic sea ice system have several consequences. Changes to sea ice cover can: alter surface albedo, increasing the amount of energy being absorbed by the Earth; negatively influence the Earth's energy balance; influence heat and gas exchange between the ocean and the atmosphere; and, lead to negative impacts on the polar ecosystem (Serreze and Barry, 2005; AMAP, 2012). The modification of the sea ice cover has impacts on several stakeholders. Since significant declining trends in sea ice extent and thickness have started to occur, indigenous and local peoples' livelihoods have been challenged, while interest in access to resources and transportation in the Arctic has increased.

Furthermore, marine hazards associated with sea ice have increased, biological systems are experiencing negative effects, and Arctic amplification has intensified. Arctic amplification is significant because the process has accelerated the declining trends in sea ice that are associated with increased warming and sea ice depletion in the Arctic further (AMAP, 2012; Serreze and Barry, 2011).

Sea ice dynamics are equally a key component as the thermodynamics of the ice. Advection of sea ice out of the Arctic through conduits such as Fram Strait and the Canadian Arctic Archipelago (CAA) is a major contributor to the overall loss of sea ice extent in the Arctic. This export has also been observed as a principal sink for multi-year ice (MYI) and overall sea ice drift has been an integeral component of the loss of older ice (Meier, 2017). Kimura et al (2013) found that winter sea ice drift has a strong influence on the subsequent summer ice cover in the Arctic. In recent years, mean sea ice drift speeds have increased (Rampal et al., 2009; Spreen et al., 2011; Kwok et al., 2013). Between 1992 and 2009, Spreen et al. (2011) found an overall trend of increasing sea ice drift speeds of 10.6% per decade and in some regions of the Arctic showing increased rates upwards of 16%. Large-scale positive trends in wind speed are observed over a large fraction of the Central Arctic where drift speed trends are the highest (Spreen et al., 2011). Despite the belief that wind stress has a major influence on ice drift speed (Colony and Thorndike, 1984; Sameleson, et al., 2006) the recent trends of increasing sea ice drift speeds are not proportional to wind speeds for the same time period in all regions of the Arctic. The results from Spreen et al. (2011) show correlations between basin-wide trends of wind and sea ice drift speeds between $r = 0.4$ to 0.52 and the results suggest that a fraction of observed increasing trends in sea ice drift speeds for the central Arctic Ocean can be attributed to wind, but not over the entire basin.

The changes in drift speeds are likely related to sea ice thinning resulting in changing internal ice forces (Haas, 2017; Spreen et al., 2011).

As mentioned, the export of sea ice occurs through two major conduits from the Arctic Basin – Fram Strait and the CAA (e.g. Kwok et al., 2004; Howell et al., 2013). Sea ice advection through Fram Strait is well documented and a lot is known about the behaviour of sea ice in that region. Conversely, relatively little is known about the advection of sea ice through the CAA, in particular through Nares Strait, a major channel of the CAA. Researchers – such as Kwok, Munchow and Melling – have observed sea ice dynamics in Nares Strait using satelitte observations and model simulations (e.g. Kwok, 2005; Kwok et al., 2010; Munchow et al., 2006; Ryan and Munchow, 2016). This thesis will utilize observational (buoy) data to evaluate the forces driving sea ice motion within Nares Strait.

1.1 Research Questions and Objectives

The goal of this work is to 1) study sea ice drift variability in Nares Strait using data from sea ice drifting buoys, and 2) to investigate which of the physical forcings on sea ice drift are most dominant in Nares Strait. The questions this thesis will attempt to answer include:

1. What is the drift speed of sea ice through Nares Strait, for the years 2009, 2010, 2011 and 2014? How do the dynamics of sea ice vary from year to year?
2. What factors drive variability of sea ice dynamics within Nares Strait?

1.2 Structure of Thesis

Chapter 2 provides a brief background on the dynamics of sea ice and deconstructs the momentum balance of sea ice drift. Information on tools and methods used to acquire in situ observations of drift from sea ice drifting buoys is provided. This chapter also examines the current state of sea ice dynamics in the Arctic Ocean, and an analysis of available literature related to sea ice dynamics in Nares Strait.

Chapter 3 offers a description of the study site, Nares Strait. A discussion of the various datasets used in this project's analysis and the methods used to employ those datasets is conducted.

Chapter 4 presents the results from the various analyses. Various products are presented to visualize the dynamics and processes occurring during the study period. The results are followed by a discussion in Chapter 5 in relation to the study's goals and objectives. Chapter 5 addresses the study objectives and research questions in this thesis.

Finally, Chapter 6 concludes the study and summarizes the findings of the study followed by limitations of the work, and recommendations for further work on this topic.

Chapter 2
Background and Literature Review

2.0 Introduction

In this chapter, a literature review pertaining to the Arctic sea ice regime as well as the dynamics of sea ice, including the momentum balance of sea ice drift is presented. Background literature specifically on the drift of sea ice through the Nares Strait and its sea ice regime is also discussed. Past studies and literature are reviewed and summarized as a precursor to the questions, goals and objectives of this study.

In Sections 2.1 and 2.2, information about the sea ice regime of the Arctic and the importance of the existing sea ice, including the phenomenon of Arctic amplification are discussed.

Section 2.3 follows up on the dynamics of sea ice, deconstructs the momentum balance of sea ice drift and further reflects on wind-driven and ocean-driven sea ice drift as well as other components of the momentum balance of sea ice.

Sections 2.4, 2.5 and 2.6 are comprised of an overview of sea ice export from the Arctic Ocean, as well as a short analysis of sea ice drift and dynamics specifically through Nares Strait.

Finally, Section 2.7 provides a summary of the information discoursed.

2.1 The Changing Arctic Sea Ice Regime

The extent of sea ice in the Arctic Ocean typically ranges from 15.5 million square kilometers in the winter to about 6 million square kilometers in the summer; however, these numbers are changing drastically as sea ice has declined significantly in the last decade. An important objective of sea ice research is to enhance our understanding of sea ice thermodynamics and dynamics in order to provide information to improve predictive climate models. To create

accurate forecasts and climate predictions, it is important to create plans of mitigation and adaptation to the changing global climate. Although climate model simulations seem to be getting better with respect to observations versus model results, it is suggested that this maybe for the wrong reasons (Rosenblum and Eisenman, 2017). Observations are exceeding model predictions with the current decline and state of the Arctic sea ice regime (Stroeve et al., 2007). Holland et al (2010) found that the potential predictability of sea ice and how easily and accurately sea ice changes and conditions can be predicted in climate models, is much lower in the spring transition season than in the winter months. Potential predictability of the sea ice system is defined by examining how quickly model simulations deviate compared to the natural variability of the system via observations (Koenigk and Mikolajewicz, 2008). Holland et al. (2010) used was the Community Climate System Model, version 3 (CCSM3) to test three different sea ice forecast scenarios. Ensemble 1 was based on data from the 1970's where sea ice is thick (roughly 3.8 m average). Ensemble 2 was run on data based from 2016 and finally, ensemble 3 is initialized based on 2017, where conditions are more like 2007, where there was a significant loss of sea ice. Ensemble 3 shows the lowest potential predictability overall suggesting that a thinner ice regime provides little predictive capability (Holland et al., 2010).

Predictions of sea ice cover and its future are not able to be made with the current state of the regime and the high variability that exists. Climate modelling, which incorporates future predictions, have become increasingly difficult (Meier, 2017).Figure 2.1 is from the latest IPCC assessment showing that in the most recent time period, 2009-2012, there is much less of an ice extent for the Arctic and this trend is likely to continue into future years. Ice extent is derived from satellite observations (IPCC, 2013).

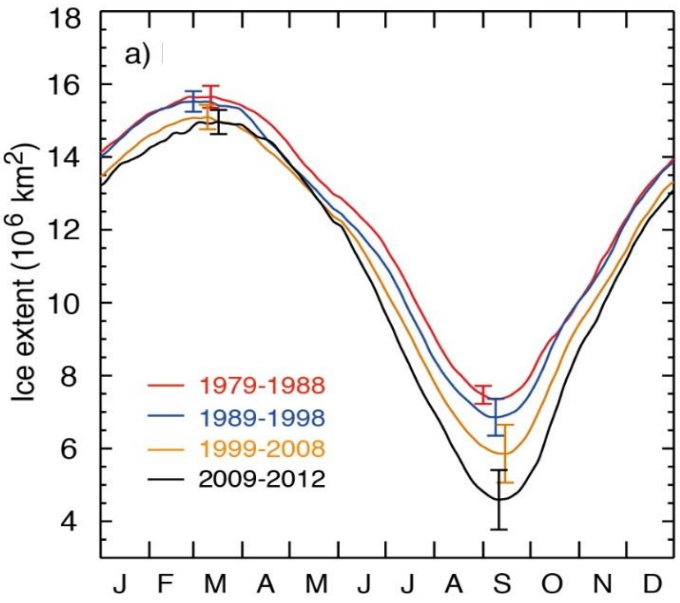

Figure 2.1 Decadal averages of daily Arctic sea ice extent (IPCC, 2013).

The changes in the global climate have resulted in Arctic amplification. Arctic amplification is the phenomenon by which surface air temperature increases are much greater in the Arctic than at lower latitudes as a response to increasing global concentrations of greenhouse gas. Arctic Amplification occurs due to decreased albedo from climate warming and ice melt, which incurs a positive feedback loop. Figure 2.2 shows the increased warming in the Arctic in comparison to the rest of the globe. This data is from January 2017, where temperatures were record highs (NASA, 2017). The amplified warming in the Arctic has resulted in longer summer melt seasons which results in less sea ice extent at the end of summer (Serreze et al., 2009). As a result, sea ice has become thinner and weaker and the areal coverage of sea ice has decreased over time (Strove et al., 2012).

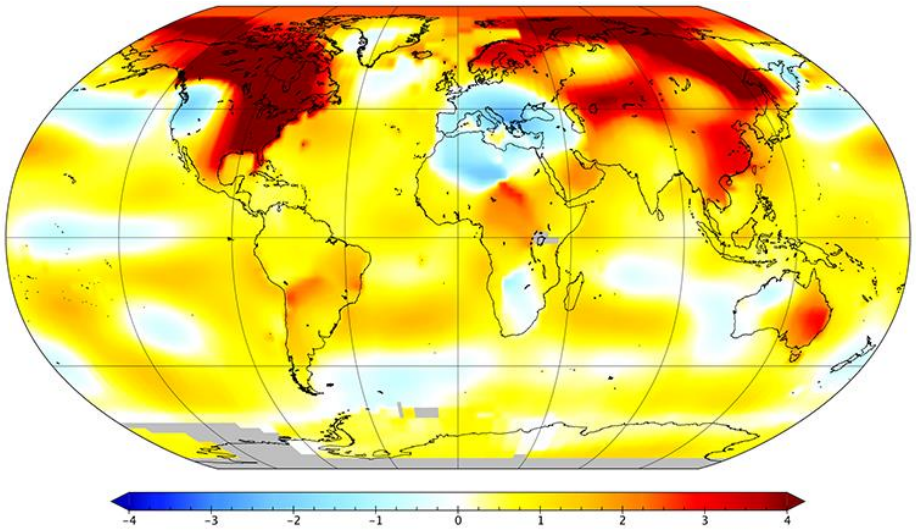

Figure 2.2 Map of global land-ocean temperature index (LOTI) anomalies (°C) from January 2017 with a base time period of 1951-1980. This map demonstrates Arctic amplification where positive temperature anomalies are greatest in the Arctic. (Adapted from NASA, 2017).

Rampal et al (2009) found that there was a positive trend for both the mean speed of ice drift and the deformation rate of sea ice 1979 to 2007; specifically, drift speed increased by 8.5% decade^{-1} in the summer months and by 17% decade^{-1} in the winter months (Rampal et al., 2009). Other studies, including Spreen et al (2011) and Rigor et al (2002), have also shown increasing trends of ice drift speed for the Arctic basin. It is noted, however, that this increasing trend is not directly correlated to, and cannot be entirely attributed to, increases in mean wind speed, but rather is also influenced by the observed declines in MYI extent and ice thickness. The changing nature of the sea ice itself is a consequence of increasing global mean surface temperatures, Arctic amplification and other climatological changes, and will have a direct effect on sea ice drift speeds and behaviors for the foreseeable future (Maslanik et al., 2007; Serreze and Barry, 2011; Haller et al., 2014; Haas, 2017). Sea ice export studies have shown a number of correlations between ice export out of the Arctic – through Fram Strait and the CAA – and sea ice thickness and age. Langehaug et al (2013) found significant correlations suggesting that an increase in ice area export

leads to a decrease in sea ice thickness. Specifically, the larger the area of ice exported from the Arctic Ocean through conduits, such as Fram and Nares Straits, the greater the amount of sea ice thinning resulting in the loss of September sea ice area (Langehaug et al., 2013). Howell et al (2013) found that the recent increase in the area of open water (ice free) in the CAA has caused an inflow of MYI from the central Arctic Ocean into the CAA. The amount of MYI within the CAA that is exported from the Arctic Ocean is significant through M'Clure Strait and the Queen Elizabeth Islands (Howell et al., 2013).

The changing climate and increasing surface temperatures does contribute to the rate of ice melt in the Arctic, as Arctic amplification (Figure 2.2). Amplified temperature anomalies in the Arctic strongly influence the extent of Arctic sea ice (IPCC, 2013; Stroeve et al, 2012; Serreze et al., 2009). However, sea ice drift speeds and the export of older, stronger, more reflective MYI out of the central Arctic Ocean, contributes to the sea ice-albedo positive feedback mechanism that exists, which is as the aforementioned driving factor of Arctic amplification. MYI typically has a higher albedo than FYI and sea ice acts as a large reflector of incoming solar radiation – the white surface of the ice can reflect up to 80% of the radiation (Kennedy, 2013; Environment Canada, 2013; van Anglen et al., 2011). As MYI exports out of the Arctic Ocean and the ice mass is changing to predominantly FYI, the overall albedo of the polar region is decreasing, suggesting more radiation is being absorbed by the ice, exposed land and open water areas of the ocean surface, which leads to increased surface warming and more sea ice melt (Maslanik et al., 2011).

2.2 Dynamics of Sea Ice

Sea ice is not a stationary material; it is in constant motion. The morphology of an ice cover depends on this fact (Lepparanta, 2011; Wadhams, 2000). Sea ice moves largely in response to

local winds and ocean currents (Thorndike and Colony, 1982). Figure 2.3 illustrates the effect of water, wind and internal stress on sea ice drift. In addition to wind and ocean forcings, there are several other forces that impact sea ice drift. A representation of the dynamics of sea ice is the momentum balance, an equation that describes the nature and magnitude of the physical forces acting on every element of the ice cover.

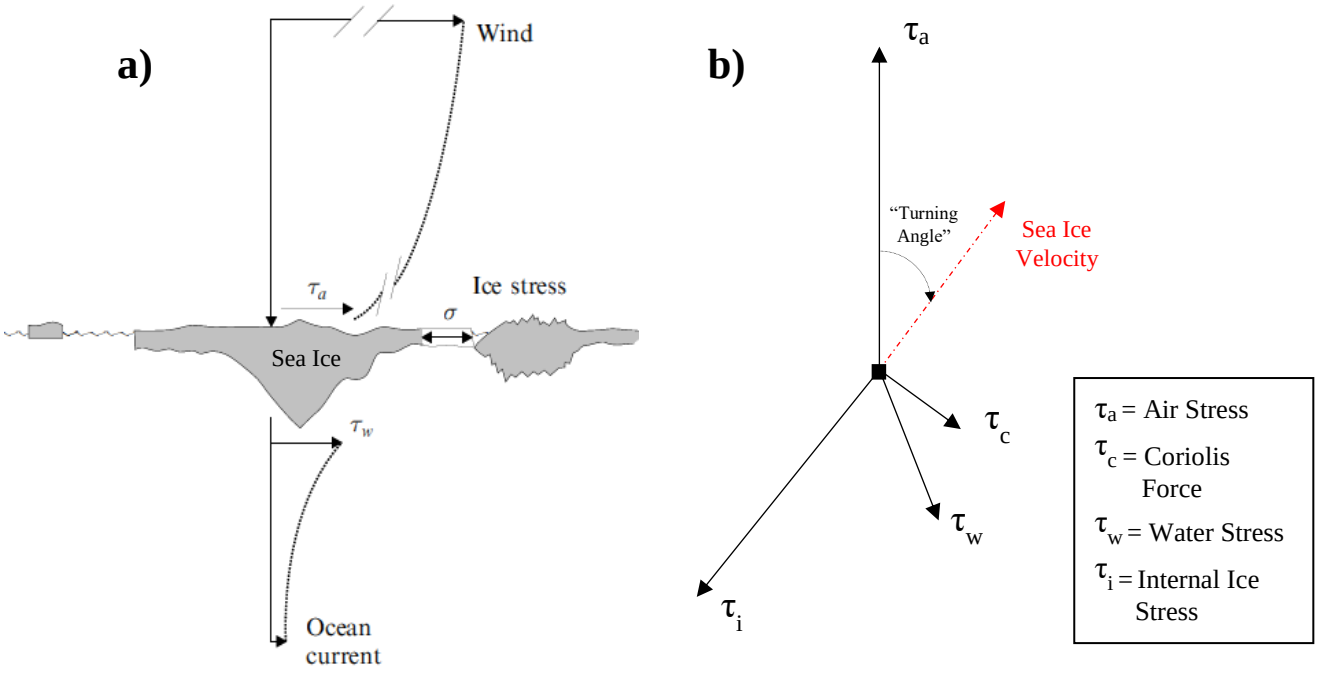

Figure 2.3: (a) Effect of water, wind and internal ice stress on sea ice (Lepparanta, 2011). (b) a schematic of the sea ice momentum balance, depicting the various forces that drive sea ice dynamics. Sea surface tilt is omitted as it is considered insignificant (adapted from Haas, 2017).

The magnitude of forces acting upon the sea ice depends on whether it is in free drift or in drift as compact ice, or in other words, ice that is consolidated. The location of the ice pack in relation to the coast is also important (Wadhams, 2000). Ice rheology, strength and deformation as well as the mass balance of the ice all play an important role in the overall dynamics of the system (Wadhams, 2000).

The sea ice momentum balance is derived by considering the five forces acting upon the unit area of the sea ice cover. Equation 2.1 describes the momentum balance,

$$M\,a = \tau_a + \tau_w + \tau_c + \tau_i + \tau_t \qquad \text{Eqn. 2.1}$$

where mass (M) x acceleration (a) of element (unit of ice) = wind/air stress (τ_a) + water stress (τ_w) + Coriolis force (τ_c) + internal ice stress (τ_i) + force due to sea surface tilt (τ_t) (Wadhams, 2000). Air stress acts upon the surface of the ice, whereas water stress has a drag effect on the underside of the ice (Lepparanta, 2011) as shown in Figure 2.3.

Variability in trends of sea ice drift in the Arctic Ocean have been linked to decadal shifts in atmospheric circulation patterns (Kwok et al., 2013). As mentioned, it is believed that atmospheric forcing, or the wind stress component of the momentum balance, is the main driver of sea ice drift (Wadhams, 2000). However, recent ice drift speeds do not seem to be directly related to the wind forcing and thus more likely linked to changes in ice thickness (Kwok et al., 2013). As suggested by Spreen et al (2011), the increase of drift speeds cannot entirely be attributed to changes in wind speed alone as the correlations between wind and sea ice drift speeds are mediocre between r = 0.4 to 0.52. It is speculated that thinning of the sea ice cover, resulting in changing internal ice stress, is contributing to the decadal increase in sea ice drift speeds (Haas, 2017; Spreen et al., 2011).

2.2.1 Sea Ice Drifting Buoys

A drifting buoy is a floating (or sitting on the surface of ice) ocean buoy. It is equipped with sensors that collect meteorological and/or oceanographic data. Data collected by the instrument are transmitted to a secure database through satellite communication away from the

study site (NSIDC, 2014). Variables that can be observed and collected from a buoy instrument include: geographic position (GPS) as longitude and latitude, atmospheric sea-level pressure (hPa), surface air temperature (°C), ice and snow thickness (m), as well as a number of other variables such as information about the condition of the instrument (i.e. battery life). In the past, buoy data were transmitted through the Argos satellite network. The Argos network is comprised of a collection of satellites that pass overhead which receive information from the buoy transmitter (Argos, 2018). However, buoys now transmit through the Iridium satellite network to a database initially managed by the owner of the instrument. Iridium is a different network of communication satellites – conducting the same way as Argos technology - and serves as a conduit of information from remote study sites to the database (Iridium, 2017). Data are typically transmitted every hour, with some variables being transmitted every three hours.

The most common types of buoys used to measure ice motion include: ice mass balance (IMB) buoys (Figure 2.4a.), ice surface velocity profiler buoys (iSVP) (Figure 2.4b.), and compact air-launched ice beacons (CALIB) (Figure 2.4c.). Each type varies with deployment methods as well as the data collected; some types, such as iSVP, are a much simpler model. They collect GPS, temperature and barometric pressure, as compared to other types, like IMB, which have the capability to measure more meteorological variables such as precipitation, ice properties such as ice and snow thickness, as well as GPS positions. Deployment varies in complexity. IMB's are manually intensive compared to the other types of buoys where the user is required to manually install the parts directly into the ice. iSVP buoys are simply placed onto the surface of the ice and activated by the user and, finally, the CALIBs are deployed via aircraft and dropped onto the target site after activation. The data in this project have all been obtained by iSVP instruments.

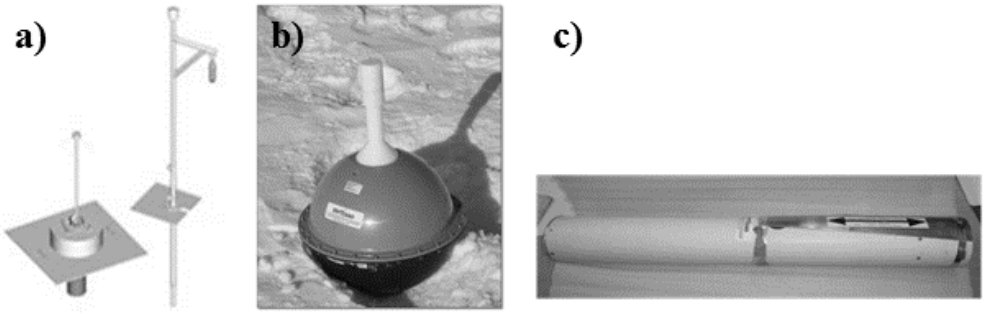

Figure 2.4: Examples of buoys used for the collection of sea ice drift data. a) illustration of an ice-mass balance buoy (IMB) b) picture of a surface-velocity profiler (iSVP) and c) picture of a CALIB. Photo sources: a) MetOcean b) Andrew Lawrence, 2014 c) Christian Haas, 2011.

2.2.2 Wind Driven Sea Ice Drift

The literature documents that wind is the primary force responsible for sea ice motion (Thorndike and Colony, 1982; Overland et al., 1984; Rigor et al., 2002; Samelson et al., 2006; Lepparanta, 2011; Spreen et al., 2011; Gimbert et al., 2012). Furthermore, the literature notes that winter ice motion can be mainly attributed to the wind field (Kimura and Wakatsuchi, 2000; Kimura et al., 2013). Wind applies force to the surface of the ice. Rough surfaces such as large pressure ridges, act as a sail to the wind and can cause the ice to drift at a higher velocity (Lepparanta, 2011). Figure 2.5 illustrates the influence of wind on sea ice drift, where wind stress is applied to the surface of the ice. In general, MYI has a higher drag than first-year ice (FYI) because FYI tends to be smoother and has not endured a high degree of deformation (Wadhams, 2000).

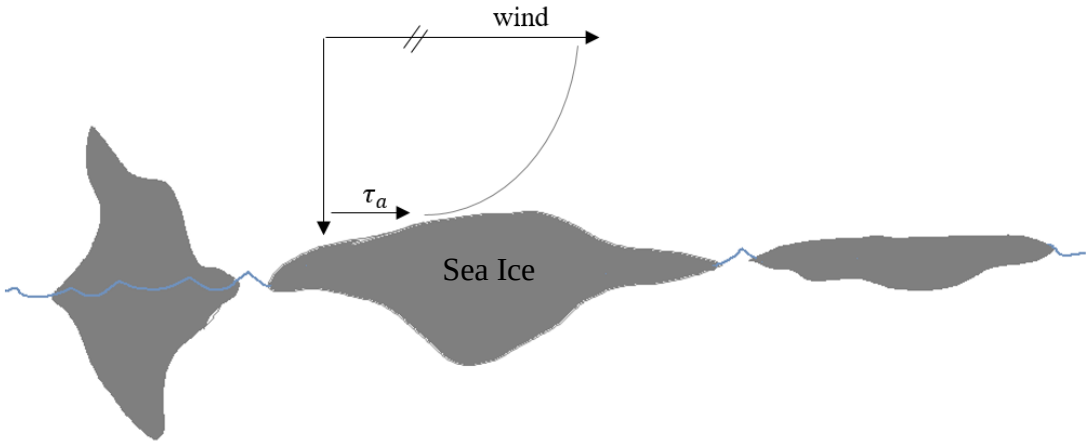

Figure 2.5: Illustration of the wind stress component of the momentum balance. Wind acting upon the surface of a floe of sea ice.

The force exerted on the surface of the ice by wind is proportional to the wind speed. This relationship is linked by the constant of proportionality called the drag coefficient; the drag coefficient is a function of the roughness of the surface (Wadhams, 2000). Equation 2.2 defines the wind stress component of the momentum balance – i.e. the force per unit area exerted by wind on ice – and illustrates the drag coefficient,

$$\tau_a = \rho_a C_a |\boldsymbol{U_a} - \boldsymbol{U_i}|(\boldsymbol{U_a} - \boldsymbol{U_i}) \qquad \text{Eqn. 2.2}$$

where τ_a is wind stress, ρ_a is air density, C_a is the ice-air drag coefficient, $\boldsymbol{U_a}$ is the wind velocity (measured conventionally at 10 m above the surface) and $\boldsymbol{U_i}$ is the velocity of the ice. The ice-air drag coefficient (C_a) is a function of the physical roughness of the surface of the ice. C_a typically ranges from 1.4 to 2.1 x 10^{-3} (Wadhams, 2000). There are two kinds of surface roughness that are observed in sea ice. Small-scale roughness describes the roughness of level (undeformed) portion of the ice surface, which includes snow covered ice in the winter or melt pond covered ice in the summer. Large-scale roughness relates to the formation of pressure ridges, rafted ice and other

deformation features (Wadhams, 2000). Another attribute to the roughness of sea ice is the number of edges exposed on an ice floe. The higher the concentration of sea ice, drag decreases due to less floe edges (Lupkes et al., 2012).

Most of the principles mentioned on ice dynamics refer to a free drift condition of sea ice for ice motion. Conceptualizing sea ice motion is simplest when considering sea ice in free drift. Sea ice in free drift is defined as ice that is not consolidated or floes are not constricted by surrounding ice floes or colliding with neighboring floes. Free drift means that there is no presence of internal ice stress upon the ice (Wadhams, 2000) and drift speed and direction are closely related to Ekman transport and geostrophic wind (Haas, 2017). When ice is in free drift the internal ice stress term of the momentum balance is omitted (Wadhams, 2000; Weiss, 2013). There is also an assumption that the unit reference area of ice cover moves as if it were an isolated object, such as a single ice floe. The ice will begin to drift in the direction of the wind (F) but as the ice is in motion, the Coriolis force increases, and the ice drift is deflected to the right of the wind – also known as the "turning angle" of the ice drift (shown in Figure 2.3). Generally, ice drift direction is to the right of the wind vector and the turning angle is 18° in the northern hemisphere (Haas, 2017). As the ice picks up speed, the Coriolis force becomes stronger and the ice drift will accelerate as a function of the wind until it hits a threshold. The ice will come to a rest eventually to the east of the starting point which has "traced out" half a loop. The drift will begin this sequence again and repeat; these "loops" are called inertial loops or oscillations and are often evident in the trajectories of ice floes and icebergs under varying winds or no wind (Wadhams, 2000; Gimbert et al., 2012). Oscillations in sea ice drift can be prompted by atmospheric events, such as storms or moving fronts (Gimbert et al., 2012) These shapes and directions is illustrated in Figure 2.6, where the effects of the types of forces on the ice are illustrated.

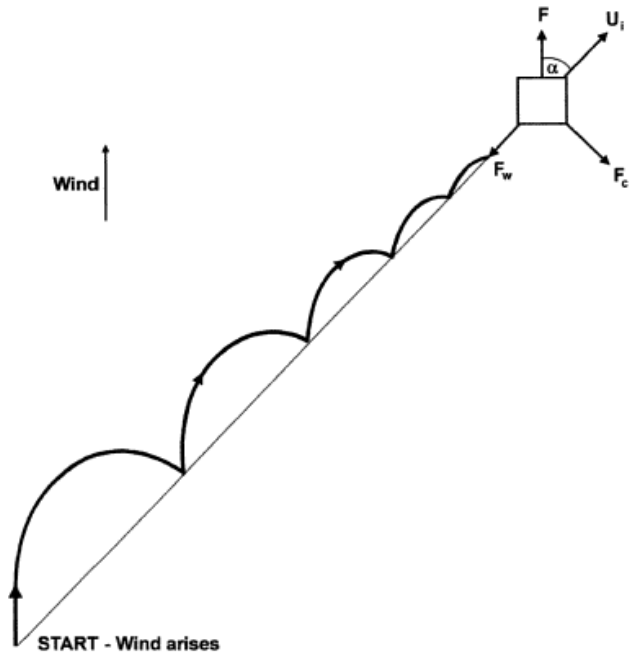

Figure 2.6: Forces on, and the motion of the ice floe in free drift; the formation of inertial loops (Wadhams, 2000).

Although the dynamics of sea ice are strongly influenced by surface winds, there is also an influence of the distance of the ice to the coast. In the summer there is less coastal influences due to more open water along the coast from melting landfast ice and alternatively, in the winter, there is a coastal influence present with the accumulation of landfast ice (Thorndike and Colony, 1982). The contributions to ice drift from other components are discussed in Sections 2.2.3 and 2.2.4.

2.2.3 Ocean Driven Sea Ice Drift

In addition to wind stress, water stress represents a dominant component of the momentum balance of sea ice drift. Water stress is represented by τ_w in Equation 2.1. Figure 2.7 shows the force of water stress acting upon the underside of a floe of sea ice.

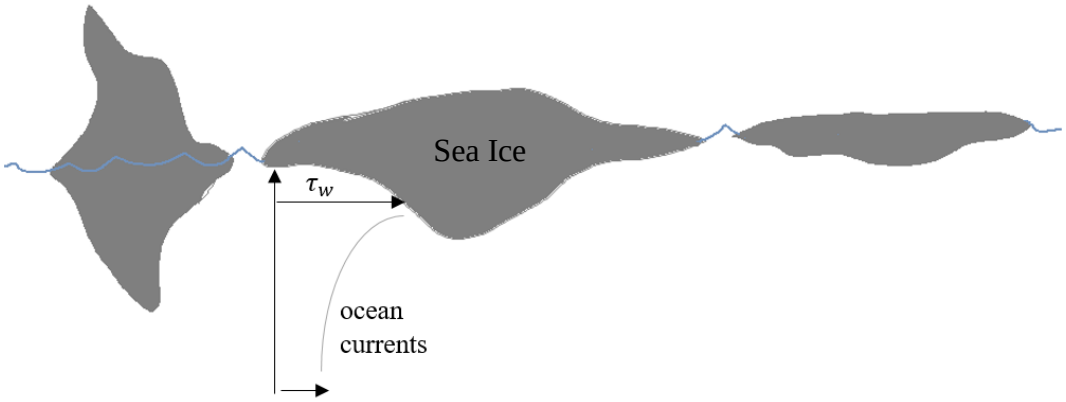

Figure 2.7: Illustration of the water stress component of the momentum balance. Ocean currents acting upon the underside of a floe of sea ice.

Closer to the ocean surface, currents are faster and stronger and are greatly influenced by surface winds and the global temperature (NOAA, 2011). As mentioned, ice surface roughness and the drag effect from wind stress increased drift speed as the degree of roughness on the surface of the ice acts as a sail; however, ocean related drag behaves the opposite and has a dampening effect on the ice velocity and movement – only if the ocean current direction is different than wind direction because ocean current speeds are slower than wind speeds. (Lepparanta, 2011).

The pattern of changing speeds and directions corresponding to near-surface winds and ocean currents is called Ekman transport. This is similar to the turning angle determined by wind and is the process by which the direction of the wind influences the ocean currents and deflects, or rotates, as you move down from the boundary at the surface of the water. In the theoretical form of atmospheric and oceanic Ekman layers below the sea ice, ocean currents are deflected 45° to the right of the wind (Lepparanta, 2011). Wind drives the ice and the frictional drag of the ice itself puts the surface waters in motion. Stress that is produced is transmitted down through the layers of the water column and the current strength decreases as it diffuses through the profile (NASA,

2018). The Coriolis effect drives this process; the near-surface layers are set in motion, each at a different angle (Wadhams, 2000) and this also suggests that the stress acting upon the ice is stronger closer to the surface. Figure 2.8 illustrates this process. It was theoretically thought that the combined influence of friction and the Earth's rotation produces a current spiral in the wind-driven layer of the ocean (Hunkins, 1966). Hunkins found that the effects of Ekman transport was included in the understanding of ice motion through a 1966 study. As mentioned, this is best described in situations of free drift ice. When ice is consolidated, the oscillations and spiral effect of Ekman transport are damped by internal ice stress (Gimbert et al., 2012).

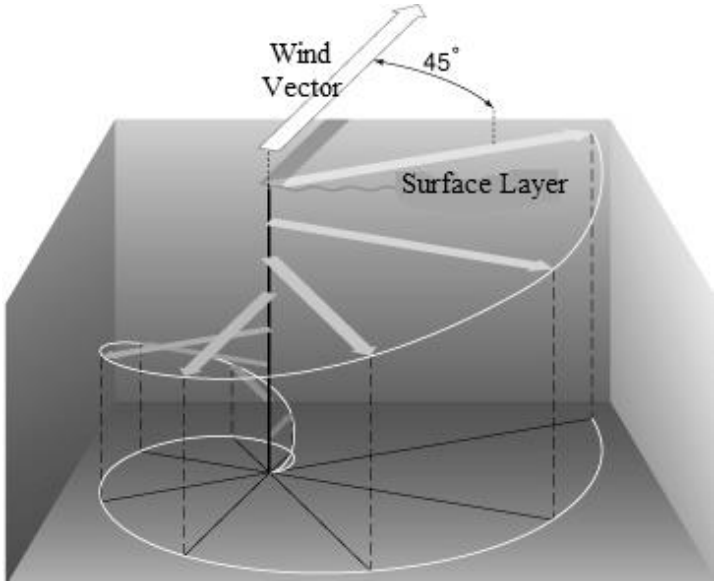

Figure 2.8: Illustration of the Ekman spiral in an "ice-free" ocean. Water at the surface moves at a 45° angle to the right of the wind vector. At deeper layers the strength of the water motion decreases and the turning angle increases. (Adapted from NASA, 2018).

The force wielded by the relative motion of water on the bottom of the ice represents the same form as air stress on the ice surface (Wadhams, 2000). The force of water stress on drift speed is proportional to the ocean current speed. Equation 2.3 states the water stress component of the momentum balance – i.e. the force per unit area exerted by ocean currents on the ice,

$$\tau_w = \rho_w C_w |\boldsymbol{U_w} - \boldsymbol{U_i}|(\boldsymbol{U_w} - \boldsymbol{U_i}) \quad \text{Eqn. 2.3}$$

where τ_w is water stress, ρ_w is water density, C_w is the ice-water drag coefficient, $\boldsymbol{U_w}$ is the water velocity (measured under the ice at the bottom of the boundary layer, i.e. at a depth of ~ 1 to 2 m) and $\boldsymbol{U_i}$ is the velocity of the ice. C_w is a function of the physical roughness of the bottom of the sea ice, so this component varies with ice type, like the ice-air drag coefficient varies with ice type as well. As MYI is rougher than FYI, MYI typically has a higher C_w than FYI. A typical value for the ice-water drag coefficient is 4 x 10^{-3} but is a function of the roughness of the ice, so values do vary with ice type (i.e MYI is rougher than FYI) (Wadhams, 2000). Typically, an ice floe that has a high ice-air drag coefficient will also demonstrate a high ice-water drag coefficient because the surface and bottom roughness of sea ice are well correlated (Wadhams, 2000).

2.2.4 Other Components of Sea Ice Drift

Air and water stress are typically the most dominant terms of the momentum balance of sea ice by an order of magnitude (Colony and Throndike, 1984; Wadhams, 2000; Haas, 2017). While these two terms play a vital role in sea ice drift speeds, particularly when sea ice is in free drift or in the summer months when ice is less consolidated (Steele et al., 1997; Wadhams, 2000), there are three more terms to the sea ice drift equation to consider (Equation 2.1). These are the sea surface tilt (τ_t), the Coriolis force (τ_c), and the internal ice stress (τ_i). The sum of τ_t and τ_c is small (Steele, et al., 1997). τ_t incorporates the fact that the earth is not a flat surface; Equation 2.4 is an expression of stress from sea surface tilt,

$$\tau_t = -m\ g\ grad(H) = -\rho_i\ h\ g\ grad(H) \quad \text{Eqn. 2.4}$$

where *grad(H)* is the gradient of elevation of the sea surface with respect to the geoid, *m* is the mass of the ice, *g* is gravity, *h* is ice thickness and ρ_i is the density of the ice. It is noted that over

a period of days, sea surface tilt is minute (Wadhams, 2000). Equation 2.5 demonstrates the magnitude of the Coriolis force

$$\tau_c = 2\, m\, \boldsymbol{\omega}\, \boldsymbol{U}_i\, sin\phi \qquad \text{Eqn. 2.5}$$

where m is the mass of the element (ice), $\boldsymbol{\omega}$ is the angular velocity of the Earth in radians, $\boldsymbol{U_i}$ is the ice velocity and ϕ is the latitude. The Coriolis force is at its maximum value at the Poles and zero at the equator (Wadhams, 2000); this is why it is important to consider when investigating Arctic sea ice motion. It is noted that the Coriolis force is negligible on a human scale, as we do not sense this force, but it is essential in defining motions of sea ice, global winds and ocean currents at a geophysical scale (Wadhams, 2000).

The fifth component of the momentum balance of sea ice that has not yet been discussed is the internal ice stress (τ_i). τ_i plays an important role in the winter months, when sea ice is consolidated and/or in narrow channels as well as restricted bodies of water, such as the conduits within the CAA. τ_i describes the total force acting upon a unit area of ice cover (Wadhams, 2000). It is difficult to parameterize in a model due to differential winds and various currents that act upon different areas of an ice floe or consolidated ice sheet (Wadhams, 2000). Steele et al. (1997) investigated the force balance of sea ice in a numerical model and ultimately worked to define an ice pressure parameter, P^*. They determined that P^* is primarily a function of mean ice thickness and velocity. They also found that water drag and the internal ice stress gradient often behave in a similar way and that on smaller spatial scales – such as the region of Nares Strait – internal ice stress is a stronger forcing than water stress (Steele et al., 1997). Although the consensus for ice drift of the central AO is that wind stress is the dominant force, considering internal ice stress will be important for this thesis due to the constricted geography of Nares Strait.

2.2.5 The Case of Compact Ice Drift

Dynamics of sea ice is well understood in free drift theory as previously described. However, this theory only works best for isolated ice. Ice is not in free drift in all instances. The free drift theory of wind and ocean stress effects on sea ice works for floating ice – such as ice floes or icebergs in open water, for diffuse ice covers such as marginal ice zones, and for parts of the Antarctic sea ice regime. For other types of zones or regions of ice, where ice motion is restricted by the presence of surrounding ice or coastlines, another solution needs to be considered. As noted, for the central Arctic pack, as well as for ice situated in channels, straits and basins – places restricted by land boundaries – it needs to be understood how stress is transmitted through the ice pack and how ice cover responds when it is not free to drift without restrictions (Wadhams, 2000). This study observes ice motion through a relatively narrow strait and this alternative concept will be reviewed.

To address the stress that is transmitted through the ice pack, the role of internal friction is to be considered. Other components of the sea ice regime need to be observed such as ice rheology and the rate and level of ice deformation. Lepparanta (2011) describes five main consequences to sea ice drift associated with a higher level of internal friction: 1) A portion of the mechanical energy to be used for drift is translated to the deformation of ice; therefore, overall drift speed is decreased 2) if external forcings, such as wind or ocean, do not reach the limit to make ice move, ice is then motionless, 3) ice is more rigid than the atmosphere and ocean, therefore spatial variations of forcings show up in sea ice velocity fields, 4) narrow deformation zones manifest, specifically at the edge of landfast ice and parallel to coastlines, and 5) the internal stress field within the ice cover can transfer mechanical energy over long distances (Lepparanta, 2011). There are a lot of other factors to consider when examining sea ice motion. This thesis will focus on the

external forcing of wind as well as internal ice stress using sea ice concentration as a proxy. Figure 2.9 shows the compactness of ice versus dimensionless drift speed, which is the observed ice drift speed scaled by theoretical free drift speed as a function of compactness. As the amount of "compactness", or ice coverage is increased, the dimensionless speed decreases suggesting that as ice becomes consolidated, the number of forces acting upon it increases and ice motion becomes slower and more complex (Lepparanta, 2011).

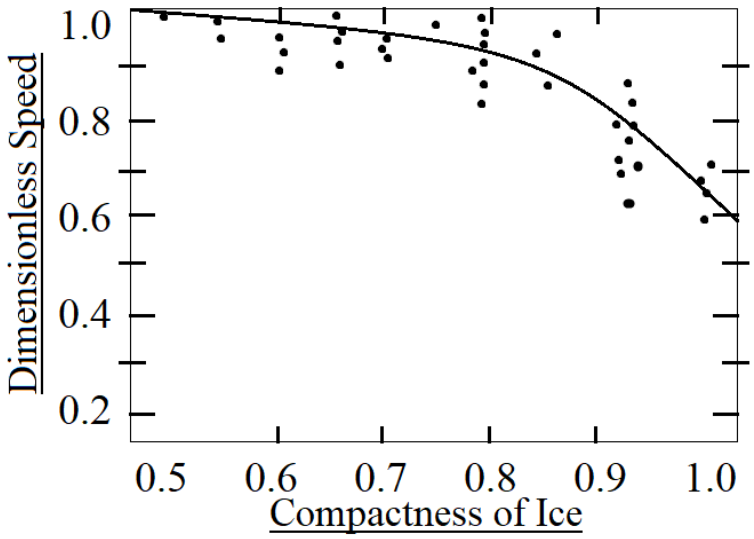

Figure 2.9: Some observations of drift speed in various ice compactness conditions. Drift speed is presented as dimensionless speed where the observed ice drift speed is scaled by the theoretical free drift speed as a function of ice compactness (Adapted from Lepparanta, 2011).

Additionally, in respect to internal friction and considering ice motion in the presence of compact ice, any period during which the sea ice is landfast should be identified further to understand the specific dynamics and forcings at work on the sea ice at a given time (Wadhams, 2000). Ryan and Munchow (2016) define the landfast ice season within Nares Strait to be when average daily sea ice drift speeds are less than 0.025 m/s (2.16 km/d) for 10 consecutive days. By

taking a closer look at the fast ice season within the study period, further understandings of the physical forces can be obtained.

2.2.5.1 Sea Ice Concentration Data through Ice Charts

Internal ice stress will be important in the investigation of the variability of ice drift though Nares Strait. In order to quantify that portion of the momentum balance, sea ice concentration information is imperative. Mean sea ice concentration can be obtained from sea ice charts. Regional weekly ice charts from the Canadian Ice Service (CIS) are obtained and analyzed for this work.

Ice charts in Canada are developed and distributed by the CIS. Ice charts illustrate and communicate ice conditions at the time of development. Charts are produced in a number of capacities: daily charts for specific areas and weekly charts for regions of the Arctic (Nares Strait falls within the Eastern Arctic chart produced by CIS). Charts are made for sea ice, lake and river ice and ice of land origin conditions. They are considered in the production of ice hazard warnings, short- and long- range forecasts of ice conditions and seasonal outlooks for the regions where ice is present. The charts are of utmost importance to icebreaker captains, commercial shipping interests and fishing vessels to help navigate ice infested waters. Both total ice concentration (ice cover) and ice stages of development (ice types) are reported by the ice charts (MSC, 2005).

Ice charts are derived from a combination of remote sensing observations, primarily synthetic aperture radar imagery, sea ice model forecasts and field observations. This information is translated into an ice chart using Geographic Information Systems (GIS) software (MSC, 2005). The charts that are of interest to this study are the ice concentration charts, which tell us the concentration of ice in a particular area. Ice concentration on ice charts is reported in tenths.

The CIS uses the "egg code" to provide specific details about the ice at *x* location. Figure 2.10 is a summary diagram of the "egg code" and its corresponding values and definitions. Appendix A shows the full definition of the egg code. These eggs overlie each specific ice region (polygons) on the charts. This study is most interested in the information that is included in the top row of the egg code (total concentration).

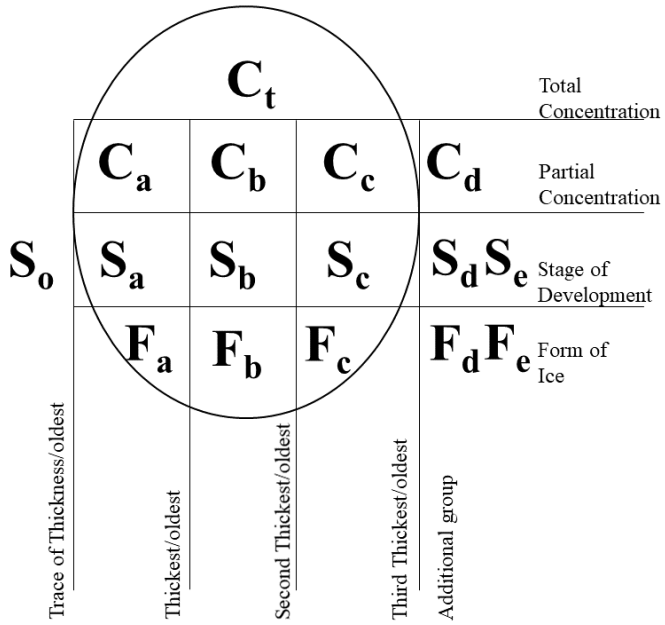

Figure 2.10: A summary diagram of the "egg code" and the meanings of values and information stored within the symbols (Adapted from MSC, 2005).

2.3 Sea Ice Export from the Arctic Ocean

As mentioned previously, the declining Arctic sea ice cover is not only attributed to melting sea ice, but also to the redistribution of sea ice from the Arctic Ocean as well. Sea ice is exported from the Arctic Ocean through several gateways; exchange typically occurs in the summer months between May and November (Kwok, 2005; Howell et al., 2013). The CAA and Fram Strait are the two major pathways that connect the Arctic Ocean to the Atlantic Ocean (Munchow and Melling,

2008). In a recent study, Howell et al. (2013) estimate sea ice area flux between the Arctic Ocean and the M'Clure Strait and the Queen Elizabeth Islands (the west and north coast of the CAA) for the study period of 1997-2012 for the months of May to November. They found that during the study period, the sea ice within the CAA was almost entirely landfast throughout the study period. When ice was not landfast, the ice is in drift motion and it is advected from the Arctic Ocean into the CAA. The advection of sea ice from the Arctic Ocean to the CAA is important as it provides the CAA with another source of MYI, apart from in situ production of MYI via the development of FYI. MYI from the Arctic Ocean poses a hazard to marine operations in this region. Howell et al. (2013) also confirms a hypothesis from Melling (1995) which was that the primary source of MYI in the CAA has shifted from MYI developed in situ within the CAA to MYI advected from the Arctic Ocean (Howell et al., 2013). Nares Strait (refer to Figure 3.1) is a narrow passage within the Eastern High Arctic, which connects the Lincoln Sea to Baffin Bay. It forms the northeastern edge of the CAA, between Ellesmere Island and the west coast of Greenland. It is believed that Nares Strait is a major conduit for sea ice export from the Arctic Basin (Kwok, 2005) despite its smaller dimensions, contributing to the inflow of MYI into the CAA. To compare, Howell et al. (2013) found mean sea ice area export through M'Clure Strait to be 21 x 10^3 km^2 and 8 x 10^3 km^2 through the Queen Elizabeth Islands – both of which are the western coast of the CAA – during a 1997 to 2012 study period. Over a study period of 1997 to 2009, sea ice export through Nares Strait was 42 x 10^3 km^2 (Kwok et al., 2010). Fram Strait still exhibits the largest export from the Arctic Basin with 88 x 10^4 km^2 sea ice through this conduit (Smedsrud et al., 2017).

Kimura et al. (2013) conducted a study to explore the relationship between winter sea ice motion and summer sea ice extent. Sea ice redistribution during the winter is one of the most vital aspects to consider in examining summer sea ice extent. They found that there were high

correlations between winter sea ice motion and the minimum ice extent in the subsequent autumn in several regions of the Arctic Basin. This supports the idea that the divergence or export of sea ice in the winter is consequential to a thinner ice cover. However, it is important to note that areas that were restricted by bounding topography, i.e. smaller channels and straits, such as the CAA, displayed non-significant r values (in the range 0.0 - 0.3) This includes the correlation reported for Nares Strait (r = 0.1). It was also concluded that the interannual variability of total ice area in September is large around the marginal ice zone and large variability in December ice motion is noticeable near the coast (Kimura et al., 2013). The research from this study suggests that sea ice imprints a memory and that what occurs in a given winter has consequences for the following year or season.

The declining trend in Arctic sea ice extent in recent years has not only affected the total sea ice coverage but has also introduced a change in the nature of the ice itself. MYI in the AO accumulates along the northwestern coastlines of the CAA due to the typical anticyclonic Beaufort Gyre; this ice represents some of the thickest and oldest sea ice in the Arctic (Wholleben et al., 2012). Maslanik et al. (2011) in their study found that the amount of MYI in the central Arctic Ocean has decreased significantly, correlating with a decrease in Arctic sea ice extent. Figure 2.11 shows the distribution of sea ice age at the annual sea ice extent minimum for 1985-2017. The Arctic sea ice regime was once dominated by MYI and it has largely been replaced by seasonal FYI (Derksen et al., 2012). Model results indicate that sea ice thinning may be due to a redistribution of thick MYI from the Arctic Ocean into the marginal seas (Haas et al., 2006). When sea ice becomes thinner and weaker, the rate of export can increase exponentially. Pfirman et al. (2014) found that extensive changes in the fate of sea ice exported from the Arctic and the travel time of older, MYI have increased exponentially. They concluded that the changes they observed

partially explain the decrease in thicker, older sea ice in the central Arctic Ocean (Pfirman et al., 2014). As sea ice is a dynamic material, the decrease in sea ice extent is not only attributed to melting sea ice (thermodynamic processes) but to dynamic processes as well. Sea ice exporting from the Arctic Basin to sub-Arctic seas through various gateways has contributed to the further depletion of the volume of Arctic sea ice.

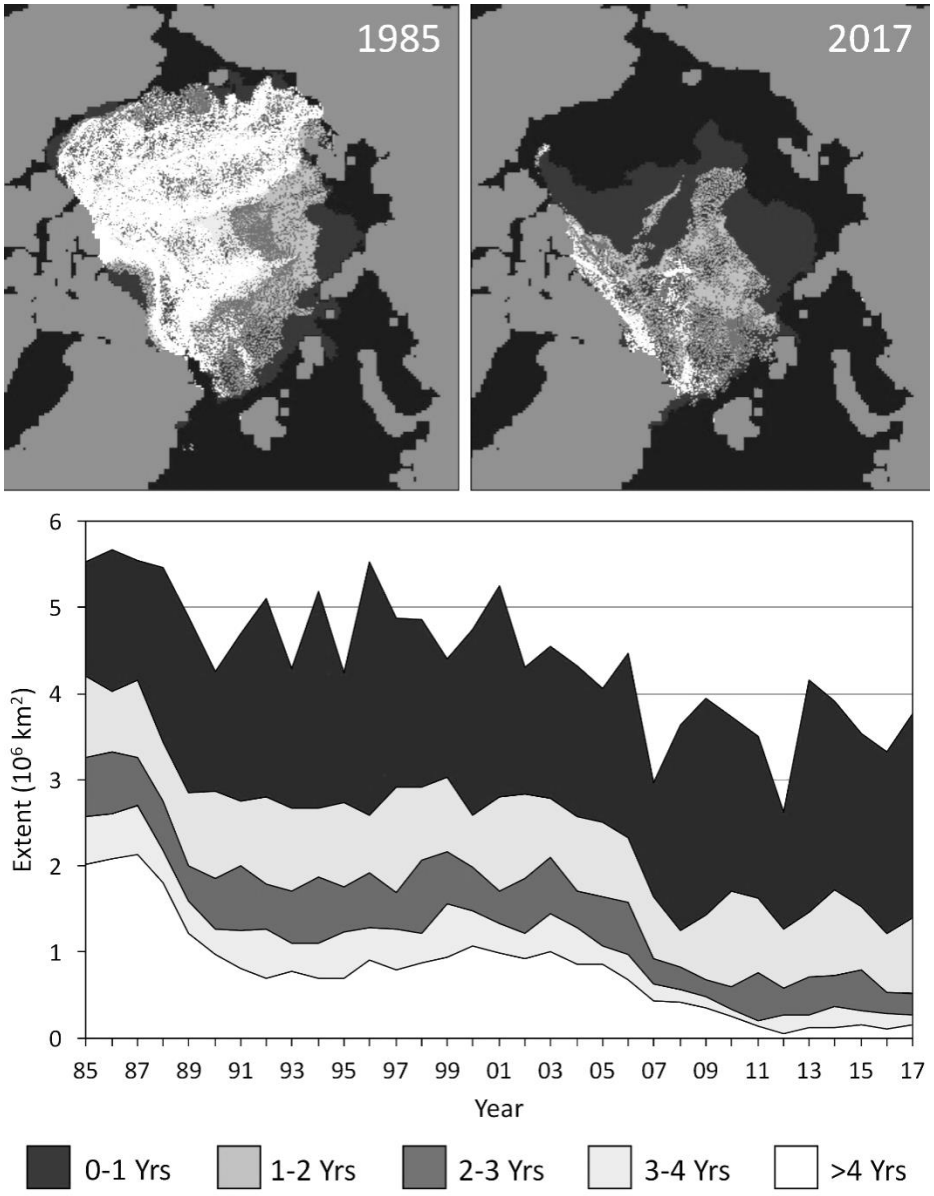

Figure 2.11: Arctic sea ice age distribution at the annual minimum ice extent 1985-2017. This graph shows a decline in sea ice age over time with most sea ice less than a year old in the last five years (adapted from NSIDC, 2017).

2.4 Sea Ice Drift through Nares Strait

Nares Strait is one of the conduits for sea ice export and mass flux of freshwater (FW) from the Arctic Ocean. Strong persistent winds also may play an important role on the ice and FW balance. Within Nares Strait, sea ice drift is most active after July and ice drift typically ceases in

motion mid- to late- winter when the ice cover once again becomes landfast. The timeline of ice drift within Nares Strait can be ascribed to the formation of ice arches associated with the consolidation of MYI. The process of ice arch formation effectively acts as a dam for southward sea ice drift (Kwok, 2005). The ice arches block the advection of sea ice from the Arctic Ocean, via the Lincoln Sea. Strong northerly winds are fundamental for the necessary conditions for arch development by removing young sea ice as quickly as it is produced (Ingram et al., 2002). It is important to understand landfast ice conditions within Nares Strait to fully understand the sea ice dynamics of the region (Ryan, 2005). Ice arching is a phenomenon that is common in the narrow passages of the CAA and the process of ice arch formation is important in confining sea ice within the Arctic Ocean. The earlier the consolidation of sea ice occurs, the longer the stoppage period in which ice is not advected from the Arctic Ocean through the strait (Kwok, 2005).

Ice arches within Nares Strait typically form between the early- and mid-winter months. The accumulation of landfast ice and the development of ice arches occur at Robeson Channel (the northern mouth of Nares Strait, at the southern limit of the Lincoln Sea) in the north and at Kane Basin near the south of Nares Strait. There is a stretch of ~450 km between these two locations (Kwok et al., 2010). These ice arches usually collapse by early to mid-summer (Decker, 2010). Kwok et al. (2010) found that the average date of formation of the northern arch was around January 12 ± 44 days and the average date of development for the southern arch was February 2 ± 44 days. The ice arches typically collapse after an average of 184 ± 10 days (Kwok et al., 2010).

There are a few benefits of ice arches forming within the strait. Ice arches ultimately control ice drift and, therefore, this phenomenon controls the flux of sea ice from the Arctic Ocean. As Nares Strait is a major gateway for ice and FW from the Arctic, the stoppage that occurs along with the formation of ice arches stabilizes the flux of sea ice. Without the event of a stoppage of

ice flow throughout the year, sea ice drift speeds, and the resulting flux, can amount to very high quantities of both FYI and MYI leaving the High Arctic and almost doubling amounts in recent years. Arches may also increase the strength of ice once formed due to thermodynamic ice growth (Kwok et al., 2010).

Kwok et al. (2010) performed a study on ice advection through Nares Strait for the period of 1997 - 2009. In 2007, ice arches failed to form in Nares Strait resulting in the highest outflow of Arctic sea ice occurring within the 13-year time period (1997-2009). Kwok et al. (2010) found that the sea ice area flux through Nares Strait was 42 x 10^3 km^2 compared to 33 x 10^3 km^2 (Kwok, 2005) averaged for 1997-2009 and 1996-2002 respectively, with 2007 exhibiting an area outflow of 87 x 10^3 km^2 (Kwok, et al., 2010). The flux measurements for 2007 doubled in comparison to previous years (Figure 2.12). The year 2007 was also a significant year for the entire Arctic system, where the Arctic sea ice cover experienced unprecedented loss. There was a correlation between ice arching and sea ice extent in this time interval (Kwok, et al., 2010).

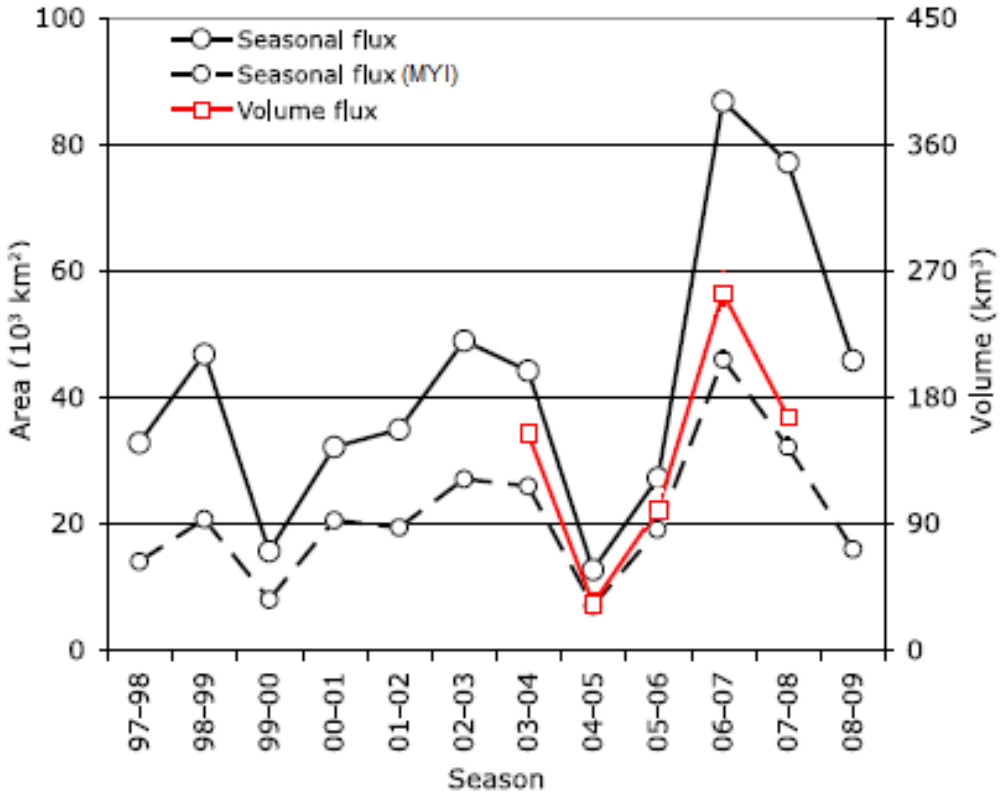

Figure 2.12: Sea ice area and volume flux for Nares Strait, 1997-2009. Total sea ice area flux (solid black line), MYI area flux (black dashed line) and sea ice volume flux (red solid line). Season is defined as September through August. In 2007, flux doubled compared to previous years (Kwok et al., 2010).

Little is known about which physical force is most dominant on sea ice motion through Nares Strait. Samelson et al. (2006) investigated this question using a combination of satellite observations (manual ice tracking) and model estimates of low-level winds. The study was conducted during two periods – January to February 2004 and November to December 2004. The year 2004 and these months were specifically chosen because of distinctive ice-motion events that were recorded through continuous observation of ice in Nares Strait. In Nares Strait, pack ice typically consolidates anytime between November and April, forming ice arches consecutively at Robeson Channel and Kane Basin – as mentioned previously. This study found stronger evidence for atmospheric control versus oceanic control of sea ice drift through the strait. Their results

suggested that the shutdown of ice drift - through the formation of fast ice and ice arches - and sea ice flux through the strait, can both be defined by wind stress and atmospheric cooling.

2.5 Summary

This chapter outlined the background information and literature important to this thesis. Sea ice is continuously in motion and the changes to the sea ice regime are due to both dynamic and thermodynamic processes. Over the last decade, Arctic sea ice has continued to deplete and the extent of ice cover in the Artic continues to decrease.

The momentum balance of sea ice drift considers the five forces acting upon a unit of sea ice. Sea ice is influenced by wind (or air) stress, water stress (stress from ocean currents), internal ice stress, Coriolis force and sea surface tilt. For unconsolidated ice that is in a state of free drift, wind is the dominant force driving sea ice drift. Internal ice stress plays an integral role on the drift of sea ice when it is compact, generally in the winter months as well as in areas that are restricted by bounding topography and coastlines – such as Nares Strait.

Sea ice drift speeds within the Arctic Basin have increased in recent years, but this cannot be entirely attributed to increased wind speeds. Instead, the literature suggests that the increase in drift speeds are due to the thinning of sea ice and the loss of MYI from the Arctic Ocean. This is largely due to sea ice thinning and becoming weaker due to the warming climate. As a result, tremendous changes to the sea ice regime in the Arctic have occurred.

Nares Strait is of importance to the changes in the ice regime of Arctic Ocean because it is a major pathway of sea ice export from the Arctic Ocean. The balance of the system in Nares Strait, and other micro-regions of the Arctic, are integral to the global climate system (Samelson and Barbour, 2008). Nares Strait is characterized by the formation of ice arches in the winter months,

which slow or prevent the advection of sea ice from the Arctic Ocean to Baffin Bay. This study examines the dynamics of sea ice in this narrow channel to better understand the behavior and influences of sea ice drift in this location.

Chapter 3
Study Site, Data and Methods

3.0 Introduction

This chapter outlines the data and methods used to answer the research objectives of this thesis. Section 3.1 outlines the study site, Nares Strait, and its geographic characteristics. This section also outlines the geographical sub-regions of Nares Strait that are referred to in this study. Section 3.2 describes the data used for the project. Three data sets are used: buoy trajectory data, meteorological data and sea ice concentration data. Finally, Section 3.3 introduces the methodologies used to analyze each of these datasets.

3.1 Study Site

The region of interest for this study is Nares Strait. Nares Strait is a stretch of water that connects the Lincoln Sea (to the North) and Baffin Bay (to the South); it is located between the east coast of the CAA – specifically Ellesmere Island – and the west coast of Greenland (Munchow and Melling, 2008). Nares Strait is roughly 500 km long and 40 km wide – a relatively narrow passage compared to other waterways throughout the CAA. Figure 3.1 is a map showing the study area for this thesis including associated bathymetry and surrounding topography of Nares Strait.

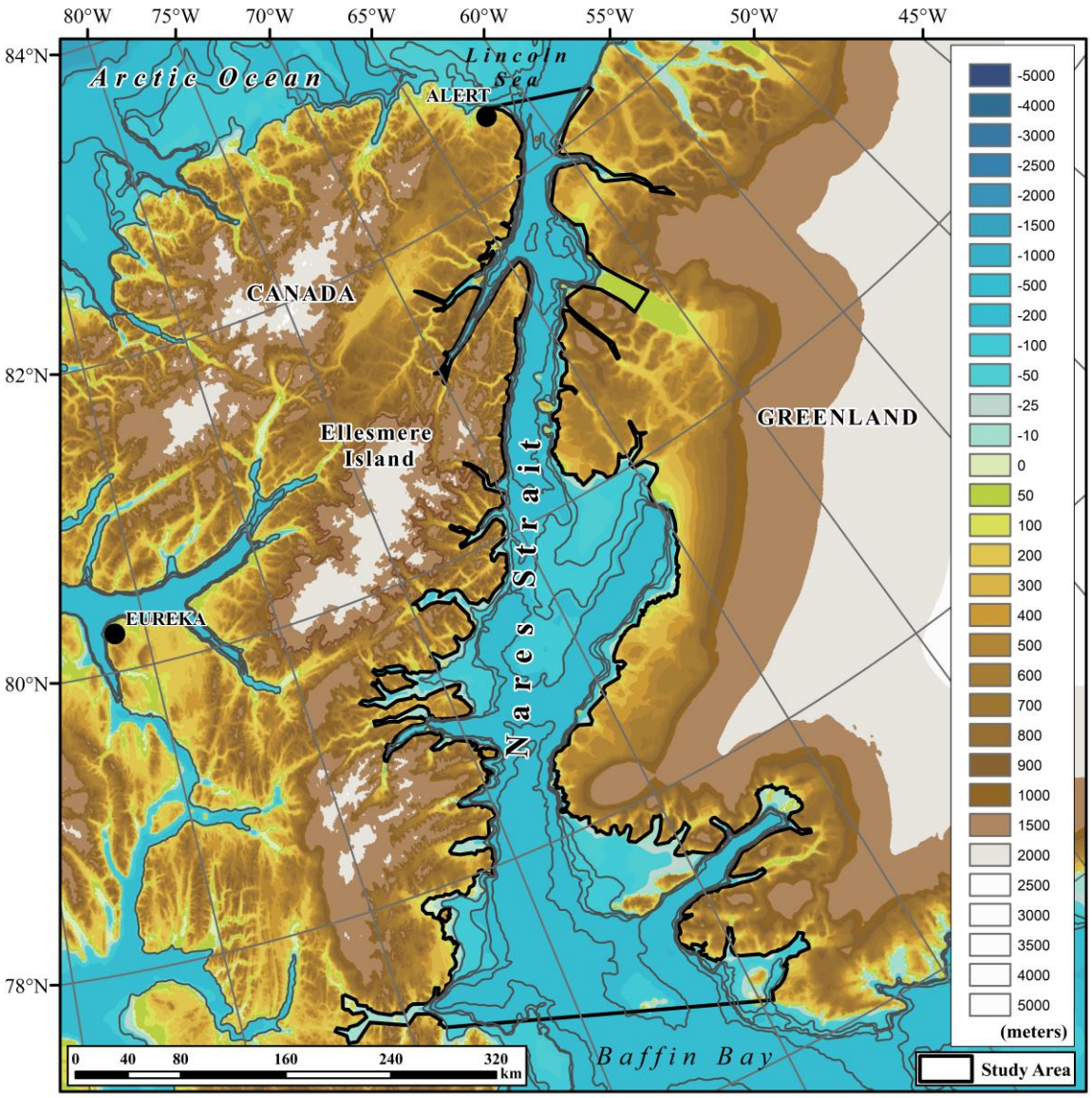

Figure 3.1: Map showing the study area – Nares Strait in the Canadian High Arctic – bathymetry and the surrounding topography (adapted from the IBCAO, version 3.0 at 500 m resolution, 2012).

Nares Strait is a unique region as it is bounded by steep topography on both its western (CAA) and eastern (Greenland) edges. The mountainous landscape surrounding the strait has a great influence on the meteorological components of the environment. Mountainous landscapes are apparent from Figure 3.1. Within a 25-kilometer buffer of the coastline of Nares Strait,

maximum elevations reach 1859 m a.s.l. with a mean elevation of 545 m a.s.l. (IBCAO, 2012) and steep terrain begins to rise up within 5 kilometers of the coast (Samelson and Babour, 2008). Due to the narrow width of the strait, as well as the bounding topography, this channel is inclined to unique meteorological characteristics, which include extreme, persistent winds. For instance, Nares Strait frequently exhibits strong along-channel winds and ocean currents that flow from north to south (Samelson and Barbour, 2008). In contrast to the steep topography that lines the coast of Greenland and Canada, Nares Strait exhibits a shallow bathymetry with a maximum depth of 1015 m and a mean depth of 295 m, relative to the rest of the Arctic Basin which has a maximum depth of 5557 m and a mean depth of 1327 m. (IBCAO, 2012).

As mentioned, Nares Strait connects Baffin Bay to the AO via the Lincoln Sea. Sadler (1975) found that about 15% of the total outflow of water from the Arctic Ocean transits though Nares Strait. Oceanic data are scarce for Nares Strait due to its remoteness and the complexity of the region. Also, instruments that are deployed in Nares Strait often are damaged and rarely survive the weather and environment (Shroyer, et al., 2015). The consensus through research and literature is that there is a strong north to south flow of water, mostly due to the strong southward flow of wind (Sadler, 1975; Samelson and Barbour, 2008; Shroyer, et al., 2015). There is a strong southward flow from the Arctic Ocean (North to South) of wind and ocean currents also due to the geostrophic current incurred from sea surface tilt (Christian Haas, personal communication, November 14, 2017). Munchow and Melling (2008) investigated ocean currents in Nares Strait and quantified specific characteristics using an array of ocean sensing instruments. Data showed that Kennedy Channel (top-mid Nares Strait) has strong, southward flow of water on the western side of the channel. Kennedy Channel has a vertically averaged magnitude of about 7 cm/s (~6 km/day). A slower ocean current on the eastern edge of the channel heads north with a depth mean

of roughly 4 cm/s (3.5 km/d). It was also noted that the exhibited ocean currents behave much differently under landfast versus mobile ice conditions (Shroyer, et al., 2015). Near the south end of Nares Strait at Lancaster Sound, near-surface current speeds range from 9 to 52 km/d (Addison and Bourke, 1987).

3.1.1 Geographic Sub-Regions of Nares Strait

Nares Strait is composed of several named geographic regions and water bodies. For this study, the channel is divided into four sub-regions where data and analysis are sub-divided accordingly to look at the spatial variability of sea ice drift within Nares Strait. Figure 3.2 shows the four sub-regions of Nares Strait. From the north to south these sub-regions are: Robeson Channel, Kennedy Channel, Kane Basin and Smith Sound. These regions will be mentioned throughout the study to address spatial variability of sea ice drift in Nares Strait and to further analyze each buoy trajectory. The most notable differences between the four sub-regions are their coastlines and water area. For example, Kennedy Channel is much narrower than the others (consistently ~39 km wide through the sub-region, compared to ~170 km wide in Smith Sound), and given the steep topography that lines the coast of the entirety of Nares Strait, this area behaves much like how a wind tunnel does (Addison and Bourke, 1987). Sea ice concentrations differ between the four regions as well. Through investigation of sea ice charts from the CIS, which will be discussed in Section 3.3. Sea ice concentrations are more variable during the summer months and range from very high coverage (70-100% ice coverage) in the northern part of the strait (Robeson Channel and Kennedy Channel) to much lower percentages of ice concentration (20-60% total ice coverage) in the south (Smith Sound). During the winter months all regions of the strait are above 60% total ice coverage which is considered to be consolidated ice cover.

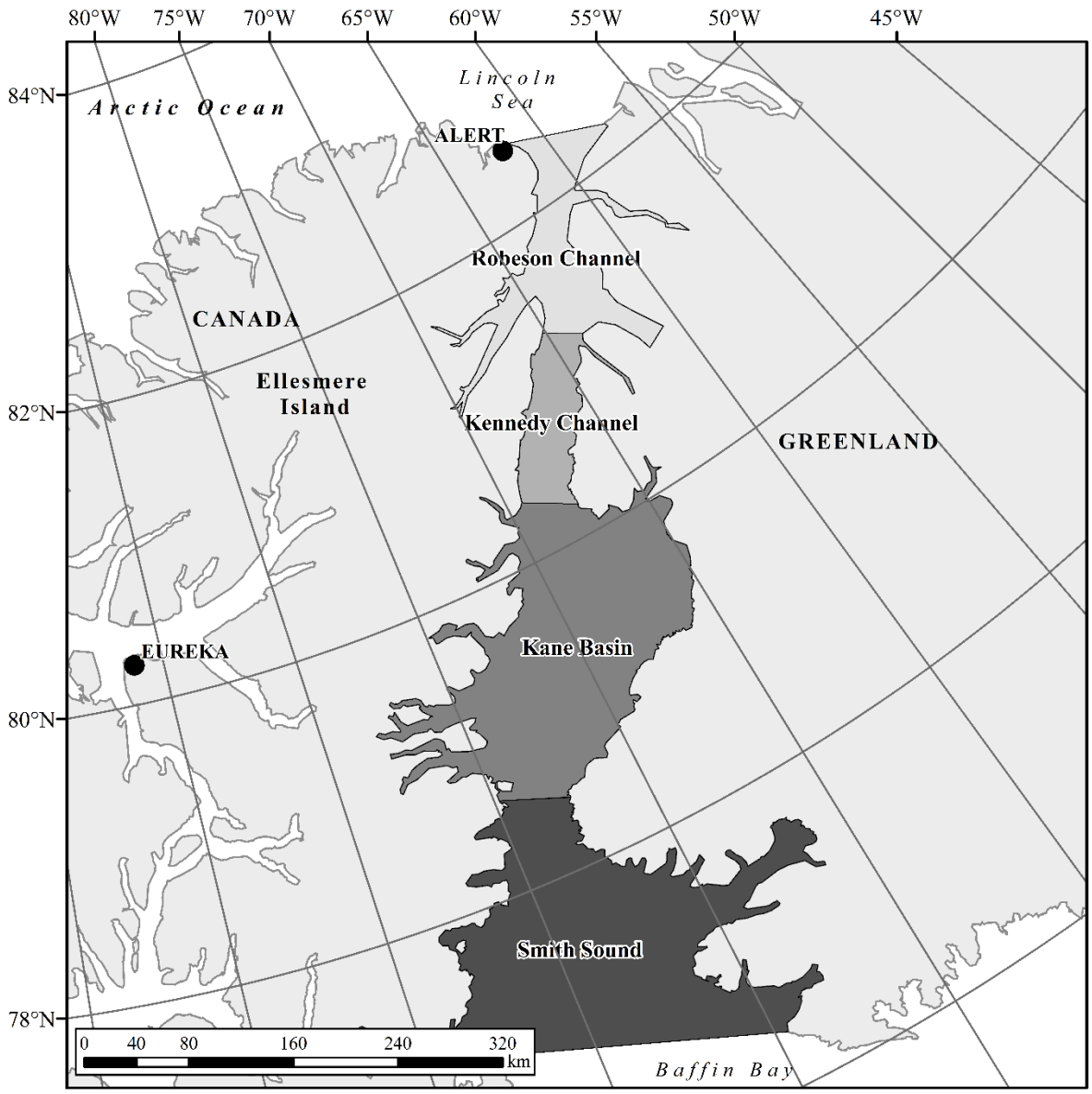

Figure 3.2: Map showing four sub-regions of Nares Strait: (from north-south) Robeson Channel, Kennedy Channel, Kane Basin and Smith Sound.

3.1.2 Climatology of Nares Strait

Maxwell (1981) conducted a comprehensive study of climatic regions of the CAA. Maxwell described Nares Strait as unique from the rest of the CAA due to various storm systems that continue northward from Baffin Bay up through the strait. These storm systems that move

northward to Nares Strait are enough to influence unique sea ice dynamics in Nares Strait. Sea ice consolidates later (February to March) in Nares Strait which is later than the other narrow channels of the CAA (Maxwell, 1981).

Precipitation is more than 200 mm annually surrounding Nares Strait due to the mountainous topography, however, the average precipitation of Nares Strait is less than 200 mm, and less than 100 mm in some places. Temperatures are also variable in and surrounding Nares Strait. The mean annual temperature range in Nares Strait is 38°C with minimum mean daily temperatures of -35°C to -28°C during the winter months and reaching maximum temperatures slightly above 3°C, in July (Maxwell, 1981).

Winds within Nares Strait have been reported to be predominantly from the northwest direction (Steffen, 1986). In another study, Ito (1982) observed that wind speed and direction were mainly controlled by the topography of Greenland and Ellesmere Island. Additionally, winds were found to be strongest in the middle of the strait and were weaker towards both coasts (Ito, 1982). Maxwell (1981) also state that the downslope from either Ellesmere Island or Greenland cause turbulent and frequent strong winds in the winter. Figure 3.3 shows a model output of 10 m winds through Nares Strait. Strong southward winds through the strait are indicated here.

More recent observations of the climatology of Nares Strait suggest significant regime changes, including an increase in temperature, which is reminiscent of the broader global climatological changes. Decker (2010) investigated climatological and cryospheric profiles of Nares Strait using remote sensing. Decker found that surface air temperatures have increased 0.3°C to 0.8°C per decade. Summer temperatures were warmer by 1°C to 3°C during 1978-2009 than during 1953-1972 (Decker, 2010).

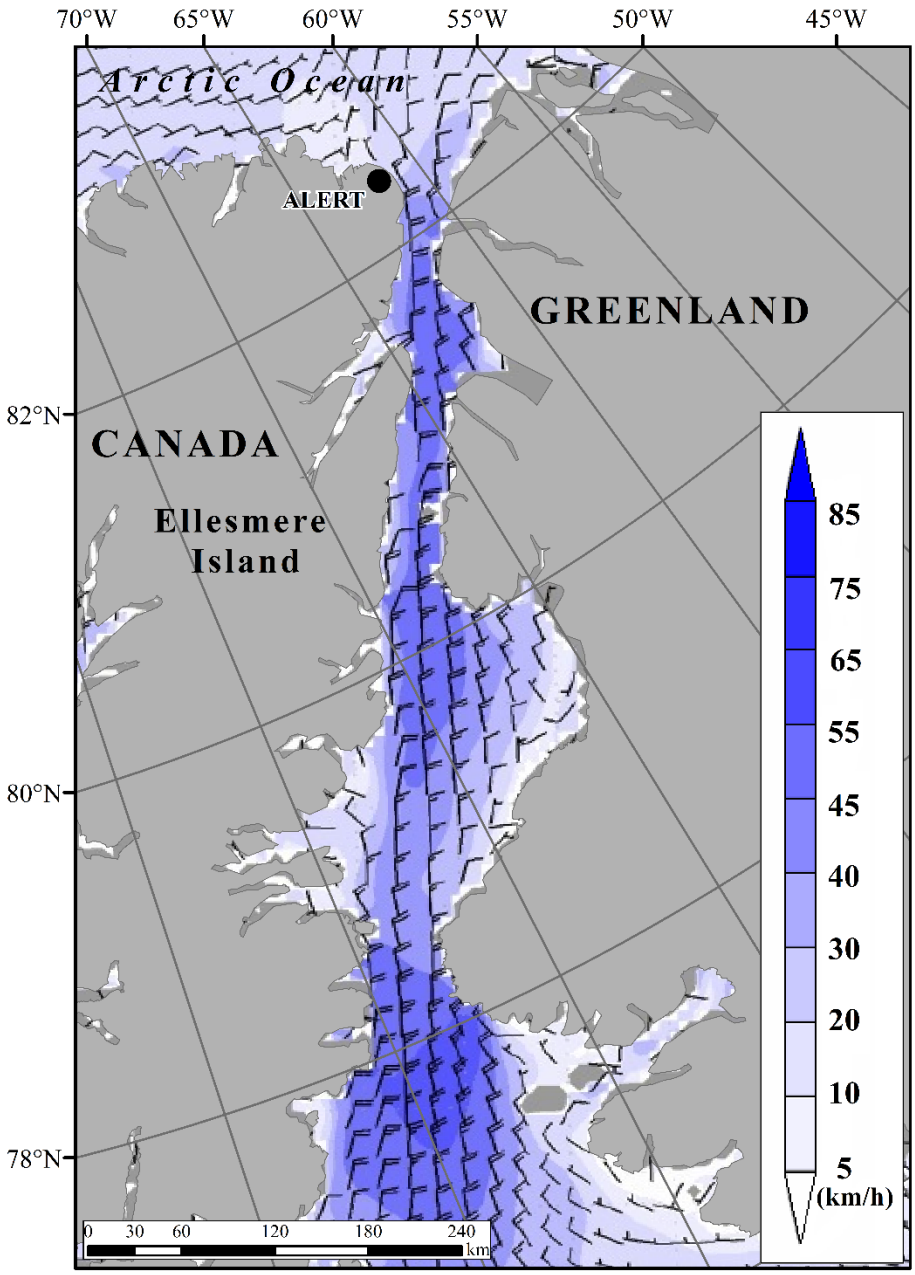

Figure 3.3: Modelled 10 m wind field for April 3, 2009 at 00:00 UTC indicating strong southward atmospheric flow through Nares Strait (Adapted from Decker, 2010)

3.2 Data

Data used for this project come from a variety of. These data have been collected from pre-existing sources, quality checked and combined. Table 3.1 summarizes the data used for this study.

Table 3.1: Summary of data used for study, data type and source.

Data Set	Data Type	Source	Comments
Buoy Data	Data output from drifting buoys - GPS location	International Arctic Buoy Program[†], Dr. Christian Haas	**Limited Data One buoy trajectory per year for years: 2009, 2010, 2011, 2014
Meteorological Data	Data output from weather stations - Wind Speed (km/h) - Wind Direction	3 Weather stations: Alert (Environment Canada[§]) Hans Island (SAMS[*]) Littleton Island (SAMS[**])	Daily averages calculated from hourly data
Sea Ice Charts	Weekly Regional Ice Charts - Eastern Arctic	CIS Data Archives[‡]	Used GIS to get weekly results

[†]www.iabp.apl.washington.edu
[‡]www.ec.gc.ca/glaces-ice
[§]www.climate.weather.gc.ca/climate_data
*www.dalriada.sams.ac.uk/aws_hans
**www.dalriada.sams.ac.uk/aws_littleton

3.2.1 Buoy Data

Buoy information for Nares Strait is limited in comparison to other regions of the Arctic Basin. Buoy data for the study area has been collected since 2005 by Dr. Christian Haas. Table 3.2 summarizes data points used for analysis of sea ice drift. Figure 3.4 is a map of the buoy trajectories from the data used for this thesis.

Table 3.2: Summary of buoys analyzed in this thesis. Data from four buoys, which passes through Nares Strait during four different years (2009, 2010, 2011, 2014) were analyzed. Buoys are listed with buoy type, start and end dates of their passage through Nares Strait and the number of data points (GPS positions) recorded by the buoys within Nares Strait.

Buoy ID	Year	Starting Latitude	Starting Longitude	Ending Latitude	Ending Longitude	Buoy Type	Start Date	End Date	Days in the Strait	Number of Points
1	2009	82.416	-60.646	77.148	-75.646	iSVP	09/01	10/20	49	390
2	2010	82.312	-58.950	77.110	-75.152	iSVP	08/27	09/17	21	165
3	2011	82.411	-60.438	77.010	-76.821	iSVP	10/14	12/09	56	1805
4	2014	82.261	-58.02	77.507	-76.201	iSVP	10/07	11/17	41	989

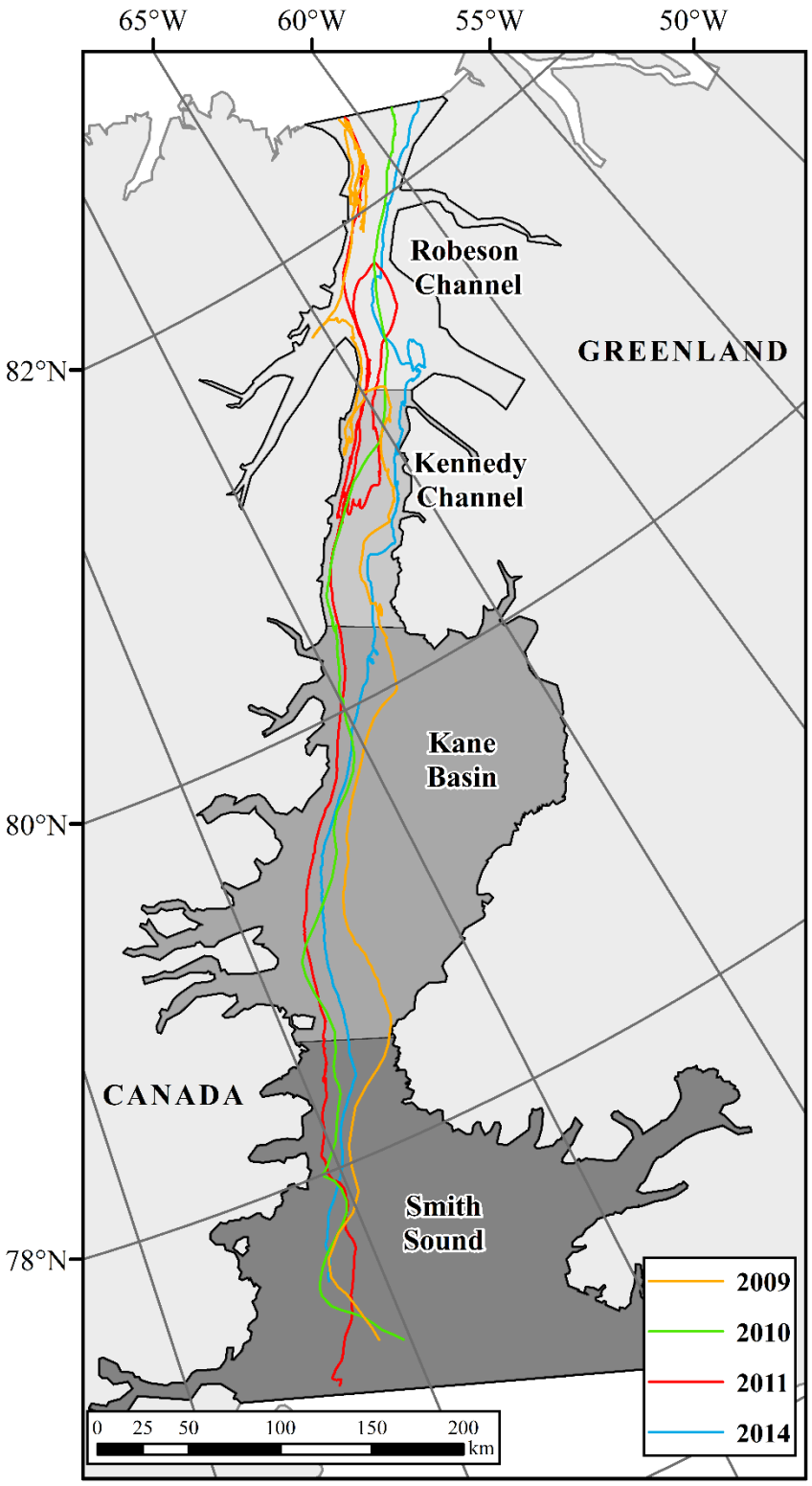

Figure 3.4: Map showing the trajectories of the four buoys used for this thesis. Trajectories are from 2009 (gold), 2010 (green), 2011 (red) and 2014 (blue). Buoy data courtesy of C. Haas (York University).

3.2.2 Meteorological Data

Nares Strait has not been monitored and studied as intensively as other regions of the Arctic. Due to the remoteness and extreme weather of the region, data acquisition remains difficult. Fortunately, there are three automatic weather stations located along the strait. The stations utilized for this study are located at Alert, Hans Island and Littleton Island. The locations of these stations are shown in Figure 3.5. The weather station at Alert is operated by Environment Canada, and data were retrieved from Environment Canada's Historical Climate Data Archive (www.climate.weather.gc.ca/climate_data). The weather stations at Hans Island and Littleton Island were operated by the Scottish Association for Marine Science (SAMS). Operation of these two stations was terminated in 2016.

Wind speed and direction data are most relevant for this study and were obtained from these three weather stations. While these stations also recorded air temperature data, it is not necessary to discuss temperature as a controlling variable for ice drift as it is redundant with ice concentration in this instance. Wind speed and direction data are important to correlate with sea ice drift speed to determine the significance of wind stress on the momentum balance of sea ice in Nares Strait.

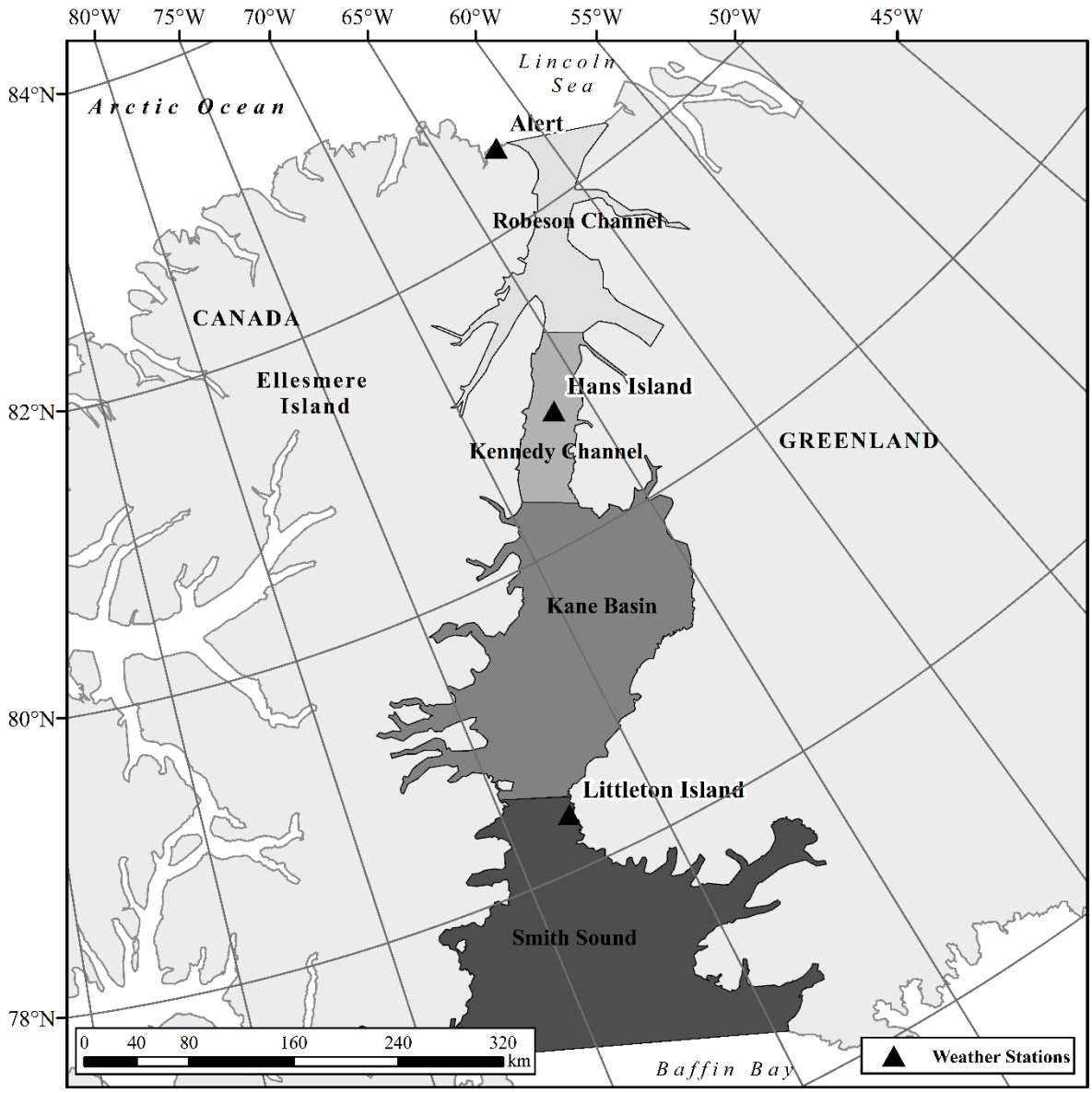

Figure 3.5: Map showing the location of weather stations from which meteorological data (wind speed and direction) has been obtained. From north to south: Alert (Environment Canada), Hans Island (SAMS) and Littleton Island (SAMS).

Data from each weather station are applied to the relevant and appropriate region of the strait determined by vicinity. Table 3.3 shows which weather station is applied to which region of Nares Strait. It is important to note the use of data from both Hans Island and Littleton Island weather stations for Kane Basin. The distance between the two weather station locations was

divided in half where Kane Basin included areas covered by both stations. Using latitude and longitude (GPS positions from the buoys) weather station observations were applied to the corresponding buoy observation using the corresponding datetime.

Table 3.3: Weather station data used for each sub-region of Nares Strait based on vicinity.

Region (North to South)	Weather Station Used
Robeson Channel	Alert
Kennedy Channel	Hans Island
Kane Basin	Hans Island/Littleton Island
Smith Sound	Littleton Island

3.2.3 Sea Ice Concentration Data

Sea ice concentration data are obtained from weekly regional ice charts from the CIS. Regional ice charts show the analysis of ice conditions for a region and are produced weekly. There are two variations of the charts: total ice concertation and stage of development. For this study, total ice concentration charts were used. CIS Ice Analysts derive ice charts from satellite imagery, weather and oceanographic information as well as visual observations from Ice Service Specialists operating in the field from ships and aircrafts (Environment and Climate Change Canada, 2016). As these products are only issued once a week, on Mondays, daily total mean ice concentration for the three days preceding and following ice chart issuance are assumed to be equal to the total ice concentration reported on that week's Regional ice chart.

3.3 Methodology

The analysis of data for this study consists of the collection and the combination of data of the study period, and to present and correlate the data in a meaningful way to address the research

questions of this thesis. There are three main components of this study's methodology: 1) the analysis of sea ice drifting buoys, 2) the examination of meteorological characteristics, specifically wind speed and direction, and 3) the analysis of sea ice concentration within Nares Strait. Calculations were done using Wavemetric Inc.'s IGOR Pro data analysis software (see Appendix B). Microsoft Excel was used for data organization. Recorded and provided data was at variable time intervals. Daily averages were calculated to standardize each of the datasets and to account for missing hourly data points. The daily averages of all three components (buoy drift data, wind speed and direction, and ice concentration) underwent correlation analysis to determine the strength of the relationships that exist between sea ice drift in Nares Strait and these physical forcings, which contribute to the momentum balance of sea ice.

3.3.1 Buoy Analysis

The fundamental aspect of this project is an analysis of the drift trajectories recorded by a series of drifting buoys through Nares Strait. The analysis of drifting buoy trajectories provides a measure of displacement (ice motion) from point A to point B. Equation 3.1 calculates displacement,

$$d = \sqrt{\Delta x^2 + \Delta y^2} \qquad \text{Eqn. 3.1}$$

where d is the displacement (or distance), Δx is the change in northing (m) and Δy is the change in easting (m). Figure 3.6 shows the concept of measuring displacement between ice floe locations.

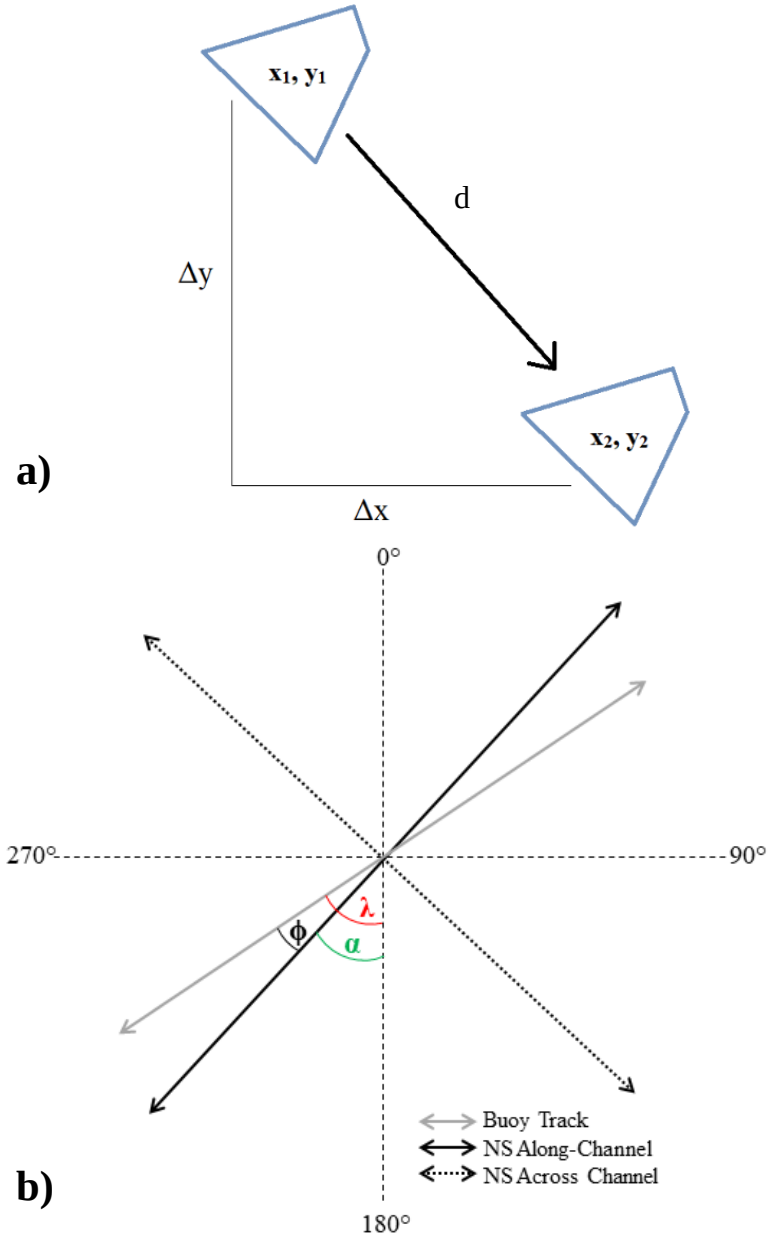

Figure 3.6: a) Illustration of the concept of measuring displacement between ice floe positions. b) conceptual diagram of identifying λ, α, and ϕ (Eqns 3.3 to 3.5b) relative to the bearing of Nares Strait.

Given a known displacement and time between two observed buoy positions, drift speed (D_s) can be calculated. Equation 3.2 is used to calculate D_s,

$$D_s = \frac{d}{t} \qquad \text{Eqn. 3.2}$$

The analysis of the buoy ice drift data consists of four main processes: 1) To collect and consolidate ice drift data from drifting buoys that have a trajectory through Nares Strait. This step includes extracting the components from the buoy output that is relevant to this work, i.e. date/time, latitude and longitude. 2) To calculate displacement between buoy GPS positions (Eqn. 3.1) and the corresponding speed of ice drift (Eqn. 3.2). 3) To determine the direction of ice drift, relative to true north (λ) and relative to the along channel bearing of Nares Strait (ϕ), and to determine buoy displacement in the along and across channel directions. When displacement is calculated, a distance vector is obtained. Equation 3.3 is used to determine the direction of ice drift relative to true north (λ),

$$\lambda = atan2(\frac{\Delta northing}{\Delta easting}) \qquad \text{Eqn. 3.3}$$

where *Δnorthing* is the change in latitude, taken from the buoy GPS positions and *Δeasting* is the change in longitude. Equation 3.4 is used to find the direction of ice drift relative to the along channel bearing of Nares Strait (ϕ),

$$\phi = \lambda - \alpha \qquad \text{Eqn. 3.4}$$

where α is the along channel bearing of Nares Strait (41.81º). Equation 3.5a and b are then used to calculate the along channel (northing) displacement and across channel (easting) displacement respectively,

$$easting = d \cdot \cos(\phi) \qquad \text{Eqn. 3.5a}$$

$$northing = d \cdot \sin(\phi) \qquad \text{Eqn. 3.5b}$$

These are used to calculate along channel and across channel ice drift speeds using Equation 3.2. 4) Finally, daily averages of drift speeds are calculated for each buoy and are correlated with daily average wind speeds, and total mean sea ice concentration values for each of the four sub-regions within Nares Strait. This analysis is conducted separately for each year. Flow charts illustrating the data pre-processing and analysis steps for each data set considered in this study are provided in Appendix C. IGOR scripts used to carry out the calculations described above are provided in Appendix B. Appendix C.1 shows the buoy analysis.

3.3.2 Meteorological Analysis

As mentioned, meteorological data are scarce for this region. Weather data are limited due to the remoteness of the region and the small number of automated weather stations operating in or near Nares Strait. Like the buoy analysis, much of this portion of the analysis involves cleaning the dataset, to check for instrumentation errors, and to consolidate the data from various stations into one standardized format. To clean the dataset, gaps in observations are identified and filled in according to previous and subsequent observations. The time interval between observations vary between years of data collected as well as between the weather stations.

Daily maximum, minimum and mean wind speeds were calculated for each station. Wind direction is recorded by the weather stations as an azimuth and a daily average azimuth is calculated as well. Additionally, wind speed, like drift speed, can be deconstructed into along and across channel directional components. Along channel and across channel wind speeds are calculated to be correlated with the corresponding along and across channel drift speeds – for a more detailed correlation analysis. Equation 3.6 is used to find wind direction relative to the along channel downwind bearing of Nares Strait (ϕ),

$$\phi = W_d - \alpha \qquad \text{Eqn. 3.6}$$

where α is the bearing of Nares Strait (221.81º) – converted to the downwind direction (41.81º + 180º) – and W_d is the wind direction. Equation 3.7a and b are used to find the along channel and across channel wind speeds respectively,

$$W_{SAL} = s \cdot \cos(\phi) \qquad \text{Eqn. 3.7a}$$

$$W_{SAC} = s \cdot \sin(\phi) \qquad \text{Eqn. 3.7b}$$

where s is the wind speed (km/h).

As the time intervals between buoy readings and the automated weather station observations are not consistent, daily averages are appropriate for correlating the weather data with sea ice drift speed. Appendix C.2 illustrate the data analysis procedure used to generate wind speed and direction data. The IGOR code used to calculate wind speed and direction data is provided in Appendix B.3.

3.3.3 Analysis of Sea Ice Charts

Mean total ice concentrations are obtained from weekly regional ice charts issued by the CIS. The ice concentration data provided in the weekly charts are considered to be valid for ± 3 days from the charts date of issue. As ice concentration varies throughout the strait, the geographical sub-regions of Nares Strait identified for this study (Figure 3.2), are used to extract ice concentration for a given time and location based on the buoy point and date. Ice concentration values are known from the egg code embedded in the ice charts. This spatial analysis is completed

using ArcGIS (ESRI, 2017). Appendix C.3 illustrate the workflow of obtaining and populating daily total mean ice concentrations.

As the weekly regional ice charts are obtained in ArcInfo interchange files, they must first be imported into ArcGIS and converted to a shapefile so that they can be manipulated and the attribute information, such as the total sea ice concentration reported in the egg codes, can be extracted. Using the shapefiles created for the geographic sub-regions for Nares Strait, the ice charts are clipped to the study area, as the regional ice charts cover the entire Eastern Canadian Arctic (which comprises the eastern half of the CAA and Baffin Bay). A series of calculations within the table in ArcGIS are used to calculate a final mean sea ice concertation. Before each step of calculations can be conducted, polygons classified as fast ice, land and ice shelves are removed as to not include in ice concentration values. 1) Total area of the basin is calculated by Equation 3.8,

$$A_T = \sum_{j=1}^{n} A_{pj} \qquad \text{Eqn. 3.8}$$

where A_p is the area of each polygon (calculated using the field calculator in ArcGIS). A_T is used at a later stage of the calculations. 2) Equation 3.9 calculates the ice area of each egg code polygon,

$$A_{i\_p} = C_i A_p \qquad \text{Eqn. 3.9}$$

where C_i is the ice concentration. 3) Next, total ice area is found using Equation 3.10,

$$A_{Ti} = \sum_{j=1}^{n} A_{i\_pj} \qquad \text{Eqn. 3.10}$$

4) Finally, total mean ice concentration of the sub-region is found using A_{Ti} and A_T in Equation 3.11.

$$\overline{C_i} = \frac{A_{Ti}}{A_T} \qquad \text{Eqn. 3.11}$$

3.3.4 Correlation Analysis

The final step in this work is to correlate the results of each of the three data sets. To measure the strength of the relationship between the variables of interest, Pearson Correlation Coefficients (*r)* are used. Equation 3.12 is used to calculate *r*,

$$r = \frac{\sum_{i=1}^{n}(x_i - \overline{x})(y_i - \overline{y})}{\sqrt{[\sqrt{[\sum_{i=1}^{n}(y_i - \overline{y})^2]}}} \quad \text{Eqn. 3.12}$$

where n is the sample size, x_i and y_i are the individual sample points (x is the independent variable – i.e. wind speed, or ice concentration – and y is the dependent variable – i.e. ice drift speed). indexed with i and $\overline{x}$ is the sample mean. Daily means calculated for each variable from the preceding analysis are used as input to the correlation analysis. In this work, correlations are considered strong if $|r| \geq 0.7$. Microsoft excel was used for the Pearson Correlation Coefficient analysis and all regression plots can be found in Appendix D.

Chapter 4
Results

4.0 Introduction

This chapter consists of five sections. Section 4.1 illustrates the direction of sea ice drift direction for each of the yearly buoy trajectories. Drift direction maps and rose diagrams are presented as evidence. Drift roses are shown for each of the four sub-regions. Section 4.2 describes the calculated sea ice drift speeds, which are categorized by year and by sub-region. Section 4.3 shows corresponding wind speed and direction data, again categorized by year and sub-region. Section 4.4 describes the calculated mean sea ice concentration data, categorized by year and sub-region. Finally, Section 4.5 presents the results from the regression analyses of sea ice drift speed with wind speed and mean sea ice concentration.

The results of this work show a wide range of variability both spatially and temporally. The factors leading to the variability of sea ice drift and drift forcings within the sea ice regime of Nares Strait will be discussed in Chapter 5.

4.1 Drift Direction

The direction of sea ice drift is derived from the changes of geographic positions of the drift buoy along the trajectory (Section 3.3.1). Figures 4.1 to 4.4 show drift speed and direction for the four sub-regions over the years of 2009, 2010, 2011 and 2014. There is a strong agreement across the four study years that sea ice drift is primarily oriented in an along-channel direction, drifting from Robeson Channel in the north, southward to Smith Sound. It is important to note, however, that there are variations in the direction at times, as seen in the drift rose diagrams, as well as in the time series of each year and sub-region. One example in 2011 can be observed in

Figure 4.3. The change in direction happens on a small spatial scale (10-45 km distance) and over a short period of time (10 days) compared to the entire trajectory through Nares Strait. These instances can be attributed to a change in wind direction, forcing from ocean stress, changes in ice concentration or internal ice stress. Of all the aspects to this thesis work, the component of direction of sea ice drift shows the least variability.

Seasonal or interannual variability is not clear when examining the direction of drift alone. However, a small amount of spatial variability is apparent when comparing the four sub-regions. Smith Sound shows the most variability with no one direction profoundly dominant. Smith Sound, as defined in this thesis, is a less constricted area of water and sea ice is generally less consolidated here and is available to move more freely. Changes in sea ice drift direction are more likely in Smith Sound than in the rest of the strait.

2009

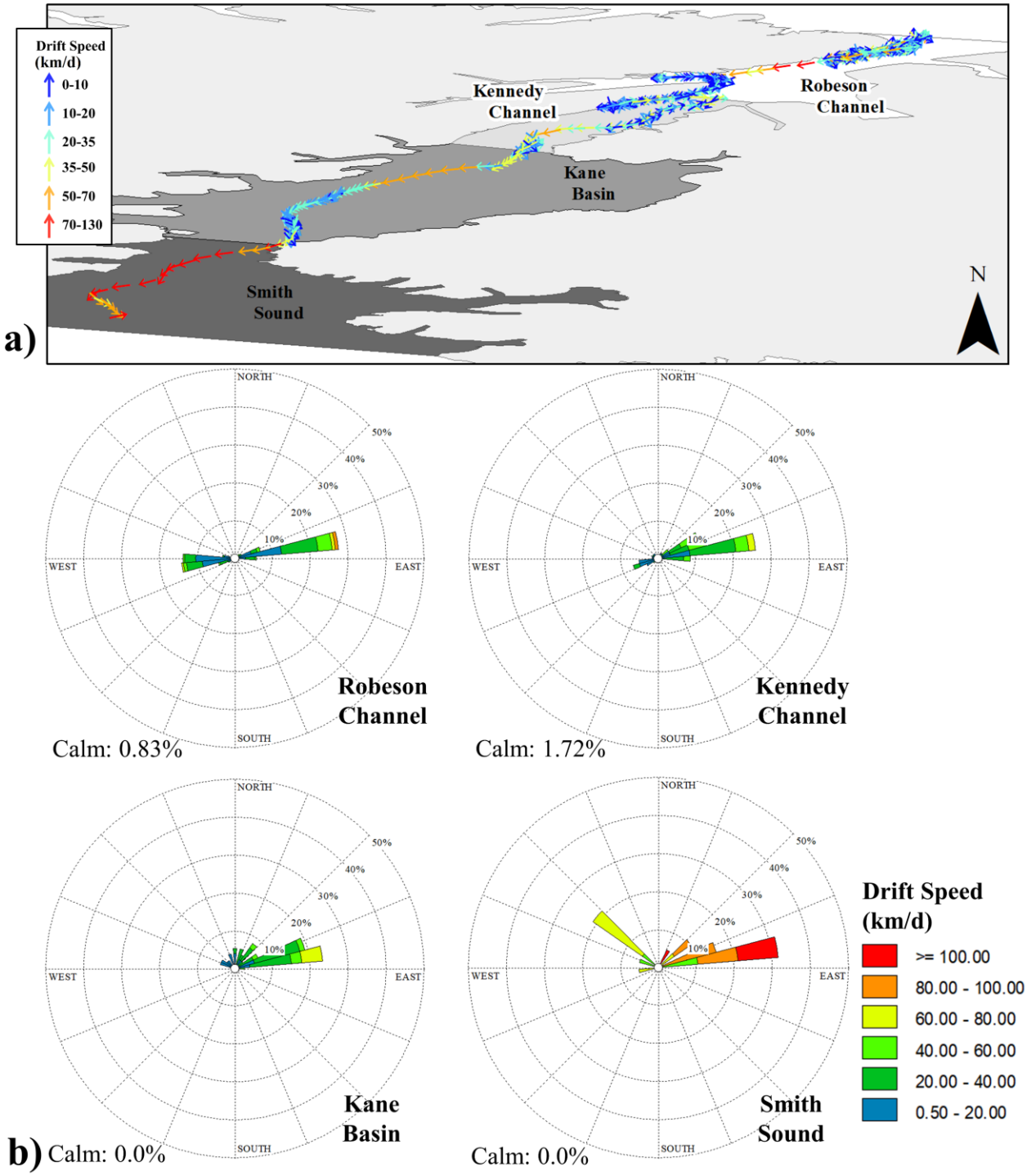

Figure 4.1: Sea ice drift direction for year 2009. a) Map of the overall drift trajectory through Nares Strait, by speed (colours) and direction (arrow direction). b) Rose diagrams of drift direction for each of the four sub-regions of Nares Strait. NOTE: these are true bearings and not relative to the along-channel bearing of Nares Strait (41.8°).

2010

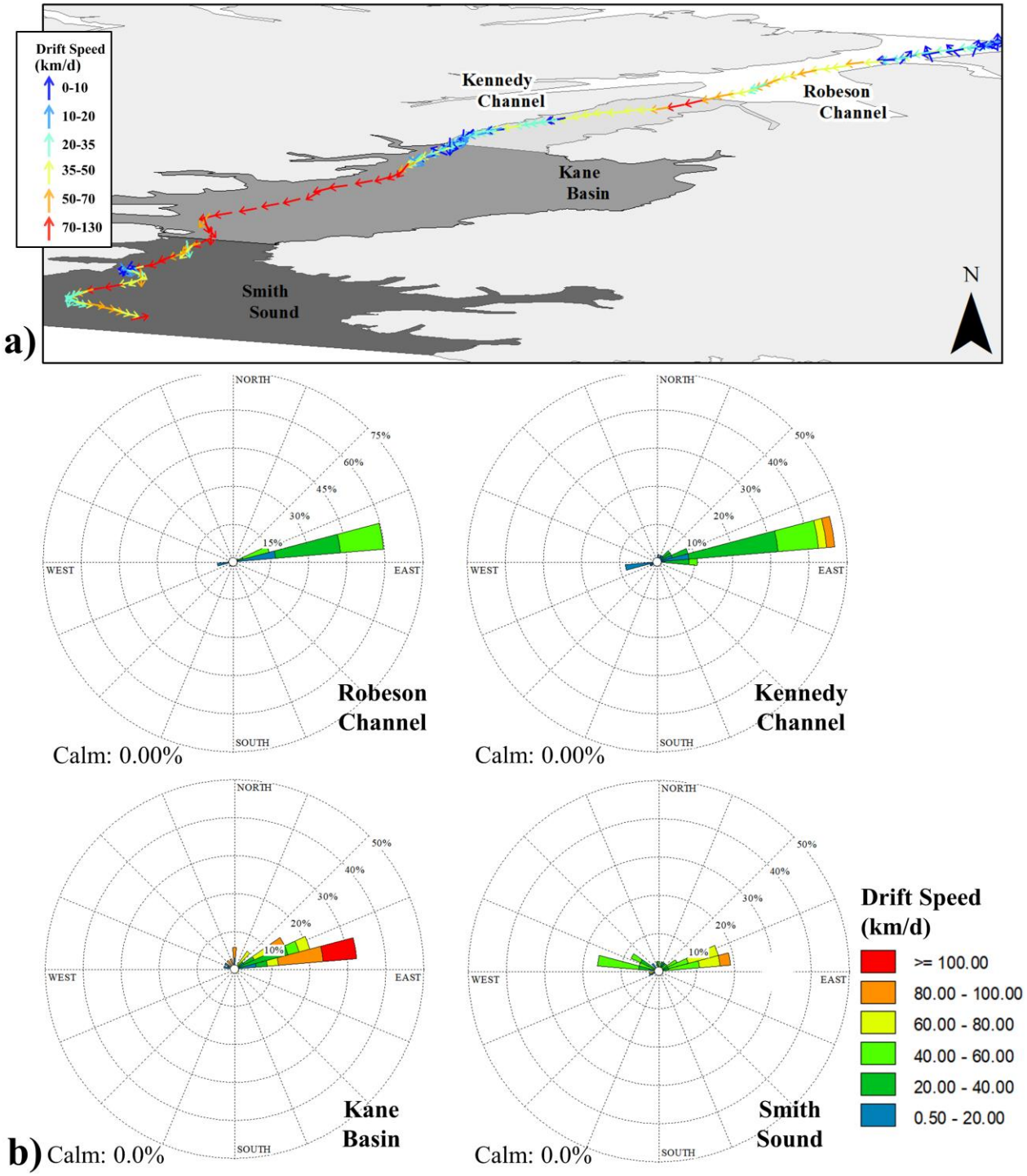

Figure 4.2: Sea ice drift direction for year 2010. a) Map of the overall drift trajectory through Nares Strait, by speed (colours) and direction (arrow direction). b) Rose diagrams of drift direction for each of the four sub-regions of Nares Strait. NOTE: these are true bearings and not relative to the along-channel bearing of Nares Strait (41.8°).

2011

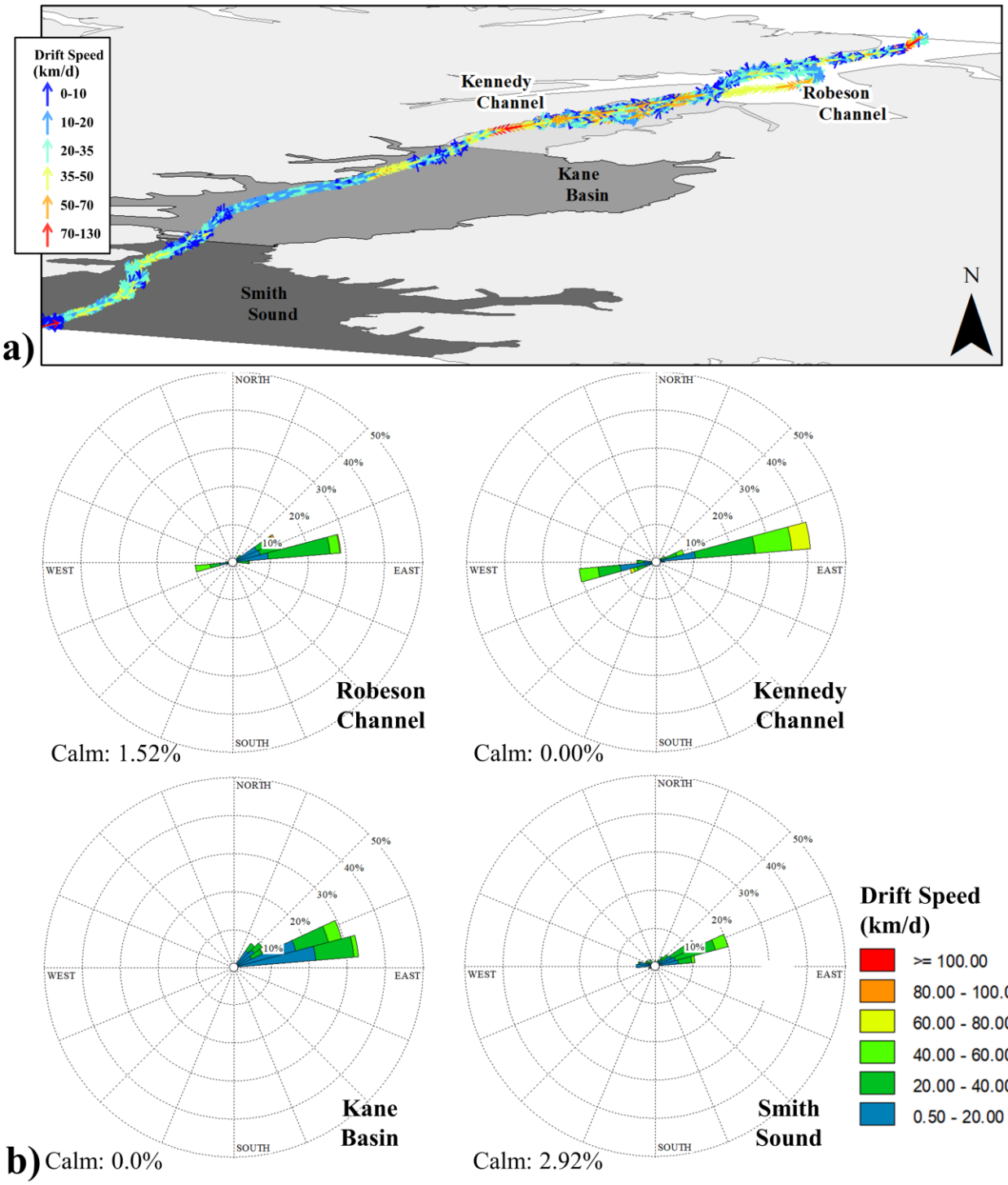

Figure 4.3: Sea ice drift direction for year 2011. a) Map of the overall drift trajectory through Nares Strait, by speed (colours) and direction (arrow direction). b) Rose diagrams of drift direction for each of the four sub-regions of Nares Strait. NOTE: these are true bearings and not relative to the along-channel bearing of Nares Strait (41.8°).

2014

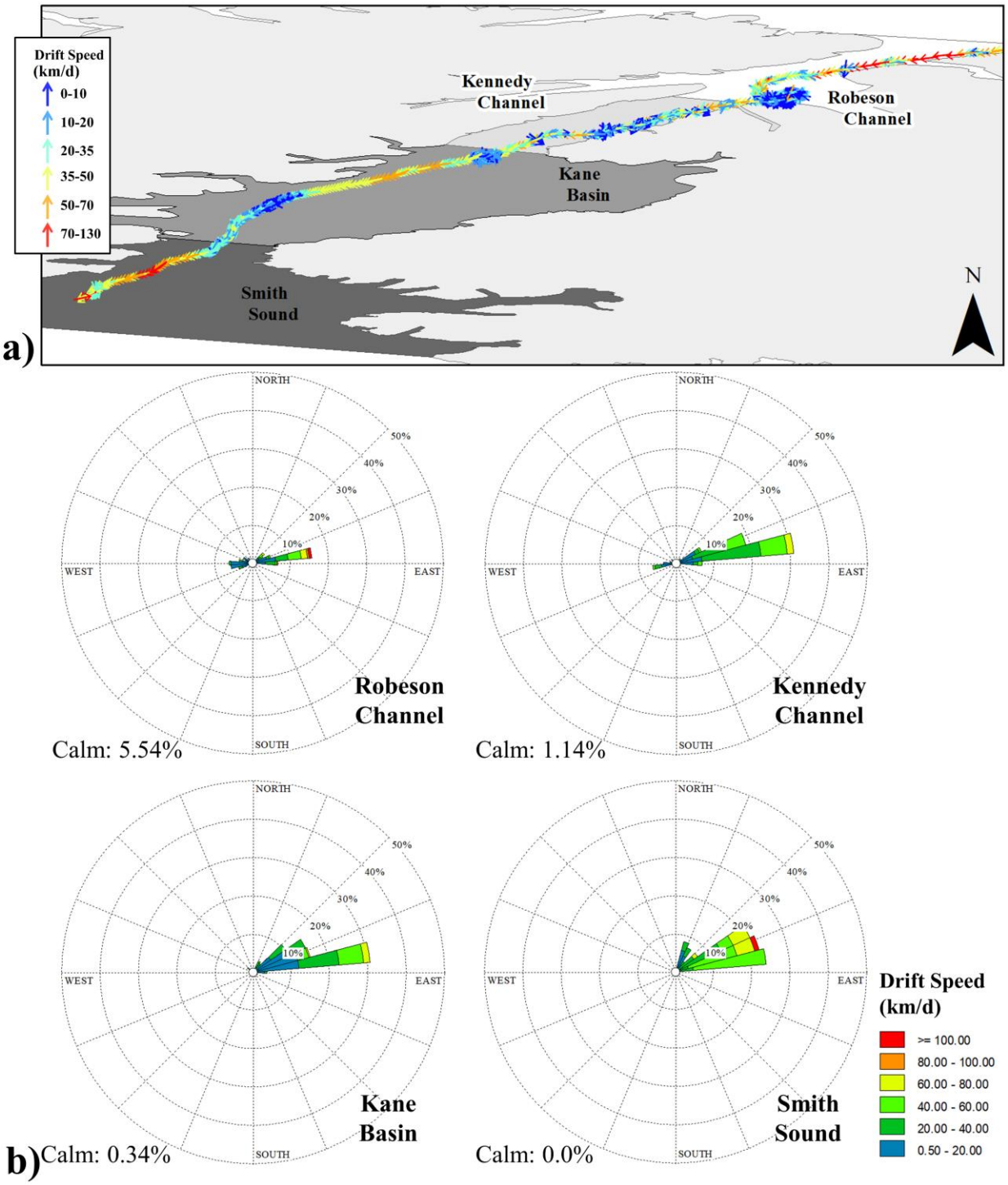

Figure 4.4: Sea ice drift direction for year 2014. a) Map of the overall drift trajectory through Nares Strait, by speed (colours) and direction (arrow direction). b) Rose diagrams of drift direction for each of the four sub-regions of Nares Strait. NOTE: these are true bearings and not relative to the along-channel bearing of Nares Strait (41.8°).

4.1.1 Turning Angles

As mention in Section 2.2.2, sea ice drift direction does have an influence from the wind direction. Sea ice direction is deflected to the right of the wind direction in the northern hemisphere (Haas, 2017). Table 4.1 shows an estimate of the turning angle of the sea ice drift direction by year and by sub-region. It is important to note that for Hans Island weather station, for the purpose of this analysis, angles were flipped to be applied to the north-east quadrant (to line up with the bearing of Nares Strait). This is assuming that the instrument may not have been calibrated properly as it is not likely the wind direction was from the northwest (Christian Haas, personal communication, November 14, 2017).

Table 4.1: Estimated turning angles (in degrees) of sea ice drift direction by year and by sub-region. The final column shows the seasonal means (2009 + 2010 and 2011 + 2014).

Year	Robeson Channel	Kennedy Channel	Kane Basin	Smith Sound	μ	
2009	49	60	59	60	57	58°
2010	45	57	63	64	58	
2011	48	64	59	53	56	51°
2014	50	57	40	33	45	

Mattson (2016) found that turning angles vary seasonally, with summer months exhibit a higher turning angle to the right (0 to 40°) than in winter months (0 to 20°). Through model simulations, Mattson (2016) also found that turning angles are higher within the CAA. Buoy tracks presented in this thesis exhibited even higher turning angles than those observed by Mattson (2016); however, late summer (58°) does shows higher mean turning angle than during the early winter season (51°)

4.2 Drift Speed

The mean daily drift speeds of sea ice (km/d) was calculated annually for each of the four buoy trajectories that pass-through Nares Strait (Section 3.3.1). Mean daily drift speeds for 2009, 2010, 2011 and 2014 were 24 km/d, 36 km/d, 20 km/d and 19 km/d, respectively (Figure 4.5). It is important to note that the 2009 and 2010 buoys drifted through Nares Strait between the months of August and October (i.e. during late summer and early fall, when ice concentration is lower) and the buoys in 2011 and 2014 passed through Nares Strait in the later months of the year (October to December, i.e. during the freeze-up period when ice concentration is higher). This explains some of the variability between the first two study years and the last two study years (Figure 4.5).

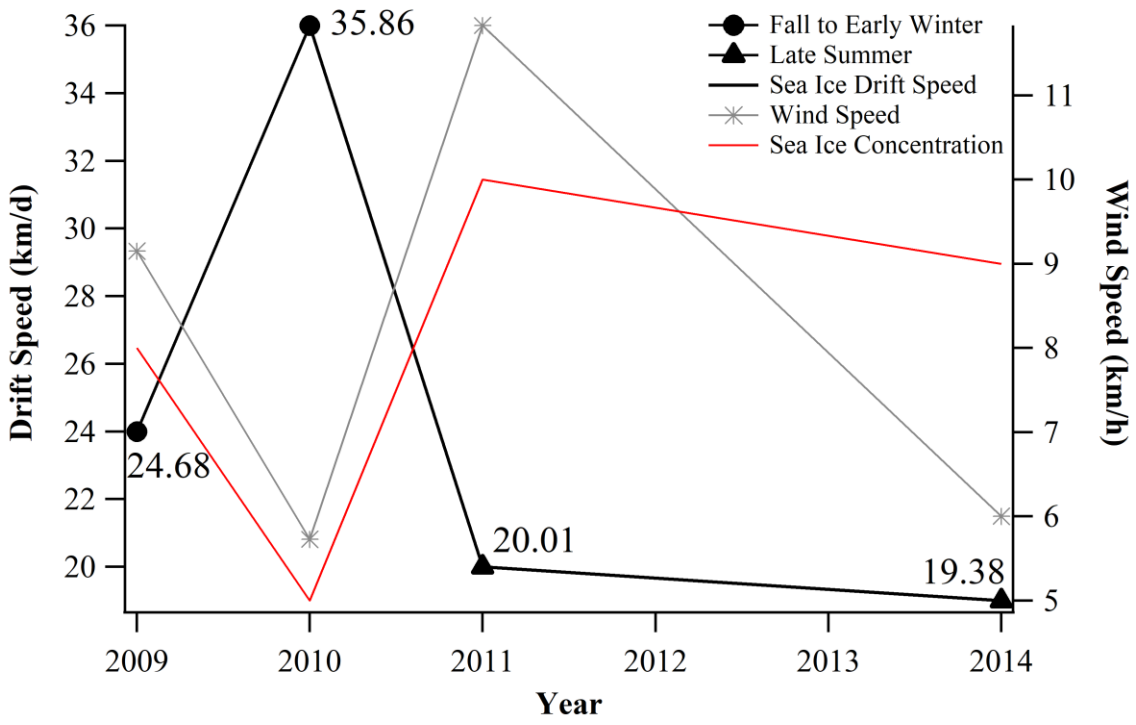

Figure 4.5: Mean daily drift speeds for Nares Strait. Speed is shown in kilometers per day.

Figure 4.6 shows the time series profiles of sea ice drift speed in each study year. The profiles are coloured to indicate the sub-region within which the buoy was located at each observation. The switch from black to red in plot c is attributed to the buoy track looping through the Robeson Channel and Kennedy Channel sub-regions – the buoy was initially moving southward and made a direction change for a period moving northward but eventually continued on the southbound trajectory.

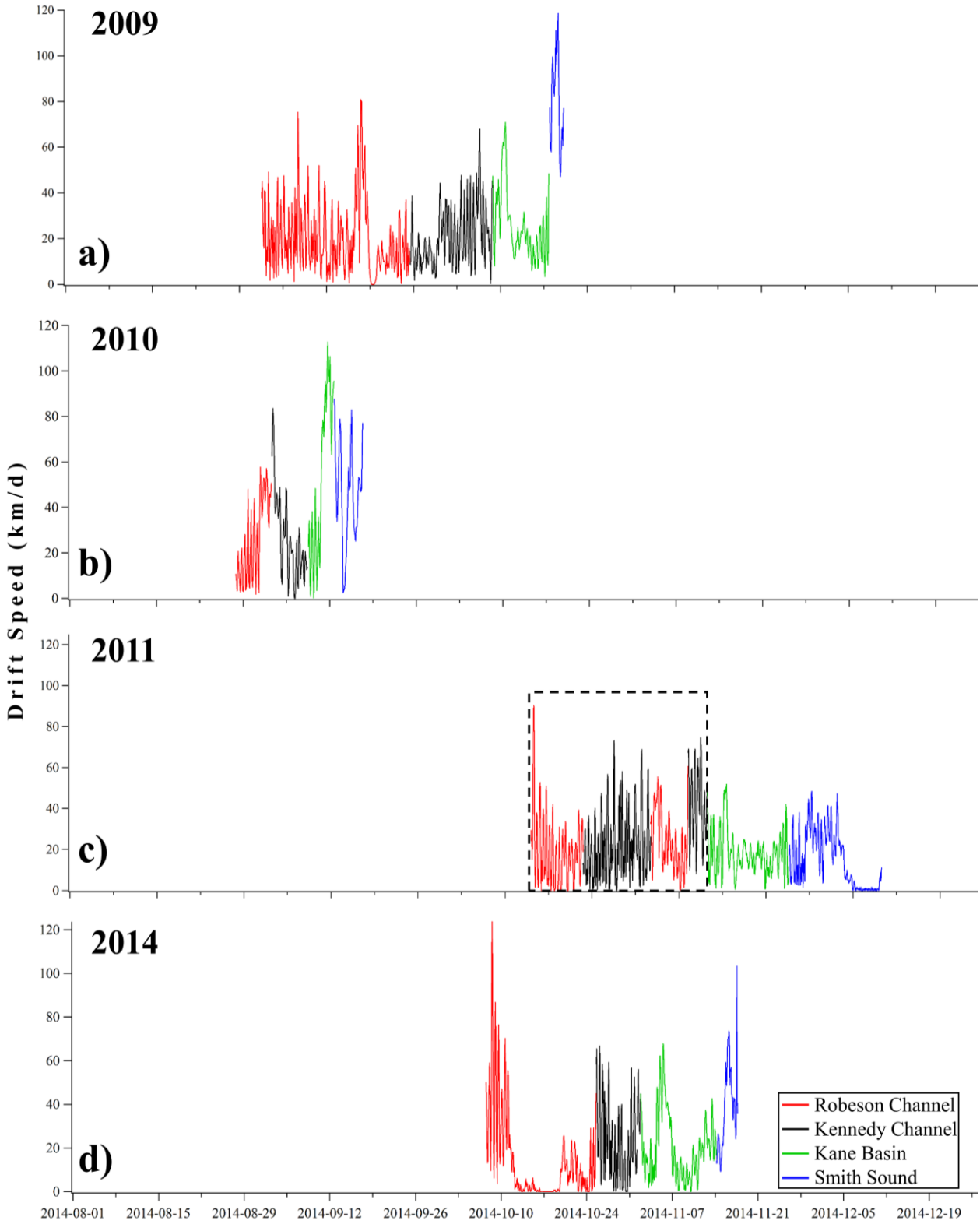

Figure 4.6: Drift speed profiles for each study year. The profiles are coloured based on the sub-region within which the buoy was located for each observation. The dashed box in (c) identifies a loop in the buoy trajectory, which intersected Robeson and Kennedy Channels.

Table 4.2 and Figure 4.7 present the annual mean of sea ice daily drift speeds by sub-region and year. Histograms of mean daily drift speeds for each sub-region and year, which illustrate the variability of ice drift, are shown in Figures 4.8 to 4.11. Generally, the wider parts of the channel (Kane Basin and Smith Sound) show faster drift speeds (30-40 km/d, relative to 10-20 km/d for Robeson and Kennedy Channels). However, there are several exceptions to this general trend. Smith Sound is most variable in average drift speeds as can be observed in the Figure 4.7. Smith Sound has the biggest range of average drift speeds over the study period.

Table 4.2: Annual means of daily sea ice drift speed (km/d) for each sub-region and study year. The annual mean and standard deviation for all observations are also shown for each study year.

Year	Robeson Channel		Kennedy Channel		Kane Basin		Smith Sound		Nares Strait	
	μ	σ	μ	σ	μ	σ	μ	σ	μ	σ
2009	19.64	9.52	20.66	8.09	25.86	13.06	80.55	4.27	24.68	17.25
2010	26.17	18.34	22.30	11.63	60.00	33.85	46.38	17.89	35.86	23.96
2011	21.32	8.39	26.60	8.62	17.89	6.07	14.63	11.41	20.01	9.76
2014	13.66	15.32	23.30	9.80	19.70	13.15	38.51	15.52	19.38	15.32
All	20.20	5.16	23.22	2.06	30.86	19.72	45.03	27.24	26.85	8.15

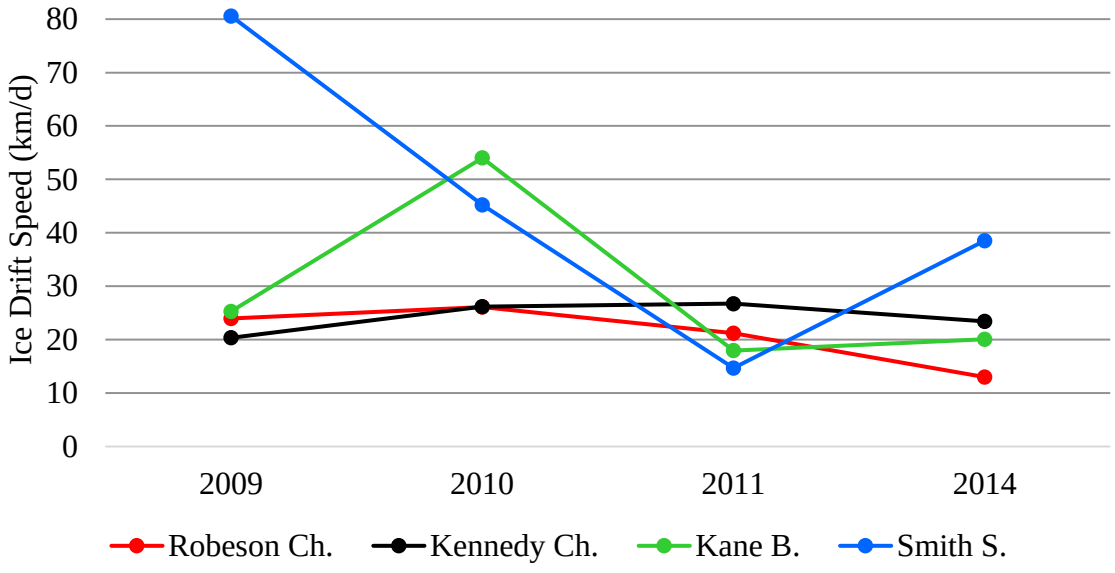

Figure 4.7: Average sea ice drift speeds (km/d) for each sub-region by year.

Another integral piece of information that can be observed from the sea ice drift speed data is the timing of (or absence of) the onset of the landfast ice season, where the ice is fastend to the coast or ocean bottom. Ryan and Munchow (2016) defined the landfast ice season within Nares Strait as a period of 10 or more consecutive days where the daily sea ice drift speed is < 2.16 km/d. this criterion was not met in any of the four study years (Table 4.3). the longest period of slow ice drift was 8 consecutive days in 2014.

Table 4.3: Summary of periods of low daily sea ice drift speed (< 2.16 km/d) and the onset (or lack thereof) of a landfast ice season in Nares Strait in each study year.*

Year	Onset of Landfast Season?	# of Consecutive Days < 2.16 km/d	Dates
2009	No	1	9/19/2009
2010	No	0	N/A
2011	No	4	12/5/2011 – 12/8/2011
2014	No	8	10/12/2014 – 10/19/2014

*Note: a landfast ice season is defined as a period of at least 10 consecutive days in which the daily drift speed of < 2.16 km/d (Ryan and Munchow, 2016).

4.2.1 Robeson Channel

Figure 4.8 presents histograms of the daily sea ice drift speeds within Robeson Channel for the four study years. The histograms are skewed right , with the drift speed being < 30 km/d for most days in which buoys were transiting this sub-region. The year 2014 shows the slowest drift speeds of the four years. The mean daily drift speed for 2014 was only 13.0 km/d, which is the slowest of all the sub-regions and of all the study years.

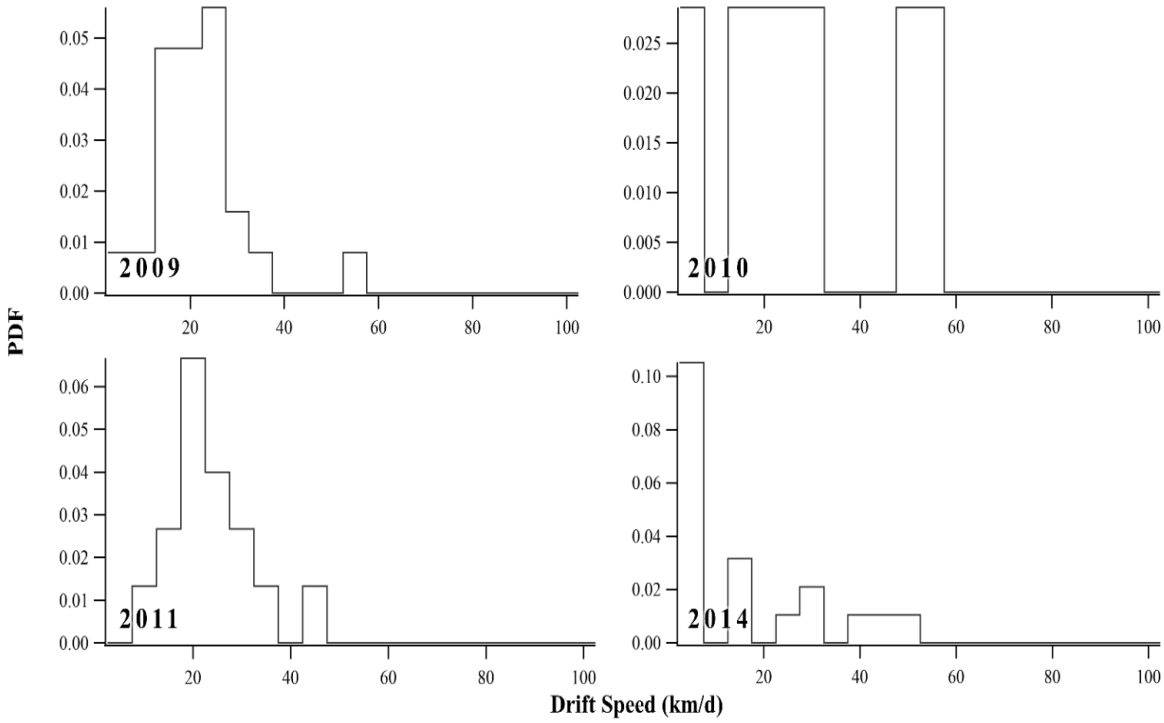

Figure 4.8: Probability Density Functions (PDF) of daily sea ice drift speed in Robeson Channel.

4.2.2 Kennedy Channel

Figure 4.9 shows the distribution of daily sea ice drift speed for Kennedy Channel over 2009, 2010, 2011 and 2014. As was observed in Robeson Channel, the distributions are generally right skewed, except for 2014, which is slightly left skewed; however, annual mean drift speeds in Kennedy Channel are typically fast than in Robeson Channel (Table 4.2). Kennedy Channel is the narrowest of the four sub-regions and exhibits an average drift speed of 20 to 26 km/d over the four study years (Table 4.2).

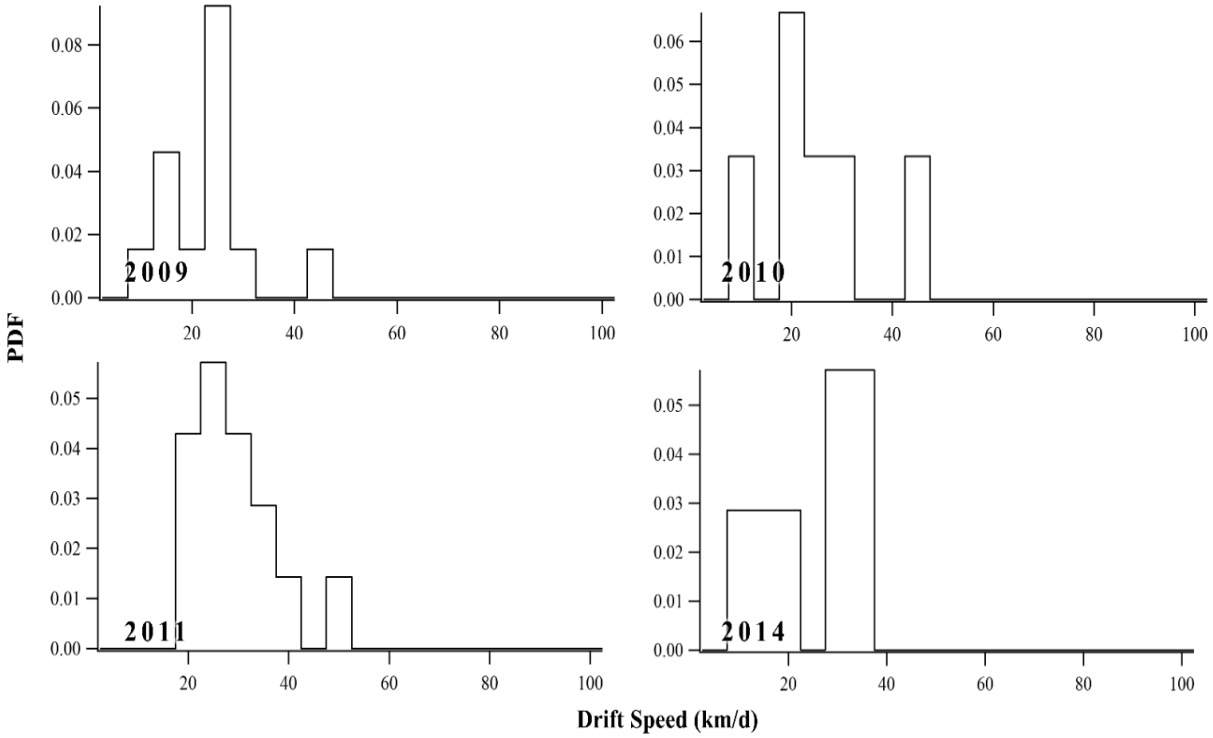

Figure 4.9: Probability Density Functions (PDF) of daily sea ice drift speed in Kennedy Channel.

4.2.3 Kane Basin

Kane Basin is the third, in consecutive order going southward, of the four sub-regions in Nares Strait. Histograms for 2009, 2011 and 2014 are right skewed, whereas 2010 show a multi modal distribution. The range of sea ice drift speed in 2010 in Kane Basin was 0.2 to 113 km/d; drift speeds were most variable in 2010 of the four years. Except for 2010, annual mean sea ice drift speeds in Kane Basin were comparable (~ 20 km/d) to those observed in Robeson and Kennedy Channels (Table 4.2).

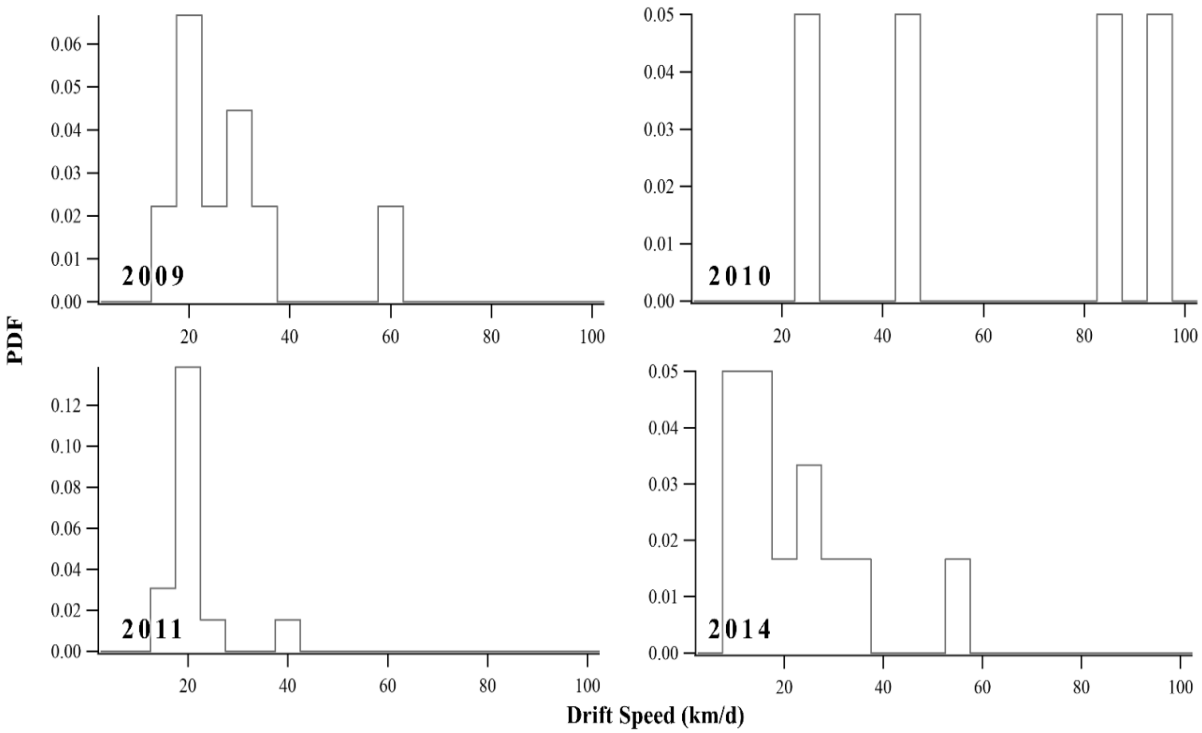

Figure 4.10: Probability Density Functions (PDF) of daily sea ice drift speed in Kane Basin.

4.2.4 Smith Sound

The annual distributions of sea ice drift speed in Smith Sound are highly variable. The distribution of daily sea ice drift speed is right skewed in 2009 and 2011, while 2010 and 2014 are both multi-modal. There is no consistency in sea ice drift speeds over the years. As will be described in Section 4.4, sea ice concentration is generally lowest in Smith Sound. Given the greater potential for sea ice to experience free drift conditions in this sub-region, annual mean daily drift speed are also typically high within this sub-region, being 81 km/d, 45 km/d, 15 km/d and 39 km/d for 2009, 2010, 2011 and 2014 respectively (Table 4.2).

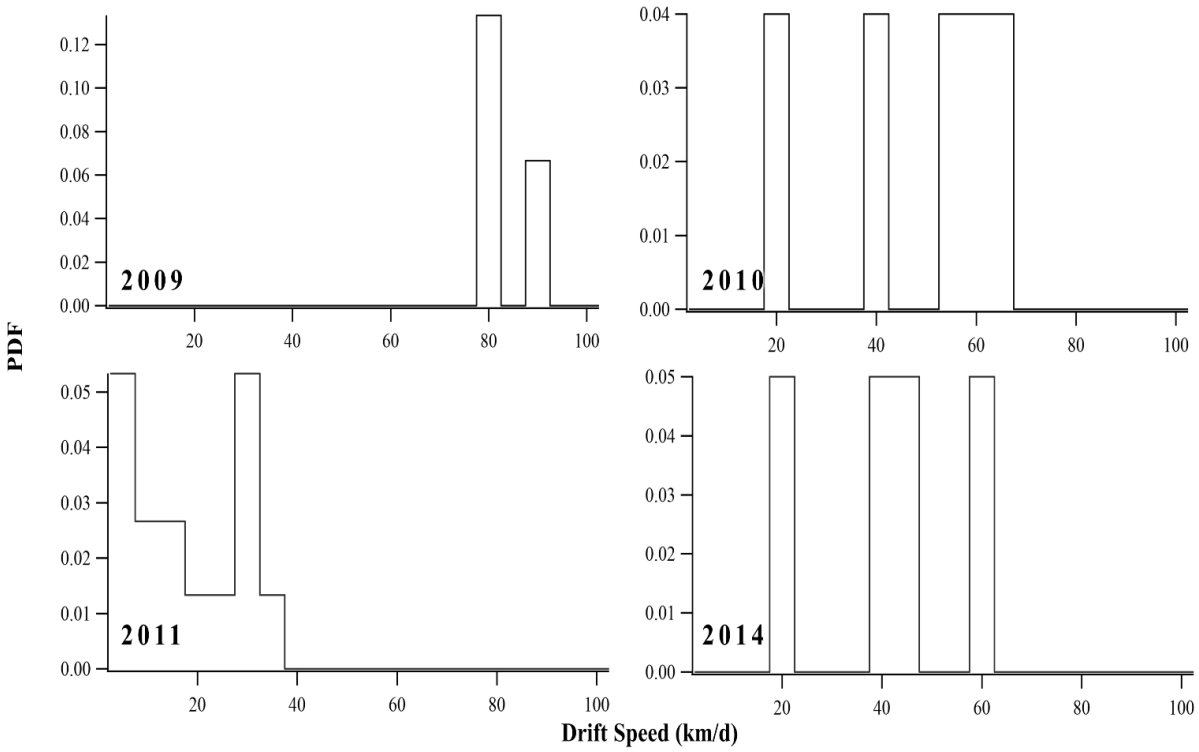

Figure 4.11: Probability Density Functions (PDF) of daily sea ice drift speed in Smith Sound.

4.3 Wind Speed and Direction

Mean daily wind speeds for each sub-region are described in Table 4.4. There is no distinction in stronger or weaker wind speeds between seasons, but, Generally, wind speeds are highest in Robeson Channel and lowest in Smith Sound. On average, 2011 exhibits the strongest wind speeds, while 2010 exhibits the weakest wind speeds. 2011 had one of the slowest drift speeds, 20.01 km/d over the entire strait and 2010 shows the highest drift speeds with an average of 35.86 km/d over the entire strait. This shows opposite observations with wind speed.

Table 4.4: Annual mean daily wind speed (km/h) for each sub-region and study year.

Year	Robeson Channel		Kennedy Channel		Kane Basin		Smith Sound		Nares Strait	
	μ	σ	μ	σ	μ	σ	μ	σ	μ	σ
2009	13.79	10.85	2.78	1.25	6.61	3.47	5.68	1.45	9.15	9.21
2010	6.19	1.10	8.42	2.48	6.46	2.18	1.27	1.64	5.73	3.19
2011	18.43	12.81	6.98	3.48	12.91	8.11	8.80	4.90	11.83	9.35
2014	6.90	4.01	1.68	1.48	7.02	3.94	6.52	3.26	6.00	4.00
All	11.33	5.06	7.18	2.81	8.25	2.70	5.57	2.73	8.20	2.51

Wind data for this work were obtained from three weather stations through Nares Strait. Alert shows the strongest winds, with very few periods of calm weather (wind speed < 0.5 m/s; Figure 4.12). winds are predominant from the northeast at Alert. Figure 4.13 shows data from Hans Island, located in the middle of the strait. The winds here are weaker and come mostly from the north-northwest. Finally, wind profiles from Littleton Island are shown in Figure 4.14. This station represents the southern end of the strait, where there is less constriction from the coasts of Greenland and Ellesmere Island. The wind rose shows weaker winds here, and prevailing winds come from the northeast. Consensus of the wind roses from all three weather stations, and for all four study years, is that the wind is generally flows along the channel from the northeast to the southwest. There are a few instances where the winds blow from the south, but it is infrequent.

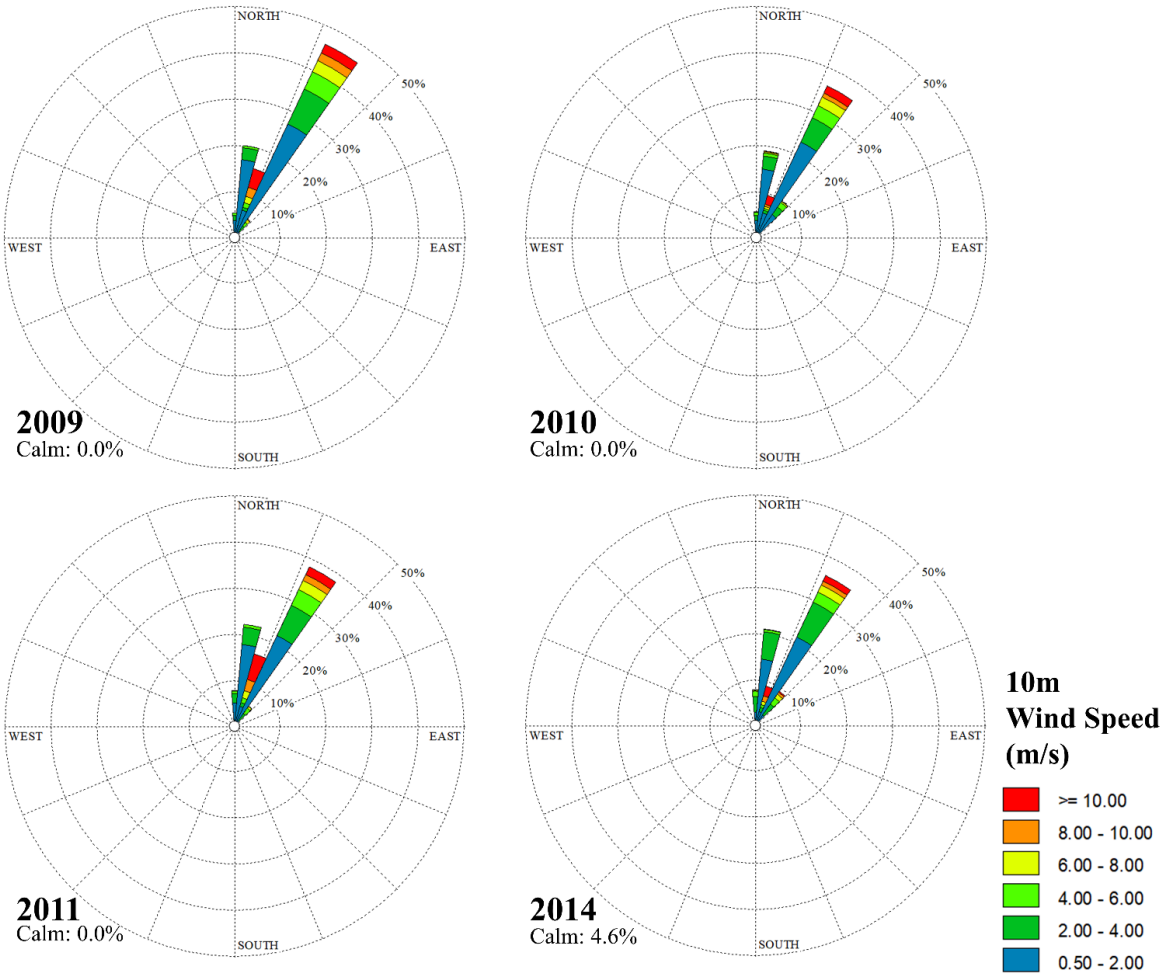

Figure 4.12: Wind speed and direction for Alert (north end of Nares Strait). Wind speeds are highest at this station, with very little calm conditions (wind speed < 0.5 m/s), and winds are predominantly from the northeast. Date obtained from Environment Canada, Historical Data – Alert Climate station.

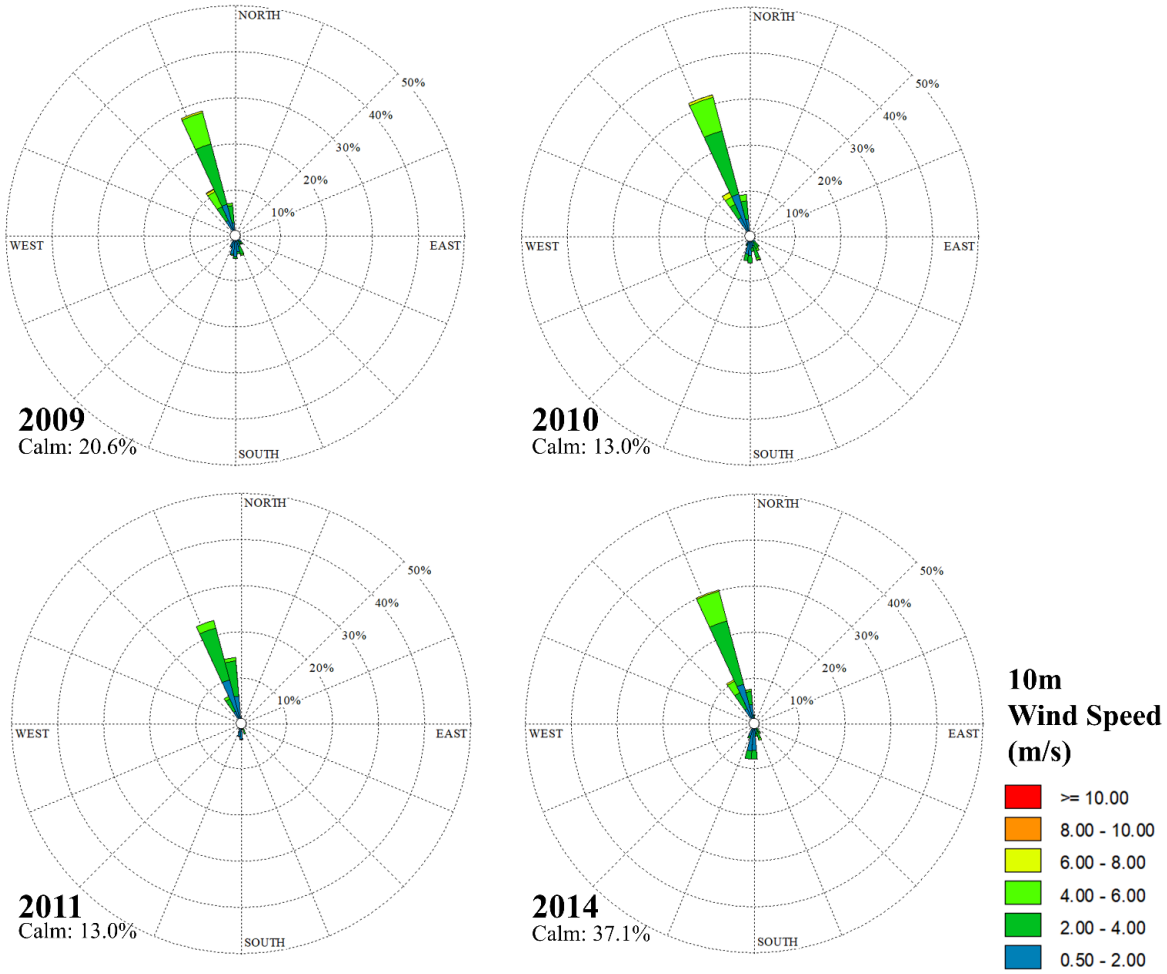

Figure 4.13: Wind speed and direction for Hans Island (mid-channel). Winds are predominantly from the north-northeast, and calm conditions (wind speed < 0.5 m/s) are common. Data obtained from SAMS. NOTE: the wind origin from the northwest is not expected and could be due to several reasons including poor calibration of the instrument.

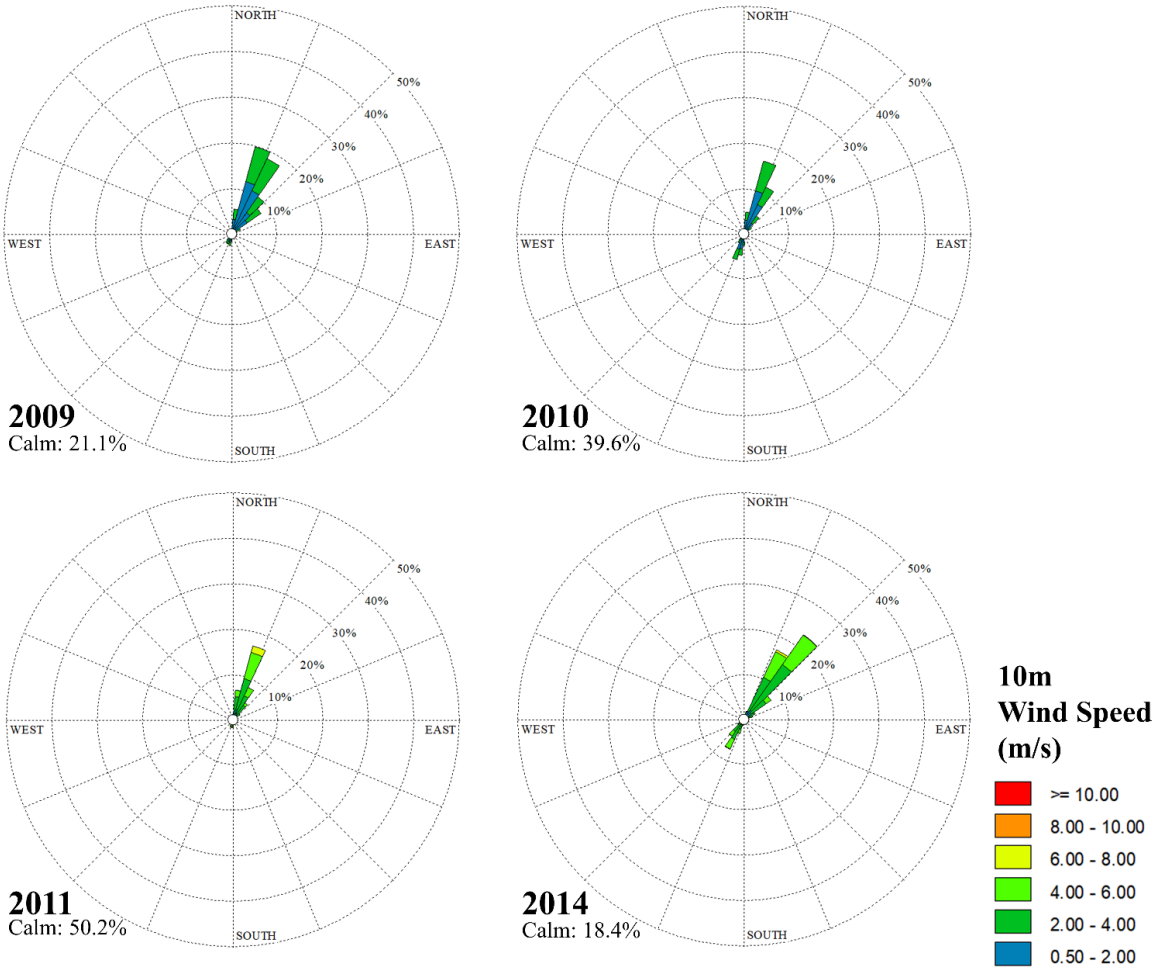

Figure 4.14: Wind speed and direction for Littleton Island (south end of Nares Strait). Winds are predominantly from the northeast, and calm conditions (wind speeds < 0.5 m/s) are common.

4.4 Sea Ice Concentration

Throughout the four study years, the mean sea ice concentration within the strait (reported in tenths) was typically greater than 6/10. This is typical of the High Arctic where, historically, there is a perennial consolidated sea ice pack. Both Robeson and Kennedy Channels have high mean sea ice concentrations in each of the four study years (≥ 7/10; Table 4.5). Robeson and Kennedy Channels are the northern portion of Nares Strait and are the sub-regions that are most constricted by coastal boundaries. Mean sea ice concentrations within Kane Basin and Smith

Sound are more variable over the four study years (Table 4.5). In all study years, the mean sea ice concentration within Smith Sound was equal to or less than the mean sea ice concentration observed in each of the three other sub-regions. Sea ice concentration within Smith Sound was < 6/10 in 2009 and 2010. Therefore, sea ice is expected to have been in a state of free drift within this sub-region in those two years. Figure 4.15 shows the distribution and profiles of mean sea ice concentration, by year, for each sub-region.

Table 4.5: Annual mean sea ice concentration (reported in tenths, 1/10 to 10/10) for each sub-region per year.

Year	Robeson Channel	Kennedy Channel	Kane Basin	Smith Sound	Nares Strait
2009	8	10	9	5	8
2010	7	7	4	2	5
2011	10	10	10	10	10
2014	10	10	10	6	9

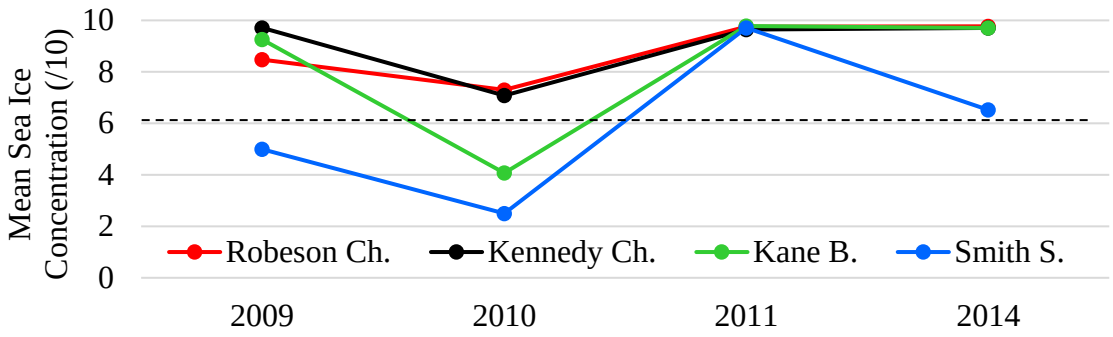

Figure 4.15: Annual mean sea ice concentration (reported in tenths) for each sub-region of Nares Strait by year. The black dashed line indicates the threshold for sea ice in free drift (< 6/10 coverage).

4.5 Regression Analysis

To quantify the relationships between drift speeds and the physical forcings acting upon it, regression analysis was performed. Table 4.6 shows the Pearson correlation coefficient values for drift speed versus wind speed as well as drift speed versus mean sea ice concentration. The colour

coding in Table 4.5 indicates the strength and sign of the correlation coefficients; green shows a positive correlation ($r > 0.7$) whereas red shows a negative correlation ($r < -0.7$). The strength of the correlation is attributed to the depth of the colours – i.e. bright green and red denote strong relationships. Correlation coefficients between buoy drift speed and physical forcings are provided for all of Nares Strait as well as by sub-region. Correlation analyses are also provided for the along-track (AL) and across-track (AC) components of the ice drift vectors derived from the buoy trajectories. Scatter plots of the data series used as inputs for each of the correlation analyses are provided in Appendix D. Select regression plots will be discussed in Chapter 5.

A general expectation of sea ice dynamics is that when W_s is higher, D_s increase, showing a positive correlation. Additionally, when mean sea ice concentration is high, D_s is slower, exhibiting a negative relationship. Looking at Nares Strait as a whole, mean sea ice concentration versus drift speed shows a negative (sometimes weak but still negative) correlation, which is to be expected. Generally, wind speed versus drift speed does show a positive relationship, apart from several instances. Another important piece to note is the change from along-channel dominant drift for 2009 and 2010 (late summer) to along-channel dominant drift for fall to early winter (2011 and 2014). These instances and more will be discussed in Chapter 5.

Table 4.6: Pearson correlation coefficient values for drift speed vs. physical forcings (wind speed and concentration). *"W_s"* is wind speed and "C_i" represents mean total sea ice concentration. "NaN" values denote where sea ice concentration did not change for the duration of the buoy passing through that sub-region. AL refers to along-channel (north-south) sea ice drift speed correlations and AC refers to across-channel (east-west) sea ice drift speed correlations. Colours indicate the magnitude of the correlation coefficients, with green indicating positive r values, and red indicating negative r values. Colour saturation increases with increasing magnitude of *r*.

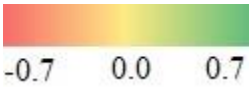

	Robeson Channel		Kennedy Channel		Kane Basin		Smith Sound		ALL	
r value	W_s	C_i	W_s	C_i	W_s	C_i	W_s	C_i	W_s	C_i
2009	0.52	-0.20	-0.13	NaN	0.83	-0.12	-0.17	NaN	0.10	-0.58
2009: AL	0.45	-0.29	-0.09	NaN	0.22	-0.06	-0.70	NaN	0.02	-0.60
2009: AC	0.36	0.07	-0.33	NaN	0.81	-0.25	0.94	NaN	0.29	-0.28
2010	-0.14	NaN	-0.74	NaN	-0.75	0.75	-0.19	0.51	-0.46	-0.51
2010: AL	-0.14	NaN	-0.63	NaN	0.11	0.79	0.05	0.14	-0.21	-0.52
2010: AC	-0.03	NaN	-0.73	NaN	-0.87	0.58	-0.30	0.25	-0.45	-0.35
2011	0.49	-0.62	0.81	NaN	-0.01	-0.36	0.12	NaN	0.21	-0.22
2011: AL	-0.46	-0.54	0.68	NaN	-0.27	-0.25	0.07	NaN	-0.21	-0.15
2011: AC	-0.23	-0.70	0.74	NaN	0.51	-0.60	0.11	NaN	0.35	-0.24
2014	0.06	-0.72	0.22	NaN	0.42	NaN	0.65	NaN	0.10	-0.43
2014: AL	0.07	-0.66	0.28	NaN	0.48	NaN	0.63	NaN	-0.11	-0.48
2014: AC	-0.04	-0.83	0.30	NaN	0.20	NaN	0.39	NaN	0.17	-0.26

Although there are things to be said in general for the entire strait, looking at individual sub-regions and combinations reveal more information about what exactly is going on during the study years. For instance, Figure 4.16 illustrates the correlations between daily sea ice drift speed and daily wind speed for each of the four sub-regions in 2009. The trends change as the buoy moves south along the strait. Robeson Channel shows a generally strong positive correlation between wind speed and drift speed (r = 0.52), whereas Kennedy Channel, shows a weak, negative correlation between these variables (r = -0.13). Contrastingly, when ice reaches Kane Basin, a very strong, positive correlations returns (r = 0.83), and finally, Smith Sound shows a weak negative correlation (r = -0.17).

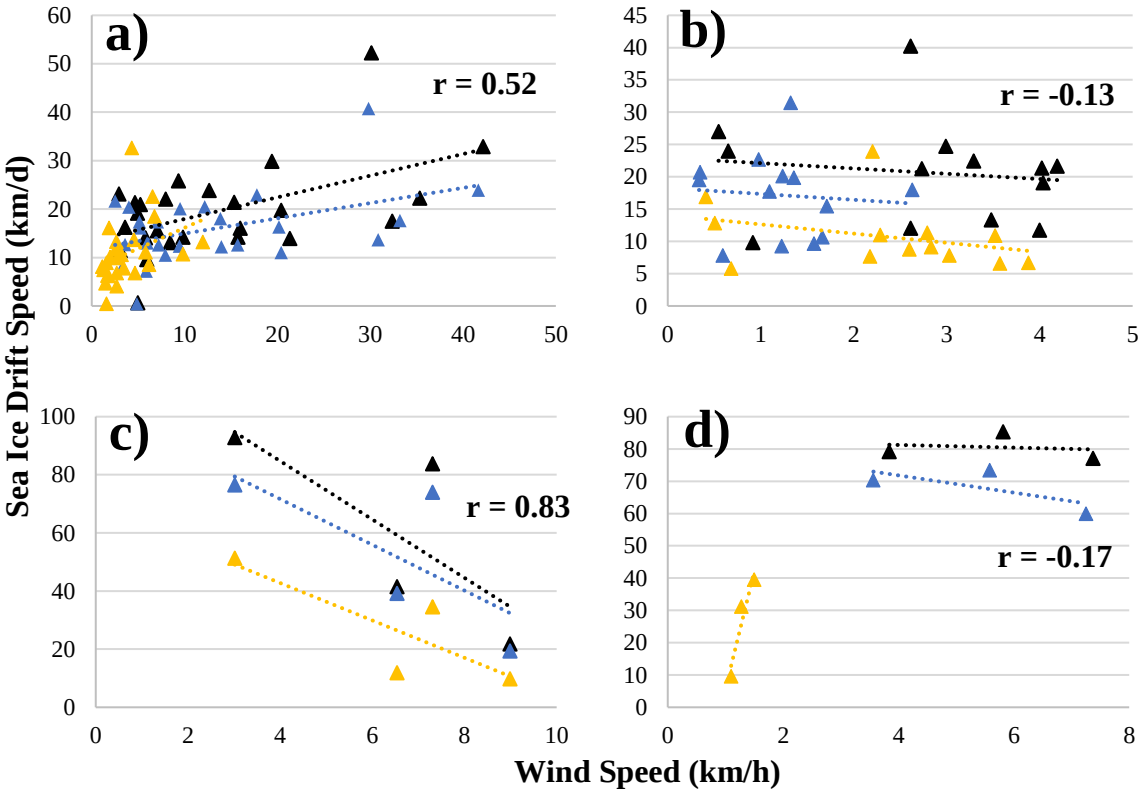

Figure 4.16: Regression plots comparing daily sea ice drift speed to daily wind speed for the four sub-regions of Nares Strait in 2009 where $r = 0.10$ for the whole of Nares Strait. Plots are provided for a) Robeson Channel, b) Kennedy Channel, c) Kane Basin, and d) Smith Sound. Along-channel shown in blue and across-channel shown in yellow. *r* value represents the overall relationship.

Figure 4.17 shows a time series of drift speed versus wind speed overlaid with sea ice concentration. Generally, sea ice drift speed trends to follow the pattern of wind speed over the time period of each buoy trajectory. However, there are exceptions to this general observation. Most notable is at the end of the buoy tracks (the right side of the plots), where the buoys are in Smith Sound, which has more open water. The correlation between wind speed and drift speed is greatly reduced here (see Table 4.6) and drift speed appears to respond strongly to the reduction of sea ice concentration in this southernmost sub-region.

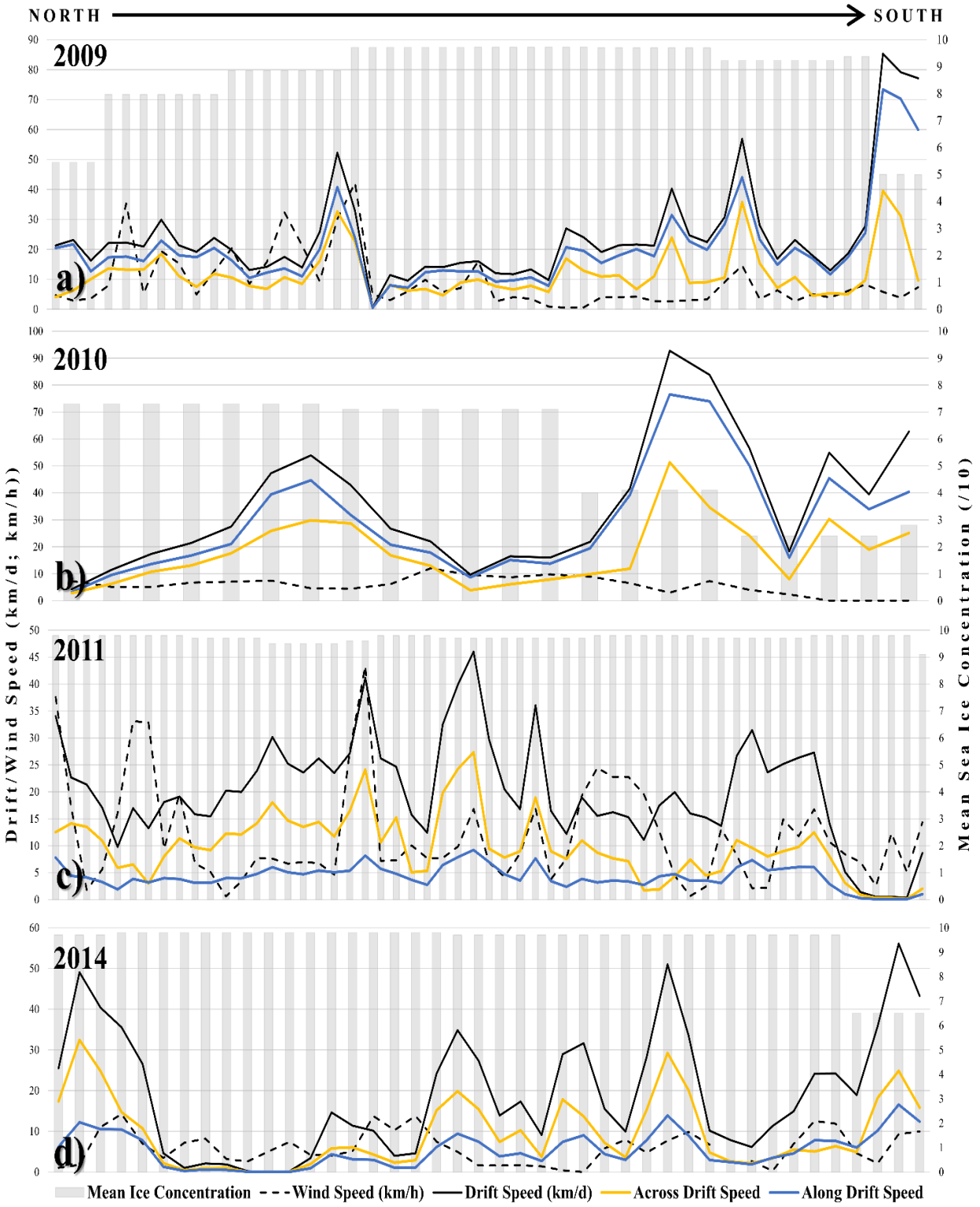

Figure 4.17: Time series of wind speed, sea ice drift and mean sea ice concentration for 2009 (a), 2010 (b), 2011 (c), and 2014 (d). Note the left y-axis values are not consistent between each of the four plots.

Chapter 5
Discussion

5.0 Introduction

In this chapter, the results presented in Chapter 4 are discussed. This discussion includes the findings of the study and what information can be obtained from these findings. A dialogue of how this work fits into the existing literature is also provided. The results of this work have been broken down into a discussion of the various types of variability that exists within the findings – i.e. the spatial, seasonal and interannual variability of the results.

The variability of the study results is discussed in Section 5.1. As mentioned, three different types of variability have been identified. Section 5.1.1 describes the spatial variability that exists between the four sub-regions of Nares Strait. Section 5.1.2 defines the seasonal variability within the study years. Section 5.1.3 discusses the interannual variability between the years within each of the two seasons that exists. Following the discussion about the variability of the study result, the limitations of this study are discussed in Section 5.2. Finally, Section 5.3 provides a summary of this chapter.

5.1 Variability

The main objective of this thesis is to examine the variability of sea ice drift in Nares Strait. The results of this work show a high amount of variability in sea ice dynamics in the strait. Various conclusions can be drawn, depending on which factor of variability is examined. Characteristics of spatial, seasonal and interannual variability can be observed from this work. This section decomposes each factor of variability in an attempt to develop a picture of the sea ice regime of Nares Strait, and to answer the questions and objectives of this study. Plots of each individual

correlation analysis are available in Appendix D and specific, case by case, plots are shown in this section.

5.1.1 Spatial Variability

In this study, Nares Strait is divided into four sub-regions (Figure 3.2). Each of the four sub-regions behave differently, showing different drift speeds as well as different identifiers of forcings on sea ice drift. It is important to note that each of the four sub-regions display different spatial characteristics as well. For example: Robeson Channel is open to the Arctic Ocean via the Lincoln Sea; Kennedy Channel is a narrow, restricted channel bound by relatively straight coast lines; Kane Basin is a restricted channel whose coastline is complex due to the presence of fiords, bays and other topographic features; and Smith Sound is open to Baffin Bay and can arguably be classified as mostly open water.

Sea ice drift analyses were broken down into along-channel and across-channel drift components. The literature suggests that there is dominant along-channel movement within Nares Strait from the north to the south (Samelson and Barbour, 2008), and after examination of the direction of wind and ice flow, there is an agreement with this thesis work, as presented in Figures 4.1 to 4.4 and Figures 4.12 to 4.14. Generally, there is no dominant difference between along and across channel drift speeds found as observed in Table 4.6. The exception to this is for Smith Sound in 2009 for wind speed versus drift speed. There is a strong negative relationship (r = -0.70) for the along-channel component and the opposite for the across-channel drift, which showed a strong positive correlation (r = 0.94) suggesting a significant change in the direction of drift.

Although there are some general remarks that can be made for the entirety of Nares Strait that agree with some expectations (Table 4.6), in comparing sea ice drift speed within the four sub-

regions, differences can be observed. Despite the ice coming from the same origin and relatively the same geographical location, drift speeds change as one moves southward down the channel. Table 4.2 lists the mean sea ice drift speed within each of the four sub-regions. The standard deviations of sea ice drift speed for each sub-region is also given, where Smith Sound exhibits the highest variability overall ($\sigma = 27.29$ km/d).

Additionally, comparing the four sub-regions beside one another, it is apparent that the dominant forcings that affect sea ice drift changes with location. As stated in Section 4.2, the wider sub-regions (Kane Basin and Smith Sound) has faster D_s overall. This is not expected, but when considering mean sea ice concentration (Table 4.5; Figure 4.15), the faster drift speeds make sense as mean sea ice concentration is lower in these sub-regions than in Robeson and Kennedy Channels generally.

Examining Table 4.6, differences between the sub-regions and their respective magnitude of relationships between wind speed and mean sea ice concentration are apparent. Referring to the example drawn for drift in 2009 (Section 4.5), it is possible that, despite sea ice concentrations for this buoy trajectory show lower ice concentrations (than 2011 and 2014), there is a build-up of pack ice on the west side of the channel where the buoy travelled along. For Smith Sound, there are few data points as the buoy did not reside in this sub-region for long (3 days) and a true comparison is difficult to make. Due to the complexity of the strait, there are a number of factors that affect the ice at any given location – which is where examining each sub-region becomes important for this work.

The following sections hone in on each sub-region, examining how ice dynamics vary on a smaller scale within the strait and attempts to identify which is the dominant term of the sea ice momentum balance equation in each sub-region to illustrate the spatial variability of Nares Strait.

5.1.1.1 Robeson Channel

Robeson Channel is the most northern of the four regions. Sea ice stays consolidated longer within this part of Nares Strait before drifting southward to Baffin Bay. This is also the location of an ice arch that typically forms in January (Kwok et al., 2010). When the ice arch does develop, or when the mean sea ice concentration is high, Robeson Channel can have a substantial influence on the rest of the ice dynamics in Nares Strait.

Variability of sea ice drift is lower here with a standard deviation of 5.16 km/d. The relationship between wind speed versus ice drift speed does show a moderately strong positive trend (Table 4.6). Figure 5.1 compares regression plots of sea ice drift speeds versus wind speed and versus mean sea ice concentration within Robeson Channel both for 2009.

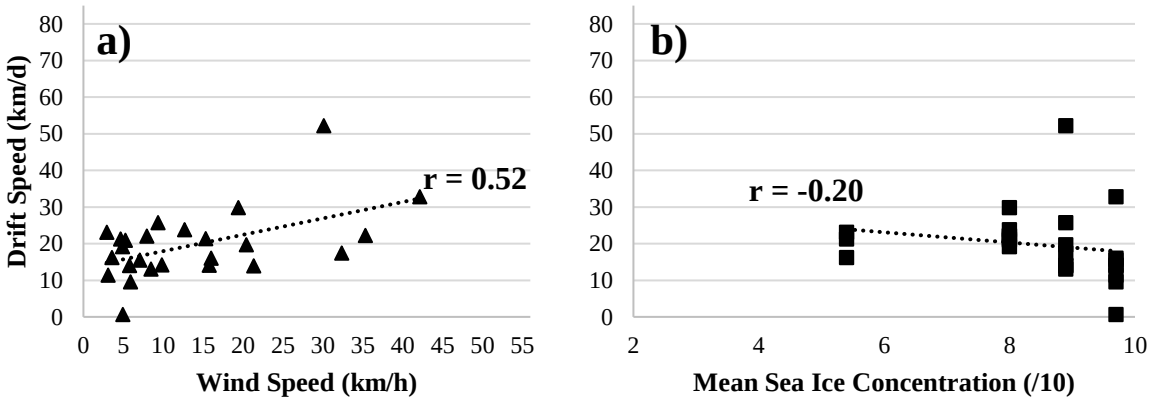

Figure 5.1: Regression plots comparing daily wind and drift speed (a) and daily mean sea ice concentration and drift speed (b) for Robeson Channel in 2009.

Wind speeds observed at Alert weather station show the strongest values, which would suggest higher sea ice drift speeds. Observations from this work show that drift speeds are generally slower (Table 4.2). Conversely, the mean sea ice concentration is high in Robeson Channel, which contributes to the lower overall drift speeds in the sub-region.

Sea ice drift speed demonstrates a weak, but negative correlation to mean sea ice concentration. A negative correlation is expected as increasing mean sea ice concentration is expected to increase the internal ice pressure which acts to reduce sea ice drift speed. The correlation between wind and drift speed is stronger overall for Robeson Channel suggesting that the wind stress term of the momentum balance is most dominant in this sub-region. However, slow sea ice drift speeds (around ~20 km/d or less) are expected here due to the high concentration of sea ice that is observed in this sub-region, even in summer months, which slows down movement and generally prevents the ice floes from experiencing free drift in this sub-region. The wind data correlated with Robeson Channel was observed from Alert weather station (Figure 4.12). Alert is open to the Arctic Ocean with little to no shelter of surrounding topography. Sea ice concentration is higher in this sub-region overall and, although drift speeds into Robeson Channel initially maybe faster due to strong persistent winds at Alert, the higher sea ice concentration does in fact slow down the sea ice drift speed. This could explain the moderately-strong positive relationship between wind speed and drift speed, but account for the observed slower drift speeds (Table 4.2).

An interesting observation from the north portion of Nares Strait (Robeson and Kennedy Channels) is a prolonged drift transit as a result of a large "loop" that occurred in 2011 that lasted ~19 days. Figure 5.2 illustrated the loop of 2011 and as a result the buoy track lasted the longest during this year. As mentioned, it is likely – due to winds and possibly ocean currents – there is a buildup of consolidated sea ice along the west side of Nares Strait. Mean sea ice concentration was high during this time period (10/10 for all sub-regions; Table 4.5) and the magnitude of internal ice stress would have been high. The buoy was transiting fast (~65 to 70 km/d) southbound and it seems to have been caught, perhaps due to a section of deformed ice, and changed direction completely. The change back to southward flow could have been instigated by a bought of strong

winds resulting to the force of the wind being strong enough to push the ice off course in the opposite direction. Further investigation into exact time snapshots (i.e. via remote satellite imagery) would be beneficial in understanding exactly what is driving this instance.

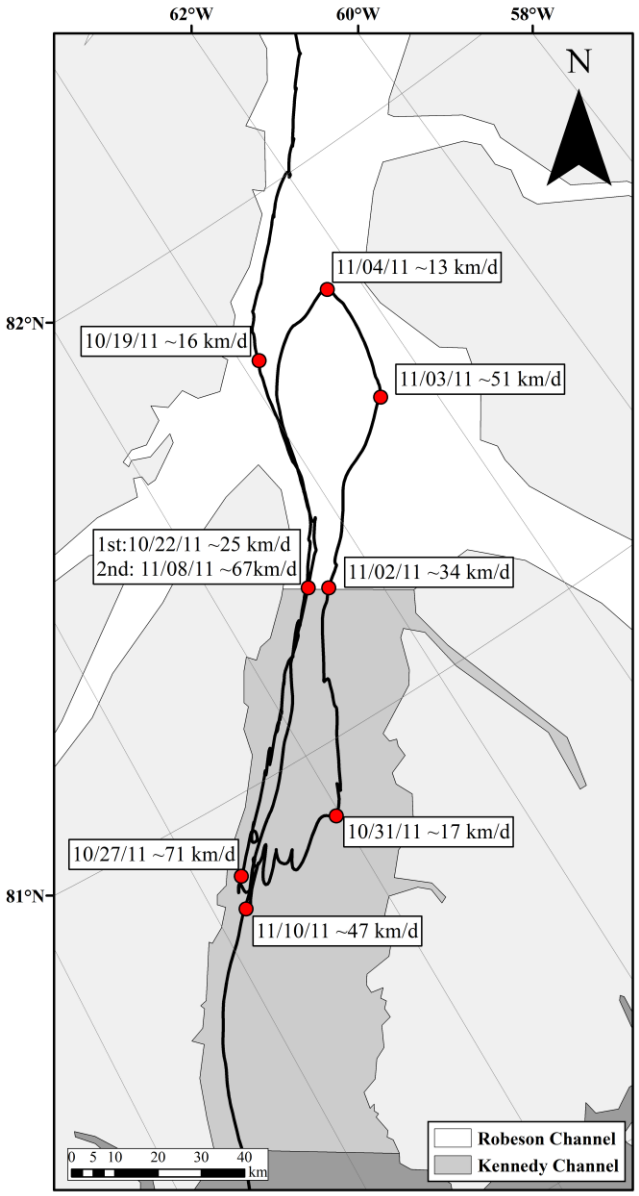

Figure 5.2: 2011 Buoy track through Robeson and Kennedy Channels. The buoy did a loop that lasted about 19 days (~10/19/2011 to 11/10/11).

5.1.1.2 Kennedy Channel

Kennedy Channel is the narrowest of the four sub-regions, and with consistently strait coast lines. As mentioned, Kennedy Channel is only ~ 39 km wide and topography likely has a large influence here. Although this sub-region has similar distribution of ice drift speeds to Robeson Channel, it does exhibit slightly higher speed values – the mode of drift speed is ~35 km/d, suggesting ice drift picks up speed through this part of the strait. Variability of sea ice drift speed is lowest in this sub-region with a standard deviation of 2.51 km/d (Table 4.2), indicating that the sea ice dynamics here are most consistent within the strait. As the channel is bounded by straight coastlines, sea ice is more constricted here with less open space to drift and move, which could account for the slower drift speeds, relative to Kane Basin and Smith Sound.

The correlation coefficients between wind speed and sea ice drift speed in Kennedy Channel show moderate to strong positive values in 2009 and 2010 and the opposite for 2011 and 2014 (moderately strong negative *r* values) (Table 4.6). There is an apparent factor of seasonality in this sub-region. During the late summer (2009 and 2010) it is possible there is a stronger influence of the water stress component of the sea ice momentum balance equation. Figure 5.3 illustrate the change from a strong negative correlation between wind speed and drift speed in 2010 to a positively strong correlation in 2011.

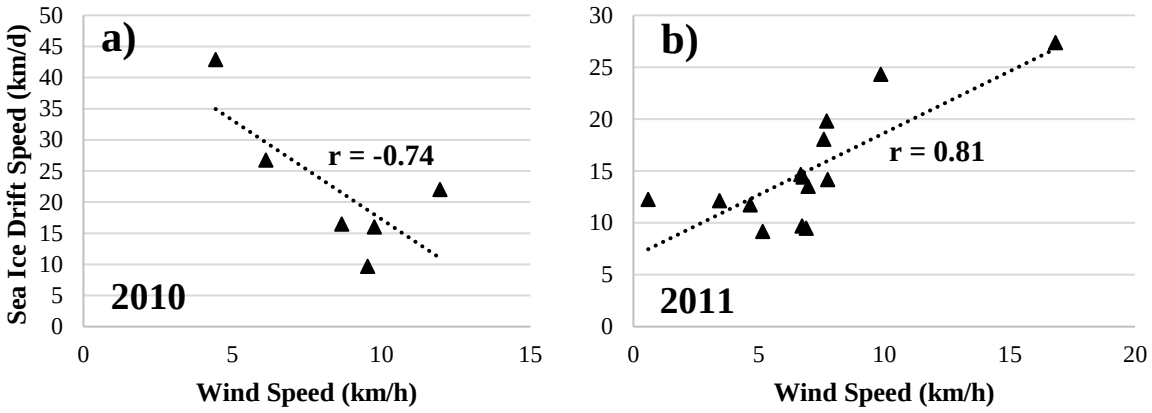

Figure 5.3: Regression plots comparing sea ice drift speed versus wind speed in Kennedy Channel for 2010 (a) and 2011 (b). *r* values are opposite for the same location between year suggesting interannual varaibility in the forcings acting on sea ice drift.

The mean sea ice concentration barely changed for this area (Table 4.5), despite the buoys drifting though this region at different times of the year (late summer in 2009 and 2010, and early winter in 2011 and 2014). Over the study period mean sea ice concentration for Kennedy Channel ranges from 7/10 – 9/10. Sea ice would not have been in free drift at any point throughout this sub-region as free drift is described when sea ice concentration is less than 60%. A meaningful analysis of the influence on mean sea ice concentration on sea ice drift speed could not be performed as the buoy did not stay long enough within Kennedy Channel to detect any changes in ice concentration.

Kennedy Channel is highly constricted by coast, which is indicative of narrowing and stronger ocean currents (NOAA, 2017). Ocean current data are sparse and generally unavailable for Nares Strait. However, there is a small subset of ocean current data available for Kennedy Channel (Section 3.1). It is known that ocean currents are strong (~ 6 km/d) and south flowing on the western side of the channel. There is also a presence of a north flowing ocean current on the east side of Kennedy Channel; however, this current is slower (~ 3.5 km/d) (Munchow and Melling, 2008). This does provide a driver for the loop discussed previously (Section 5.1.1.1;

Figure 5.2). Water stress acts on the bottom surface of an ice floe and ocean currents are not necessarily affected by a consolidated ice cover above (Lapparanta, 2011). Knowing the presence of these two ocean currents (on both the west (south) and east (north) sides of the channel), could begin to provide an understanding for this anomaly.

5.1.1.3 Kane Basin

Kane Basin demonstrates high variability in sea ice drift speeds with a standard deviation of 19.72 km/d (Table 4.2). Nares Strait is beginning to widen with more open water within this part of the strait and sea ice drift speeds increase to an average of 30.86 km/d. Kane Basin has a mix of coastal restrictions and the inclusion of bays and fiords, providing space for ice to move and interact dynamically.

In most instances examined for the previous two sub-regions, there are only small differences between along-channel and across-channel sea ice drift. For Kane Basin, especially in looking at wind speed versus ice drift speed, strength and whether the relationship is positive, or negative are variable and show more notable differences (Table 4.6). Kane Basin is wider than Robeson and Kennedy Channels (~119 km wide but varies due to various topographic and coastal features). The differences between along-channel and across-channel drift suggest that the ice is moving in various directions and noticeable direction changes are occurring. A similar pattern emerges in Smith Sound. As these sub-regions are wider and less restricted (such as like Kennedy Channel), ice is able to drift more freely.

In Kane Basin, mean sea ice concentration was low in 2010 – also as exhibited for all of Nares Strait (Table 4.5). Sea ice in Kane Basin during 2010 was in free drift (i.e. ice concentration was < 6/10). Figure 5.4 shows an example of wind versus drift speed and mean ice concentration

versus drift speed for 2010. Sea ice drift speed versus wind speed show a strong negative relationship; however, there is a strong positive relationship with mean sea ice concentration and ice drift speed (Table 4.6). When ice concentration is low, ice drift speed increases and a strong positive relationship is expected. This demonstrates that possibly internal ice stress has a strong influence on sea ice in this sub-region. When there is a significant change in sea ice concentration (which for the other study years, ice concentration is more consistent where 2010 exhibited the lowest ice concentrations (Table 4.5)) the drift of sea ice in Kane Basin responds accordingly. Less ice denotes weaker internal ice stress working against the drift of ice and therefore, faster ice drift speeds. Sea ice is showing stronger relationships (negative or positive) thus far into the examination of each sub-region. This suggests that the internal ice stress component of the sea ice momentum balance equation is possibly the most dominant for Nares Strait; this will be discussed further.

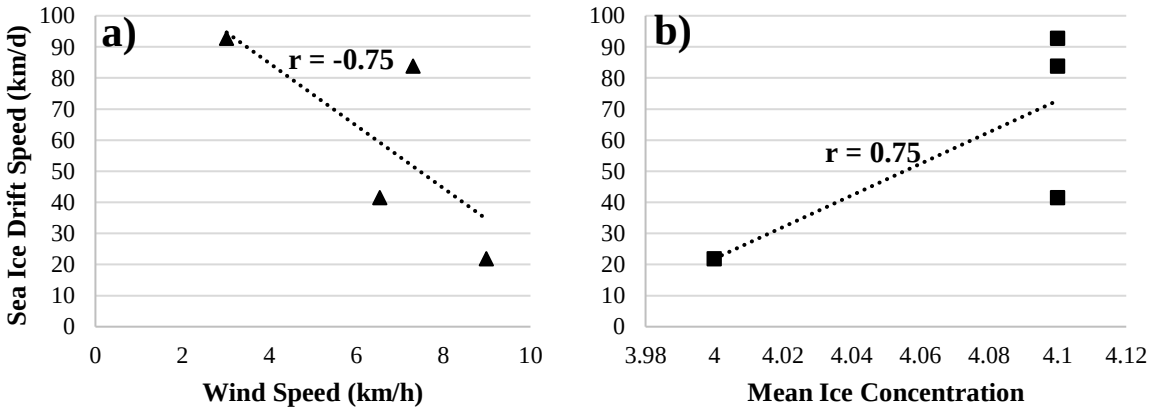

Figure 5.4: Regression plots comparing correlation of wind versus drift speed (a) and ice concentration versus drift speed (b) for Kane Basin in 2010.

5.1.1.4 Smith Sound

Smith Sound is the most southern of the four sub-regions. Like Kane Basin, Smith Sound exhibits more open water and less restrictions to ice movement as the sea ice drifts towards the Southern limit of Smith Sound and into Baffin Bay to the south. Not only is the mean drift speed the fastest here, so was the variability of observed drift speed (Table 4.2).

Smith Sound has less restrictions bounding sea ice (i.e. from the coast). Furthermore, the mean sea ice concentration in 2009 and 2010 indicate that sea ice was in fact in free drift (i.e. ice concentration < 6/10) (Table 4.5). When ice is in free drift, internal ice stress is not acting significantly upon the ice. It is important to note that ice was moving so quickly though this part of Nares Strait, the buoys drifted through Smith Sound over a span of 2 or 3 days. Ice chart data was weekly available and mean sea ice concentration did not change to permit any meaningful correlation analysis to occur (Table 4.6). But, as ice is favorable to free drift in association with the characteristics of Smith Sound, it is likely that ice concentration and coverage would have a strong correlation with ice drift speed here.

An interesting observation is the drastic difference of along-channel and across-channel correlations between wind speed and ice drift speed for this sub-region in 2009 – which is like that of Kane Basin. Figure 5.5 shows the relationship of wind speed and ice drift speed for 2009, broken down into the along-channel and across-channel components. Wind direction data did not show any significant direction changes at Littleton weather station (Figure 4.14). However, a change in ocean currents or a possible section of isolated consolidated sea ice could influence such a dramatic difference. Sea ice oscillations, which are indicative of ice in free drift (Gimbert et al., 2012) could also explain the contrast. Finally, simply the fact that the ice was moving so quickly through this

sub-region (4 days in 2009), the low sample size for correlation analysis could be responsible for this anomaly.

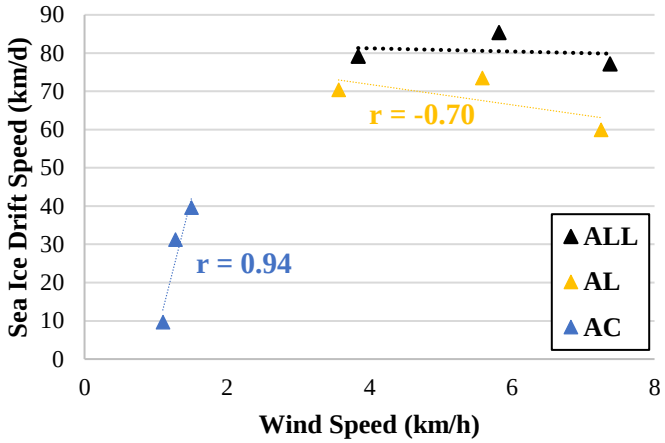

Figure 5.5: Wind speed versus sea ice drift speed for Smith Sound in 2009. Along-channel drift (AL) denoted in yellow and across-channel drift (AC) shown in blue.

Certainly, two things can be said about Smith Sound from this work: 1) sea ice drift is fastest in Smith Sound and the south end of Nares Strait, and 2) the variability of sea ice drift speed increases as the ice moves south through Nares Strait and the presence of open water increases and the magnitude of ice in free drift increases.

5.1.1.5 Nares Strait

Breaking down the entirety of Nares Strait into the four sub-regions discussed allows one to really assess the complex sea ice dynamics of the region. However, several things can be said about the strait as whole.

Correlations are moderately weak for the entire strait (Table 4.6). A general expectation from the theories of sea ice dynamics is that when internal ice stress increases, ice drift speed

decreases – showing negative correlations. When examining Nares Strait as a whole, mean sea ice concentration versus ice drift speed shows moderately weak negative relationships, but negative, nonetheless. This is in consensus with what is expected. The relationship between wind speed and ice drift speed is more variable and inconsistent. Some years show weak, but positive correlations (2009 and 2011) where 2010 and 2014 demonstrate moderately negative correlation coefficients (Table 4.6). Figure 4.5 show matching trends with sea ice drift speed and mean sea ice concentration over the study period for Nares Strait. Where sea ice concentration is higher, slower drift speeds occurred (2011 and 2014). There is not as high of an agreement with wind speed and drift speed from this figure (i.e. wind speeds changed from high to very low for 2011 and 2014 (Table 4.4), but drift speeds remained low for both years (Table 4.2)).

It is also important to note that examination of the strait entirely did not show significant differences between along-channel and across-channel drift for any of the four study years. Without looking at smaller sub-regions within Nares Strait, detailed differences are difficult to observe. But this does shed some light on the broader scale of the complexity of sea ice dynamics in this region.

The Pearson correlation results (Table 4.6) show that the internal ice stress component of the sea ice momentum balance equation is strong, but another term is dominating over wind stress when sea ice concentration is low. It is suspected that oceanic processes by proxy of the water stress term of the momentum balance is strong for Nares Strait, and possibly for other narrow channels in the High Arctic.

5.1.2 Seasonal Variability

The data in this thesis can be distinctively divided into two seasons. The buoys for 2009 and 2010 both pass through Nares Strait between August and mid-October. This period will be referred to as "late summer". The second season occurs through the months of October to December where both of the buoys from 2011 and 2014 passed through the strait and this season will be referred to as "fall to early winter".

One of the most notable differences between these two seasons is the difference in mean sea ice drift speed. Values are higher during late summer ($\geq$ 25 km/d) than in fall to early winter ($\leq$ 20 km/d; Table 4.2). This will be discussed further in the following sections.

The other important factor to note is the difference in mean sea ice concentration between these two seasons. Values for mean sea ice concentration are variable and generally lower across all four of the sub regions in late summer, with concentrations sufficiently low (< 6/10) to enable free drift conditions in Smith Sound in both 2009 and 2010 and in Kane Basin in 2010 (Figure 4.15). During fall to early winter mean sea ice concentrations remain >65% across all four sub-regions, suggesting that the majority of sea ice is compact and consolidated during this season and that free drift is not expected to occur during this season. Ice concentrations of these two seasons define the end of the melt season in late summer and the onset of ice freeze up during the fall and early winter.

Finally, contrasts can certainly be observed between seasons. A lot is to be noted about summer versus winter. Although the observation period of data for this thesis did not quite fall into the midst of winter, characteristics of winter dynamics can certainly be observed during the fall to early winter season. As these two seasons defined in this work do involve traditional

transition months (i.e. fall – October and November), expected results will not necessarily be as great or obvious.

5.1.2.1 Late Summer

Late summer corresponds with the time period where sea ice generally has reached its minimum extent in the Arctic. In this study, the two buoys that drifted through Nares Strait during late summer had the highest mean sea ice drift speeds and the most variable drift speeds (Table 4.2).

This season showed lower mean sea ice concentrations for the study period. Mean sea ice concentration values for 2009 and 2010 were 8/10 and 5/10 respectively (Table 4.5). In Chapter 2, free drift was defined by ice concentrations being less than 6/10, which means that in 2010, ice, on average, was in free drift. 2009 had a higher mean sea ice concentration; however, sea ice still is not as consolidated as it was for the fall to early winter season. This fact suggests that, theoretically, the magnitude of internal ice stress at work is less in 2009 and 2010 and could be an explanation for the higher drift speeds observed.

Additionally, given that mean sea ice concentration was lowest in 2010 (Figure 4.15), it would be expected that the correlation between mean sea ice concentration and sea ice drift speeds would be stronger. The Pearson correlation coefficients in Table 4.6 show negative trends across the board in 2010 for wind speed versus ice drift speed. Where there was enough change in ice concentration to draw any correlation information, *r* values were moderately strong and positive – which is what we expect. This likely explains the high mean sea ice drift speed for 2010. It is also expected that correlations are positive with wind speed and drift speed when internal ice stress is low, but this fact is opposite of that expectation. This suggests one more piece of suggesting

evidence that water stress is likely a strong contender for the dominant term of the sea ice momentum balance equation for Nares Strait.

Contrastingly, in 2009, correlation coefficients between wind speed and ice drift speed show positive trends with strong correlations in some sub-regions (Robeson Channel and Kane Basin). This suggests that contrasting terms of the momentum balance could be dominant in the ice drift through Nares Strait between the two years, despite the buoy transits occurring in the same months in these two years.

An average turning angle for late summer of 58° to the right was found. As mentioned, this value is higher than the model simulations of Mattson (2016); however, it still holds true to a higher turning angle for the summer months, as the fall to early winter turning angle average was found to be 51° (Table 4.1). There is not a big contrast between the two values, but the inclusion of fall – a transition season – in the two seasons considered in this study would contribute to the small observed difference between the mean turning angles of these two seasons.

When deconstructing sea ice drift speed into the along-channel and across-channel components, another dimension of seasonality can be observed. Late summer, when internal ice stress is low, shows the along-channel ice drift to be more dominant throughout the buoy transit (Figure 4.17). There are known strong north to south flow of both wind and ocean currents in Nares Strait (Samelson and Barbour, 2008). This is evidence that during low sea ice concentration periods, atmospheric and/or ocean forcings on sea ice dynamics in Nares Strait is strong.

It is a consensus within sea ice research that the summer sea ice regime is becoming more variable and less predictable. As the global temperature continues to rise, and the climate continues to shift, sea ice in the Arctic continues to be strongly affected (IPPC, 2013; Kimura et al., 2013). Nares Strait one of the few regions in the Arctic that has not shown a substantial decline in sea ice

over the past few decades (Environment Canada, 2012a). The literature shows that in fact, in the summer months sea ice dynamics are less predictable and becoming more variable. This is indicative of the massive changes that are occurring to the Arctic sea ice regime.

5.1.2.2 Fall to Early Winter

Fall to early winter buoy trajectories considered in this study had slower mean sea ice drift speeds than the late summer buoys. The 2011 and 2014 buoys trajectories had the lowest average drift speeds (Table 4.2). These two years are more consistent compared to the contrast between the mean drift speeds observed for the late summer buoys. Additionally, standard deviations of ice drift speed for 2011 and 2014 were lower (Table 4.2) than in 2009 and 2010, which conveys a lower amount of variability of sea ice drift during the fall to early winter season.

Mean sea ice concentration for fall to early winter was greater than a concentration of 60% within all sub-regions of Nares Strait in both 2011 and 2014 (Figure 4.15). Sea ice was mainly consolidated and compact during these months (ice concentrations were > 9/10 for all four sub-regions except Smith Sound in 2014). During October to December, temperatures are decreasing, and ice growth is happening at an increased rate. When the sea ice cover is compact, drift speeds are expected to be lower as the motion of the ice is restricted by internal ice stress. Where correlation analysis between mean sea ice concentration and ice drift speeds were able, *r* values were moderately strong and this was observed for all four study years (Table 4.6).

Mean wind speeds during the fall to early winter were higher than in late summer (Table 4.4). Although the wind speeds were higher than in late summer, the correlations between wind speed and ice drift speed for all of Nares Strait were weak for both 2011 and 2014 (Table 4.6). Contrastingly, the literature suggests that wind stress is usually the dominant term of the sea ice

momentum balance equation within the Arctic during the winter months (Kimura and Wakatsuchi, 2000; Kimura et al., 2013). However, it is also noted in the literature that although wind does typically make up a larger fraction of the momentum balance, this is not generally not the case with shallow seas and near coastlines (Matsson, 2016). The results presented here suggest that atmospheric forcing is not as significant in Nares Strait or that the ice field is too compact, confirming the unique characteristics and dynamics that exist in this region of the Arctic. General assumptions about sea ice dynamics cannot always be applied to narrow channels.

As with observing the overall spatial variability and patterns within each sub-region, seasonal variability can be observed within the spatial variability that exists by breaking down each sub-region again. Correlation coefficients between wind speed and ice drift are generally weak to moderate strength, except for Kennedy Channel in 2011. Where there was a large enough change in sea ice concentration and correlations with sea ice drift speed could be drawn, relationships are negative and moderate to strong. As sea ice concentrations during this season, strong negative correlations and slower drift speeds are excepted and observed. As mentioned, this is also observed throughout Nares Strait as a whole (Table 4.5); however, relationships are weaker, but still negative. Robeson Channel does exhibit very strong negative correlations between sea ice drift speed and mean ice concentration (Table 4.5). Kane Basin is interesting in that during a period where more consistency is apparent, correlations between 2011 and 2014 are opposite from one another (i.e. 2011 shows a weak negative relationship between wind speed and ice drift speed where as in 2014, wind speed versus ice drift speed exhibit weak to moderate positive correlations) (Table 4.6).

Seasonality, as previously mentioned, has an impact on sea ice drift direction as well. Unlike during late summer, the across-channel drift dominated during this season as illustrated in

Figure 4.17. Mean sea ice concentration is higher during this time, once again, suggesting that the internal ice stress component is strong. This could contribute to the ice oscillating and/or moving back and forth across the strait along with the ice pack. Additionally, an average turning angle of 51° to the right of the wind (Table 4.1) was found. The difference between both seasons' turning angles is not too significant; however, late fall to early winter is less than late summer. This agrees with Mattson (2016). This difference is likely due to the increased consolidation of sea ice, resulting in less space for the sea ice to drift, in favor of the ice to move more closely to the direction of the wind flow.

Trends in the declines of sea ice concentration, from climate change, for the Arctic as a whole are weaker in the winter (IPCC, 2013). The lower variability of sea ice drift speeds during this season support this. Several things can be drawn from this work. Firstly, slower drift speeds during early fall to late winter overall and even during a time of expected consistency, variability is observed (i.e. seasonality within each sub-region and between years). Secondly, mean sea ice concentration is high and the across-channel ice drift is dominant. Lastly, the turning angle of sea ice drift is smaller during this season.

5.1.3 Interannual Variability

The previous section investigated the seasonal variability that was observed within the data. This section will break down the pairs of years within each of the two seasons to observe interannual variability. As mentioned, the buoys from the years 2009 and 2010 drifted through Nares Strait over roughly the same months of August to October (late summer), while the 2011 and 2014 buoys drifted through the strait between October and December (fall to early winter). Because of the similarity in transit times of the 2009 and 2010 buoys and of the 2011 and 2014

buoys, interannual comparisons can be made for each of the late summer and fall to early winter seasons. It was observed that, in any given year, there is no certainty within Nares Strait with respect to sea ice motion. This, comparatively, is also apparent within the whole Arctic basin as from year to year various observations cannot be easily predicted and the outcome of annual climate and ice characteristics is never certain (Strove et al., 2010; Serreze and Barry, 2011; NSIDC)

5.1.3.1 2009 vs 2010

As discussed, during late summer buoys for both 2009 and 2010 drifted through Nares Strait. Despite having transited through Nares Strait in the same months in consecutive years, extreme differences in the sea ice drift data and the correlations between ice drift speed and wind speed as well as mean sea ice concentration are observed between these two years (Table 4.6).

While these two years had the highest mean drift speeds, 2010 exhibited substantially higher mean ice drift speeds than 2009 (Figure 4.5). The direction of drift in 2009 was generally southwards originating in the north-east but did show variability where the buoy trajectory took a turn or changed direction briefly (Figure 4.1). In 2010, the sea ice drift direction was strongly southward on the along channel plane with very little deviation (Figure 4.2). This could be one factor to account for the higher drift speed as the ice did not change its direction very much to slow down the momentum of the ice pack. Additionally, the average sea ice concentration was also much lower in 2010 (5/10) than in 2009 (8/10; Table 4.5). Therefore, the internal ice stress is expected to have been weaker in 2010, and the ice would be more responsive to air stress and water stress forcings.

Wind speeds did not correlate with the increase of drift speed between the years. 2009 showed faster wind speeds (Table 4.4), but slower drift speeds, indicating that changes in the air stress term of the momentum balance equation were not responsible for the increased drift speeds observed in 2010. Rather, this lends further evidence to the importance of the internal ice stress term of the momentum balance equation (i.e. that the reduced concentration of sea ice (Table 4.5) likely played an important role on the increase sea ice drift speeds observed in Nares Strait in 2010).

As mentioned, sea ice drift speeds were more variable in late summer than in fall to early winter, suggesting that the summer months are less consistent and less predictable. This is especially observed with comparison of 2009 and 2010. Standard deviations of ice drift speed indicate the magnitude of variability in 2009 and 2010 at 17.25 km/d and 23.96 km/d, respectively (Table 4.2). 2010 shows higher variability empirically. These buoy trajectories were observed within the same months of the year; however, these two years show a very different pictures of late summer sea ice dynamics within Nares Strait.

2010 was the eighth minimum sea ice extent on record at 4.62 million km^2, with the record lowest extent being 3.39 million km^2 in 2012 (NSIDC, 2018). Exceedingly more literature is suggesting that the decline in sea ice extent and disappearance of sea ice in the Arctic can be attributed to ice mass loss (i.e. the shrinking of sea ice extent and the thinning of sea ice cover). The high drift speed in 2010 from this data suggests that in September, where the Arctic minimum ice extent occurs, ice is moving faster and more freely, which is also contributing to the loss of sea ice in the Arctic (Spreen et al., 2011; Maslanik et al., 2007). A positive feedback is observed here as the loss of sea ice increases, the rate of drift increases, sea ice mass and thickness are decreased which accelerates further loss of sea ice contributing to possible faster moving ice out of the Arctic

(Kwok et al., 2013). Like in Nares Strait, the majority of ice drift direction is southward, away from the Arctic Basin, where sea ice is then further melted as it reaches warmer waters to the south, ultimately contributing to further Arctic sea ice loss.

5.1.3.2 2011 vs 2014

During the winter season and the onset of the colder months of the year, results from the analysis in this thesis show more consistency and less variability between years. The standard deviation of sea ice drift speed for 2011 and 2014 was 9.76 km/d and 15.32 km/d, respectively (Table 4.2), indicating less variability as compared to the late summer years. The consistency noted within the winter season drift speeds is also observed when considering the mean sea ice drift speeds for these two years (Table 4.2).

Mean ice concentration for these two years were also above 6/10, suggesting that the sea ice cover was consolidated. As any open water areas are undergoing freeze-up during this season, and the sea ice cover is thickening, ice drift becomes slower, dampened and less variable throughout this season. As a result, there is dramatically less interannual variability during the fall to early winter season, as seen in the results observed in this study for 2011 and 2014. In terms of correlations of ice drift speed with both wind speed and sea ice concentration, values showed more consistency and less variability than 2009 versus 2010. Mean sea ice concentration did not change much during these two years (Table 4.5) and correlation analysis were not possible, except for Robeson Channel. Strong, negative *r* values were observed (Table 4.6). This is expected for this season – internal ice stress increases when sea ice concentration increases. Additionally, wind speed versus ice drift speed in comparison was inconsistent between 2011 and 2014. Moderate to strong positive *r* values was observed through Kennedy Channel, however, supporting both the

expectations of the geographic characteristics influence on ice drift through Kennedy Channel as well as the literature support that wind stress drives ice motion during the winter months in the Arctic (Kimura et al., 2013).

5.2 Limitations

There are several limitations within this thesis work. As per the nature of Nares Strait and the CAA, there is the presence of perennial ice cover and consolidated ice pack throughout the strait all year round, especially at the north end of the strait (i.e. Robeson Channel, Kennedy Channel). As a result, evaluating mean sea ice concentration is integral to understanding the momentum balance of the sea ice drift regime in the region. With the ice cover being consolidated for most of the study period (i.e. free drift conditions were the exception rather than the norm), understanding and having a thorough quantitative evaluation of internal friction of the ice is essential. Unfortunately, the limited spatial and temporal resolution of the ice charts acquired from the CIS to evaluate changes in sea ice concentration, prevent a detailed analysis at the short temporal scale of the drift tracks of the buoys through the strait. Another source of mean sea ice concentration, that provides data at daily intervals with high spatial resolution (on the order of ~5 km) would be beneficial to improving our capacity to understanding the critical role that internal ice stress plays on the drift of sea ice within Nares Strait. While daily sea ice concentration data are available from passive microwave sensors, the low spatial resolution of these data products, and the influence of contamination from land area within the confines of Nares Strait, precludes the use of passive microwave data for this study region.

Secondly, to the issue of spatial resolution, a more comprehensive dataset of wind observations could provide a better understanding of the variability of the sea ice drift in Nares

Strait. It is apparent from dividing the region into four sub-regions and evaluating sea ice drift to each region, that there is a high level of variability at small scales (~50 to 100 km). Only three weather stations were available over the 400 km length of Nares Strait. These three stations are unlikely to effectively capture the true variability of wind conditions throughout the strait. More detailed observations could provide a better understanding of the correlations between sea ice drift and wind stress within Nares Strait.

The complexity of sea ice motion makes it difficult to predict where a deployed buoy will travel, resulting in difficulty planning for studies to collect observations of sea ice motion in a specific region, including Nares Strait. Despite the buoys being deployed in the same region each year, atmospheric and oceanic forcings make the buoy trajectories unpredictable. In the case of this study, buoys were deployed in the Lincoln Sea (the north entrance to the strait) with the hope that they would flow southward through Nares Strait and on to Baffin Bay. However, numerous buoys drifted eastward across the northern coast of Greenland and on to exit the Arctic Ocean via Fram Strait, or drift to the west, ending up in the Beaufort Sea or off the northwest coast of the CAA. To develop a clear picture of the sea ice regime within Nares Strait, more consistent measurements and a higher volume of buoy trajectories over a number of consecutive years are required.

Additionally, with regards to buoy and instrument limitations, this research would benefit from a larger temporal scale. If data could be obtained for multiple buoy trajectories per year, the seasonality of ice drift in Nares Strait could be analyzed in more detail. Ice arch formation is known to be an integral part of the dynamics in Nares Strait. Often, the ice arches do not form and other years they do. Literature suggests that there is no climatological relationship here, but one thing that is certain is that the presence of the ice arches have a great influence on the sea ice dynamics

of the strait. If data could be obtained before, during and/or after the formation and collapse of an ice arch, essential information could be collected about what ultimately drives the drift of sea ice in this unique region.

Finally, instrumentation errors also need to be considered. When using autonomous instruments, especially from such a remote area, the user is dependent on the instrument operating in a reliable manner. In this study, some buoys and weather stations that had occasional gaps of missing data for a few hours to, in rare cases, a few days. In order to overcome these instances of missing data, daily averages were obtained for each dataset. This averaging decreased the temporal resolution of the data, thereby limiting the potential to effectively observe variations in sea ice drift (and the forcing resulting in those changes in sea ice drift) at short (sub-daily) time scales. In some instances, there was a lot of sea ice activity during the periods of 12 hours to a day. Utilizing daily average, these instances are overlooked and cannot be effectively analyzed.

5.3 Summary

This chapter discussed the analysis, results and limitations of this thesis. Arctic sea ice conditions are becoming increasingly difficult to predict and model, due in part to the variability of sea ice dynamics, which are in part driven by global climate change.

Three scales of variability were examined with respect to sea ice drift in Nares Strait: spatial variability, seasonal variability and interannual variability.

Smith Sound was found to have the most spatial variability. This region had the fastest and more variable sea ice drift speeds of the four sub-regions. Smith Sound is the most open basin of the four sub-regions and ice is more commonly in free drift within this sub-region.

The buoy drift data showed two distinct seasons in which the buoys traversed Nares Strait. The 2009 and 2010 buoys drifted through the strait in late summer, while the 2011 and 2014 buoys drifted through the strait in fall to early winter. It is important to note that these time periods are not in the midst of summer and winter (i.e. during periods of transitions between summer and winter), but differences were still concluded from examining the data. Of the two seasons, ice drift speeds were more variable in late summer. This is in agreement with the trends of the entire Arctic system where more variability in sea ice and climate is observed within the summer months (Kwok et al., 2013; Stroeve et al., 2007; Pfirman et al., 2004).

Finally, interannual variability was evaluated by comparing drift and forcing data from 2009 versus 2010 and from 2011 versus 2014. The greatest discrepancies are observed between 2009 and 2010, which is expected as these years were in the late summer season, which also showed increased variability of sea ice drift, which is at least in part due to the lower sea ice concentrations, and associated reduction in internal ice stress, observed at this time of year.

Finally, buoy, wind and ice concentration observations from this region are limited both spatially and temporally. As a result, the conclusions that can be drawn from the analysis presented in this thesis are limited. Aspects that need improving include the need for: better resolution and coverage of sea ice concentration data; higher resolution and availability of meteorological data throughout the entire strait; and increased frequency of buoys drifting through Nares Strait.

As changes are occurring, more research needs to be conducted to get a better understanding of the changes happening in Nares Strait, which are indicative of the overall changes in the Arctic.

Chapter 6
Conclusions, Recommendations and Future Work

6.0 Conclusions

The Arctic sea ice regime is an integral part of the global climate system. To understand the rapid and accelerated rate of climate change, it is important to understand sea ice dynamics. Arctic amplification has been identified as an important factor in, and an early indicator of, climate change. Since the Arctic sea ice cover plays a critical role in Arctic amplification, improving our understanding of the behavior of Arctic sea ice, and its role in the Earth's climate system, is vital. When talking about changes to the Arctic sea ice cover, rapid decrease in sea ice extent and thickness, as well as the potential for ice-free summers by the end of this century, are often the topic of conversation. However, sea ice is not declining solely due to changing thermodynamics, it is moving and the export of sea ice from the Arctic Basin through dynamic processes is important to understand.

This thesis is aimed to answer two questions:

1) What is the drift of sea ice through Nares Strait and how do the dynamics vary from year to year?

2) What forcings dominate the sea ice momentum balance equation within Nares Strait?

Sea ice drift speeds were calculated from GPS position data acquired by four drifting buoys deployed on the surface of ice floes that transited though Nares Strait between 2009 and 2014. It was observed that sea ice drift speed increases southward through Nares Strait, with the slowest drift speeds observed in Robeson Channel (the north end of the strait) and the fasted drift speeds observed in Smith Sound (the south end of the strait). Variability of sea ice drift speed was

examined at three scales – spatial variability, seasonal variability and interannual variability. Spatially, sea ice dynamics were variable between the four sub-regions of Nares Strait. Within each of the four sub-regions, sea ice drift was most variable within Smith Sound. Seasonal variability of ice drift speed was analyzed by comparing drift data from the two buoys that transited Nares Strait in the late summer (2009 and 2010) to those transited though Nares Strait in the fall to early winter time period (2011 and 2014). Sea ice drift was found to be more variable during the late summer, when sea ice concentrations were lower. Interannual variability was investigated between the two buoys transits available for each of the late summer and fall to early winter seasons. Once again, interannual variability was higher between the late summer years (2009 and 2010) than between the fall to early winter years (2011 and 2014).

Regression analysis was used to attempt to determine which forcings dominated the sea ice momentum balance in each study year and sub-region, and for Nares Strait as a whole. Although there were instances where correlation coefficients between sea ice drift speed and wind speed or ice concentration were strong, correlations were often weak or moderate and there was uncertainty in determining which forcing was dominant in any given year, or sub-region. Consolidated ice drift (versus free drift) is difficult to understand and quantify. It is more difficult to explain the momentum balance of the sea ice in Nares Strait as the dominant terms become more variable and less predictable (i.e. from changing climatic variables such as temperature and atmospheric changes). This is like the current regime of the Arctic Basin – over the years of increasing global temperatures and changing climate regimes, sea ice has seen considerable changes and increasing variability with recent years.

It is suggested by recent scientific projections that summer sea ice in the Arctic will disappear within a generation and will have grave consequences. Nares Strait is part of a

monumental region titled “the last ice area” and the significance of this area is increasing as the Arctic sea ice extent and perennial sea ice continues to disappear (WWF, 2018). As the climate continues to change and the rate of Arctic amplification continues to increase, the predictability of the Arctic sea ice system becomes less apparent and more difficult. This in turn will affect our overall understanding of the global climate regime and may increase the uncertainty of forecasted sea ice conditions in the future.

It is important to note that the findings of this study were hampered by several limitations, including: the lack of precision and low temporal resolution of the sea ice concentration data; the sparsity of meteorological data available throughout the strait; the fact that all four buoy transits were restricted to a short portion of the year (August to December); and the fact that wind speed and ice drift data had to be averaged to daily time intervals to account for occasional missing data – this hindered the ability to investigate how sea ice responded to these forcings at times where ice drift direction or speed varied at sub-daily timescales. Despite the number of substantial limitations, all the results and analysis presented in this thesis represent an important step towards better understanding the dynamics of sea ice drift in Nares Strait. This information is a precursor that can be used to guide future research related to sea ice dynamics in both Nares Strait and the Arctic as a whole.

6.1 Recommendations and Future Work

The results presented in the study indicate that there is a need for enhanced quality and quantity of meteorological and sea ice data in Nares Strait. Several questions are important to address in future work and research on the dynamics of sea ice in Nares Strait. These include:

1) What is the sea ice thickness distribution for Nares Strait, how does it vary and is it changing?
2) Does the thickness of the sea ice in Nares Strait affect the dynamic processes? If so, at what magnitude?
3) If wind and ice concentration are not showing strong relationships via regression analysis, what other factors could be at work and how could they be evaluated? In particular, oceanographic data are required to understand the role of ocean stress on sea ice dynamics in this region.

Sea ice is thinning across the Arctic Basin and sea ice drift is accelerating across the Arctic as a whole. The acceleration of sea ice drift is not believed to be directly linked to wind and atmospheric changes, rather the trends have a relationship to sea ice thickness. To address the thinning of sea ice and alternative drivers of sea ice drift, a comprehensive study of the thickness of sea ice in Nares Strait, not just the concentration of the ice cover, is required to evaluate the level of deformation and the influence of ice characteristics on ice motion within the region.

Additionally, as it was found that another factor is likely at work at any given instance on ice motion in Nares Strait, it is important that future studies incorporate data about ocean currents in Nares Strait. It is imperative that future research studies obtain data of ocean current speeds in Nares Strait to correlate to sea ice drift speeds so that oceanic/water stress component of the momentum balance can be investigated.

Finally, the results of this work also contribute to the Arctic sea ice regime, apart from the CAA and Nares Strait. Examining the seasonality of climate variables is important. The higher variability of sea ice drift speeds observed within late summer in this study correlates with this work. It is important to note this increased variability, but as the climate shifts and changes, being

able to get an idea of what is to come will be important to adapt to these changes globally. One thing that is certain, the Arctic sea ice regime is becoming less predictable and variable as the global climate changes. Obtaining further, more detailed, observations of sea ice dynamics in all regions of the Arctic will contribute to the information needed to improve the initialization and parameterization of climate models to make better predictions of future sea ice change and, subsequently, plans of action to mitigate or adapt to these changes.

References

Addison, V., and Bourke, R. (1987). The physical oceanography of the northern Baffin Bay-Nares Strait region.

Agnew, T., Lambe, A., and Long, D. (2008). Estimating sea ice area flux across the Canadian Arctic Archipelago using enhances AMSR-E. *Journal of Geophysical Research*, C10011.

Alexander, M., Bhatt, U., Walsh, J., Timlin, M., Miller, J., and Scott, J. (2003). The Atmospheric

Response to Realistic Arctic Sea Ice Anomalies in an AGCM during Winter. *Journal of Climate (17)*. 890-905.

Arctic Monitoring and Assessment Program. (2011). *ARCTIC CLIMATE ISSUES 2011: CHANGES IN ARCTIC SNOW, WATER, ICE AND PERMAFROST*

Argos. (2018). *How Argos works?* Retrieved from: http://www.argos-system.org/argos/how-argos-works/.

Bitz, C., Fyfe, J., and Flato, G. (2002). Sea ice response to wind forcing from AMIP models. *Journal of Climate*, 522-536.

Coachman, L., and Aagaard, K. (1974). Physical Oceanography of Arctic and subArctic seas.

Colony, R., and Thorndike, A., (1985). Sea Ice Motion as a Drunkard's Walk. *Journal of Geophysical Research, (90)*, 965-974.

Colony, R., and Thorndike, A. (1984). An Estimate of the Mean Field of Arctic Sea Ice Motion. *Journal of Geophysical Research, (89)*, 10 623-10 629.

Decker, D. (2010). *Remote Sensing of the Climate and Cryosphere of Nares Strait, Northwest Greenland.* Ohio: The Ohio State University.

Derksen, C., Smith, S., Sharp, M., Brown, L., Howell, S., Copland, L., . . . Walker, A. (2012). Varibility and change in the Canadian cryosphere. *Climatic Change*.

Evironment and Climate Change Canada. (2016). *Ice and Iceberg Charts*. Retrived from: http://www.ec.gc.ca/glaces-ice/default.asp?lang=Enandn=B6C654BB-#1weekley-ice

Environment Canada. (2012a). *Nares Strait*. Retrieved from: http://www.ec.gc.ca/glaces-ice/?lang=Enandn=3D5398F0-1

Environment Canada. (2012b). *Sea Ice Dynamics*. Retrieved from: http://www.ec.gc.ca/glaces-ice/default.asp?lang=Enandn=454CAC14-1

Environment Canada. (2013). *Historical weather and climate data*. Retrieved from: http://climate.weatheroffice.gc.ca/climate_normals.

ESRI. (2017). *Importing an ArcInfo interchange file (E00)*. Retrieved from: http://desktop.arcgis.com/en/arcmap/latest/manage-data/coverages/importing-an-arcinfo-interchange-file.htm.

Gimbert, F., Marsan, D., Weiss, J., Jourdain, N.C., and Barnier, B. (2013). Sea ice inertial oscillations in the Arctic Basin. *The Cryosphere (6)* 1187-1201.

Givati, A., and Rosenfield, D. (2013). The Arctic Oscillation, climate change and the effects on precipitation in Israel. *Atmospheric Research (132)* 114-124.

Goosse, H., Fichefet, T., and Campin, J. (1997). The effects of the water flow through the Canadian Archipelago in global ice-ocean model. *Geophysical Research Letters*.

Gudmandsen, P. (2012). *2013 Regional Outlook - Nares Strait and Lincoln Sea.* University of Denmark.

Haas, C., and Eicken, H. (2001). Interannual variability of summer sea ice thickness in the Siberian and central Arctic under different atmospheric circulation regimes. *Journal of Geophysical Research (106)*. 4449-4462.

Haas, C., Hendricks., and Doble, M. (2006). Comparison of sea ice thickness distribution in the Lincoln Sea and adjacent Arctic Ocean in 2004 and 2005. *Annals of Glaciology (44)* 247-252.

Haas, C., Pfaffling, A., Hendricks, S., Rabenstein, L., Etienne, J., and Rigor, I. (2008). *Reduced ice thickness in Arctic transpolar drift favors rapid ice retreat.* University of Alberta.

Haas, C. (2010). Dynamics versus Thermodynamics: The Sea Ice Thickness Distribution. In D. Thomas, and G. Deickmann, *Sea Ice.* Blackwell Publishing Ltd.

Haas, C. (2017). Chapter 2: Sea ice thickness distribution In Thomas, D (eds.), *Sea Ice Third Edition* (pp. 42-64), John Wiley and Sons Ltd.

Hibler, W.D., Roberts, A., Proshutinsky, A., Simmons, H.L., and Lovick, J. (2006). Modeling M2 tidal variability in Arctic sea ice drift and deformation. *Annals of Glaciology (44)* 418-428.

Hibler, W. (1979). A dynamic thermodynamic sea ice model. *Journal of Physical Oceanography*, 815-846.

Hibler, W., Roberts, A., Heil, P., Proshutinsky, A., Simmons, H., and Lovick, J. (2006). Modeling M2 tidal varibility in Arctic sea ice drift and deformation. *Annals of Glaciology*, 418-428.

Holland, M., Bailey, D., and Vavrus, S. (2010). Inherent sea ice predictability in the rapidly changing Arctic environment of the Community Climate System Model, version 3. *Climate Dynamics, (36)*, 1239-1253.

Howell, S., Wohleben, T., Dabboor, M., Derksen, C., Komarov, A., and Pizzolato, L. (2013). Recent changesin the exchange of sea ice between the Arctic Ocean and the Canadian Arctic Archipelago. *Journal of Geophysical Research* , 1-13.

Hunkins, K., (1966). Ekman Drift Currents in the Arctic Ocean. *Deep-Sea Research (13)*. 607-620

Ingram, R., Bacle, J., Barber, D., Gratton, Y., and Melling, H. (2002). An overview of physical processes in the North Water. *Deep-Sea Research II (49)*. P. 4893-4906.

IPCC. (2013*). Climate Change 2013: The Physical Science Basis.* Contribution of Working Group I to the Fifth Assessment Report of the Intergovernmental Panel on Climate Change [Stocker, T.F., D. Qin, G.-K. Plattner, M. Tignor, S.K. Allen, J. Boschung, A. Nauels, Y. Xia, V. Bex and P.M. Midgley (eds.)]. Cambridge University Press, Cambridge, United Kingdom and New York, NY, USA, 1535 pp, doi:10.1017/CBO9781107415324.

Iridium. (2017). *Iridium Global Network.* Retrieved from: http://www.iridium.com/network/globalnetwork/.

Ito. H., and Muller, F. (1982). Ice movement through Smith sound in Northern Baffin Bay, Canada, observed in satellite imagery. *Journal of Glaciology (28)*.

Kennedy, C. (2013). *2012 State of the Climate: Arctic Sea Ice*. Retrieved from: http://www.climate.gov/news-features/understanding-climate/2012-state-climate-Arctic-sea ice.

Kimura, N. and Wakatsuchi, M. (2000). Relationship between sea ice motion and geostrophic wind in the Northern Hemisphere. *Geophysical Research Letters (27)*. 3735-3738

Kimura, N., Nishimura, A., Tanaka, Y. and Yamaguchi, H. (2013). Influence of winter sea ice motion on summer ice cover in the Arctic. *Polar Research (32)*. doi: 10.3402/polar.v32i0.20193

Koenigk, T., and Mikolajewicz, Y. (2008) Seasonal to interannual climate predictability in mid and high northern latitudes in a global coupled model. *Climate Dynamics*. doi: 10.1007/s00382-008-0419-1.

Kowalik, Z., and Proshuntinsky, A. (1994). The Arctic ocean tides. *American Geophysical Union*.

Kottmeier, C., Olf, J., Frieden, W. and Roth, R. (1992). Wind forcing and ice motion in the Weddell Sea region. *Journal of Geophysical Research (97)*. 20373-20383

Kwok, R., Spreen, G., and Pang, S. (2013). Arctic sea ice circulation and drift speed: Decadal trends and ocean currents. *Journal of Geophysical Research: Oceans (118)*. 2408-2425.

Kwok, R., Pedersen, L., Gudmandsen, P., and Pang, S. (2010). Large sea ice outflow into Nares Strait in 2007. *Geophysical Research Letters*.

Kwok, R. (2005). Varibility of Nares Strait ice flux. *Geophysical Research Letters (32)*.

Kwok, R., Cunningham, G., and Pang, S. (2004). Fram Strait sea ice outflow. *Journal of Geophysical Research Letters (109)*. C01009

Kwok, R. (2000). Recent Changes in Arctic Ocean Sea Ice Motion Associated with the North Atlantic Oscillation. *Geophysical Research Letters, (27)*. 775-778.

Kwok, R., Curlan, J., McConnell, R., and Pang, S. (1990). An Ice Motion Tracking System at the Alaska SAR Facility. *IEEE Journal for Oceanic Engineering*, 44-54.

Langehaug, H.R., Geyer, F., Smedsrud, L.H. and Gao, Y. (2013). Arctic sea ice decline and ice export in the CMIP5 historical simulations. *Ocean Modelling, (71)*. 114-126

Lepparanta, M. (2011). *The Drift of Sea Ice Second Edition.* Chichester: Praxis Publishing Ltd.

Lupkes, C., Gryanik, V., Hartmann, J., and Andreas, E. (2012) A parametrization, based on sea ice morphology, of neutral atmospheric drag coefficients for weather prediction and climate models. *Journal of Geophysical Research: Atmospheres*, (117). D13112

Marshall, S. (2012). *The Cryosphere*. Woodstock: Princeton University Press.

Maslanik, J., Stroeve, J., Fowler, C., and Emery, W. (2011). Distribution and trends in the Arctic sea ice through spring 2011. *Geophysical Research Letters*.

Matsson, K. (2016). Wind impact on sea ice motion in the Arctic. Department of Physics, Lund University, Sweden.

Maxwell, J.B. (1981). Climatic regions of the Canadian Arctic islands. *Arctic (34)*. 225-240

Meier, W.N. (2017). Chapter 11: Losing Arctic sea ice: observations of the recent decline and the long-term context In Thomas, D (eds.), *Sea Ice Third Edition*, (pp. 290-303), John Wiley and Sons Ltd.

Munchow, A., and Melling, H. (2006). An observational estimate of volume and freshwater flux leaving the Arctic Ocean through Nares Strait. *Journal of Physical Oceanography*.

MetOcean. (2013). *Buoys and Profilers: SVP*. Retrieved from: http://www.metocean.com/ProdCat.aspx?CatId=1andSubCatId=5andProdI.

MSC. (2005). MANICE: Manual of Standard Procedures for Observing and Reporting Ice Conditions, Revised Ninth Edition. Meteorological Service of Canada Catalogue No. En56-175/2005.

Munchow, A., and Melling, H. (2008). Ocean current observations from Nares Strait to the west of Greenland: Interannual to tidal varibility and forcing. *Journal of Marine Research*, 801-833.

Munchow, A., Melling, H., and Falkner, K. (2006). An observational estimate of volume and freshwater flux leaving the Arctic Ocean through Nares Strait. *Journal of Physical Oceanography*, 2025-2041.

NASA. (2018). *Ocean in Motion: Ekman Transport.* Retrieved from: http://oceanmotion.org/html/background/ocean-in-motion.htm.

NOAA. (2017). *Wind driven surface ocean currents*. Retrieved from: https://oceanservice.noaa.gov/education/kits/currents/05currents3.html.

NASA. (2017). *January 2017 was third-warmest January on record*. Retrieved from: https://climate.nasa.gov/news/2550/january-2017-was-third-warmest-january-on-record/.

NOAA. (2011). *Ocean currents.* Retrived from: http://www.noaa.gov/resource-collections/ocean-currents.

Notz, D. (2017). Arctic sea ice seasonal-to-decadal variability and long-term change. *Past Global Changes Magazine (25)*. doi: 10.22498/pages25.1.14

NSIDC. (2018). *ChArctic* (3.0) [Minimum and Maximum Extent Values] Retrieved from ftp://sidads.colorado.edu/DATASETS/NOAA/G01235/seaice_analysis

NSIDC. (2017). *Arctic sea ice 2017: Tapping the breaks in September*. Retrieved from: http://nsidc.org/Arcticseaicenews/2017/10/Arctic-sea-ice-2017-tapping-the-brakes-in-september/.

NSIDC. (2012). *Arctic sea ice extent breaks 2007 record low*. Retrieved from: http://nsidc.org/Arcticseaicenews/2012/08/Arctic-sea ice -breaks-2007-record-extent/

NSIDC. (2011, October 4). *Arctic Sea Ice Near Record Lows*. Retrieved from Arctic Sea Ice News and Analysis: http://nsidc.org/Arcticseaicenews/2011/10/summer-2011-Arctic-sea ice -near-record-lows/

Overland, J., Mofjeld, H., and Pease, C. (1984). Wind-Driven Ice Drift in a Shallow Sea. *Journal of Geophysical Research (89)*. 6525-6531.

Overland, J., and Wang, M. (2005). The Arctic climate paradox: The recent decrease of the Arctic Oscillation. *Geophysical Research Letters (32)*.

Pfirman, S., Haxby, W., Colony, R., and Rigor, I. (2004). Variability in Arctic Sea Ice Drift. *Geophysical Research Letters (31)*.

Rampal, P; Weiss, J; and Marsan, D. (2009). Positive trend in the mean speed and deformation rate of Arctic Sea Ice, 1979-2007. *Journal of Geophysical Research (114)*.

Rosenblum, E., and Eisenman, I. (2017) Sea ice trends in climate models only accurate in runs with biased global warming. *Journal of Climate (30)*. 6256-6278.

Ryan, P. (n.d.). *Flow Dynamics and Ice Bridge Formation in Nares Strait.* Delaware: University of Delaware.

Ryan, P; and Munchow, A. (2016). Sea ice draft observations in Nares Strait from 2003 to 2012. *Journal of Geophysical Research: Oceans (112).* doi: 10.1002/2016JCO11966.

Rigor, I., Wallace, J., and Colony, R. (2002). Response of Sea Ice to the Arctic Oscillation. *Journal of Climate, (15)*. 2648-2663.

Samelson, R., Agnew, T., Melling, H., and Munchow, A. (2006). Evidence for atmospheric control of sea ice motion through Nares Strait. *Geophysical Research Letters*.

Samelson, R., and Barbour, P. (2008). Low-level jets, orographic effects, and extreme events in Nares Strait:a model-based mesoscale climatology. *Monthly Weather Review*.

Smedurd, L., Halvorsen, M., Stroeve, J., Zhang, R., and Kloster, K. (2017) Fram Strait sea ice export variability and September Arctic sea ice extent over the last 80 years. *The Cryosphere*, (11). 65-79.

Smedsurd, L., Sirevaag, A., Kloster, K., Sortenberg, A., and Sandven, S. (2011). Recent wind driven high sea ice export in the Fram Strait contributes to Arctic sea ice decline. *The Cryosphere*, 821-829.

Statistics Canada. (2012). *EnviroStats* . Retrieved from: http://www.statcan.gc.ca/pub/16-002-x/2011001/ct016-eng.htm.

Spreen, G., Kwok, R., and Menemenlis, D. (2011). Trends in Arctic sea ice drift and role of wind forcing: 1992-2009. *Journal of Geophysical Research Letters, (38)*. L19501.

Steele, M., Zhang, J., Rothrock, D., and Stern, H. (1997). The force balance of sea ice in a numerical model of the Arctic Ocean. *Journal of Geophysical Research Letters, (102).* 21061-21079.

Steffen, K., (1986). Ice conditions of an Arctic polynya: north water in winter. *Journal of Glaciology (32).*

Stroeve, J., Kattsov, V., Barrett, A., Serreze, M., Pavlova, T., Holland, M., and Meier, W. (2012). Trends in Arctic sea ice extend from CMIP5, CMIP3 and observations. *Geophysical Research Letters*.

Stroeve, J., Serreze, M., and Drobot, S. (2008). Arctic sea ice extent plummets in 2007. *Eos*.

Stroeve, J., Holland, M., Meir, W., Scambos, T., and Serreze, M. (2007) Arctic sea ice decline: faster than forecasted. *Geophysical Research Letters (34).*

Serreze, M., Barrett, A., Stroeve, J., Kindig, D., and Holland, M. The emergence of surface-based Arctic amplification. *The Cryosphere, (3).* 11-19.

Serreze, M., and Barry, R. (2005). *The Arctic Climate System.* New York: Cambridge University Press.

Smith, S. (1997). The Scientist and Engineer's Guide to Digital Signal Processing. *California Technical Publishing*. San Diego, California.

Tang, C., Ross, C., Yao, T., and Petrie, B. (2004). The circulation, water masses and sea ice of Baffin Bay.

Thorndike, A., and Colony, R. (1982). Sea Ice Motion in Response to Geostrophic Winds. *Journal of Geophysical Research (87)*. 5845-5852.

Wadhams, P. (2000). *Ice in the Ocean*. Overseas Publishers Association.

Wang, J., Zhang, J., Watanabe, E., Ikeda, M., Mizobata, K., Walsh, J., Bai, X., and Wu, B. (2009). Is the Dipole Anomaly a major driver to record lows in Arctic summer sea ice extent? *Geophysical Research Letters (36)*

Weiss, J. (2013). *Drift, Deformation, and Fracture of Sea Ice. A Perspective Across Scales*. Springer

Wu, B., Wang, J., and Walsh, J. (2006). Dipole Anomaly in the Winter Arctic Atmosphere and its Association with Sea Ice Motion. *Journal of Climate (19).* 210-225

WWF. (2018) *The last ice area*. Retrieved from: https://arcticwwf.org/places/last-ice-area/.

Zhao, Y., and Liu, A. (2007). Arctic Sea Ice Motion and its relation to Pressure Field. *Journal of Oceanography (63).* 505-515

van Angelen, J., van der Broeke, M., and Kwok, R. (2011). The Greenland sea jet: A mechanism for wind driven sea ice export through Fram Strait. *Geophysical Research Letters*.

Appendix A
Egg Code Definition

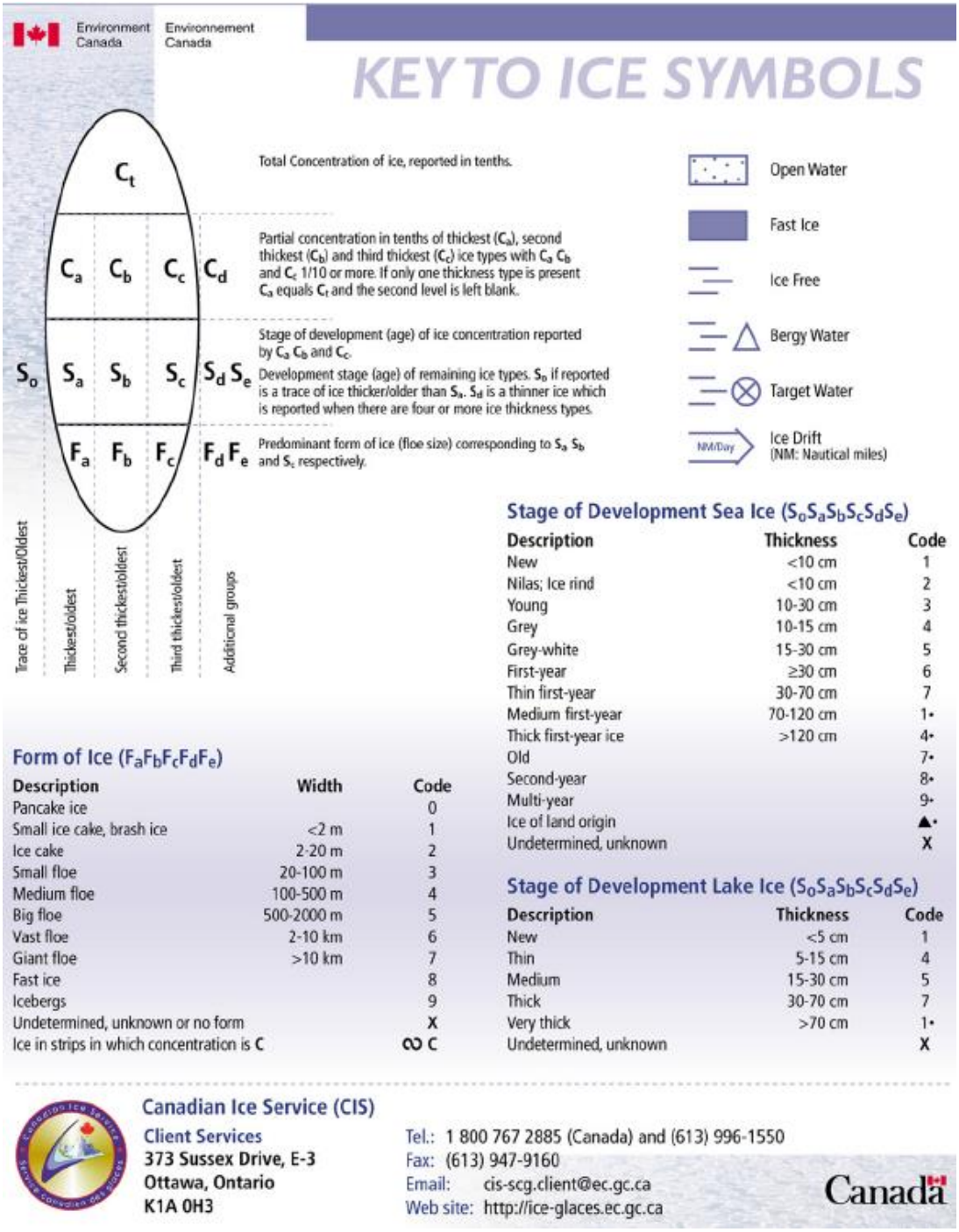

Figure A.1: Full description of the egg code and key ice chart symbols (MSC, 2005).

Appendix B
IGOR Code

B.1 Along and Across Channel Drift Speed

IGOR Pro code available upon request.

Appendix C
Analysis Procedures

C.1 Buoy Analysis

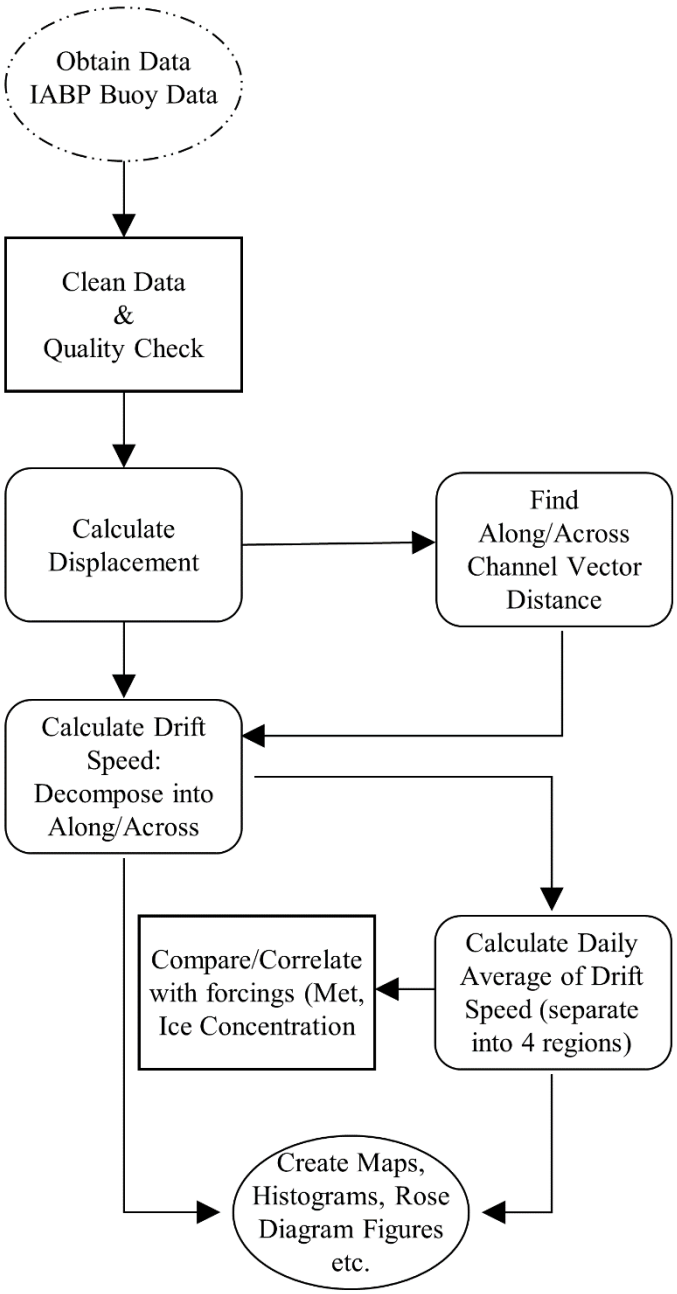

Figure C.1: Flow diagram of buoy analysis procedure.

C.2 Meteorological Analysis

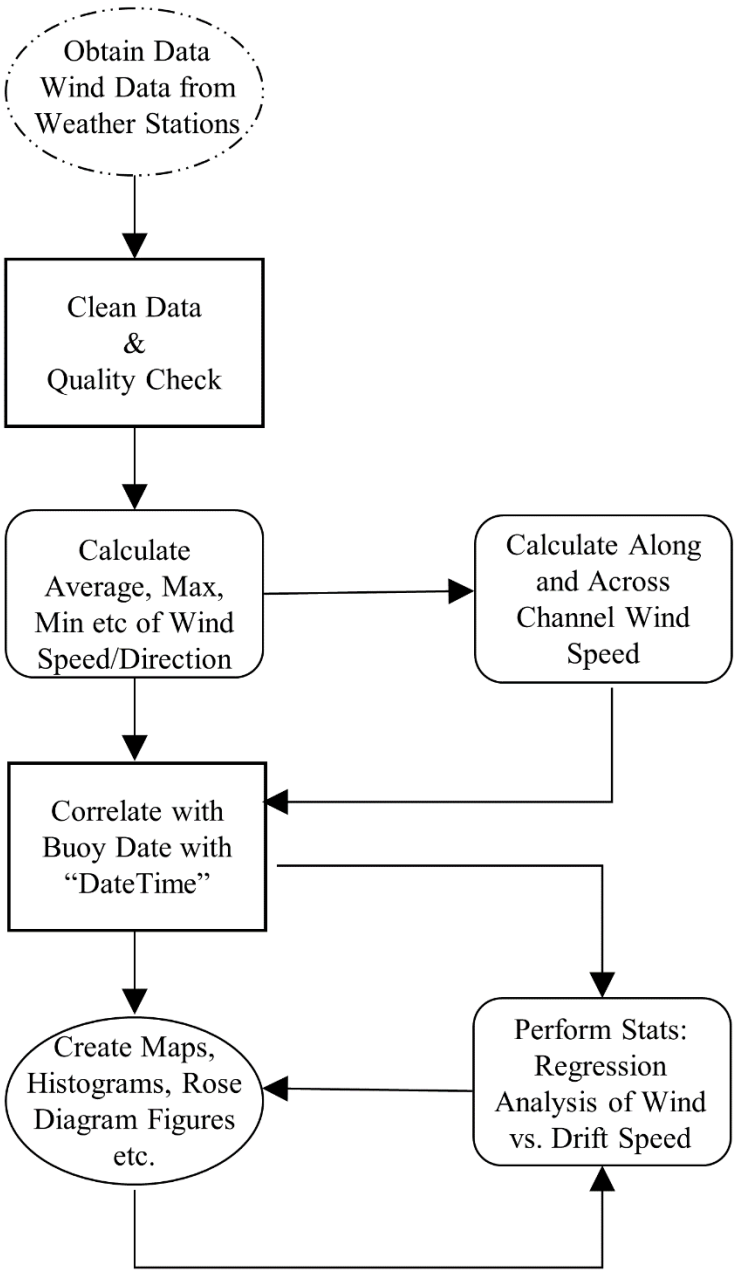

Figure C.1: Flow diagram of meteorological analysis procedure.

C.3 Ice Concentration Analysis

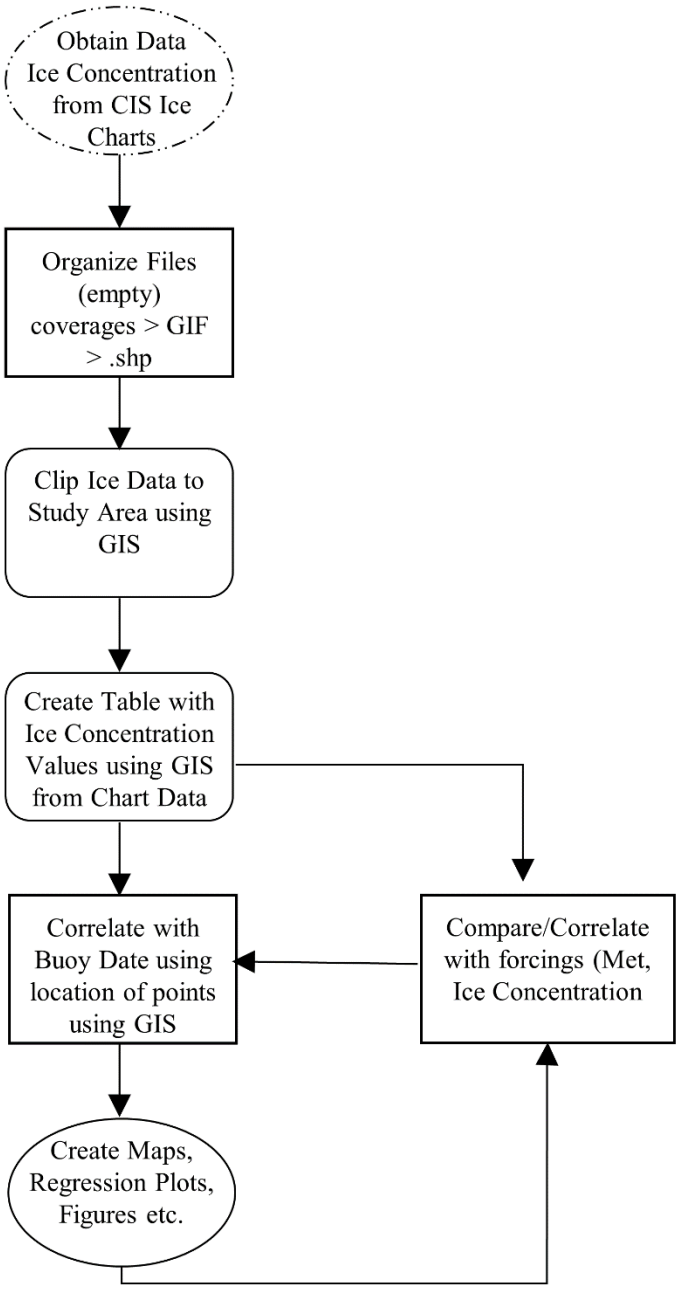

Figure C.3: Flow diagram of ice concentration analysis procedure.

Appendix D
Regression Plots

D.1 Robeson Channel

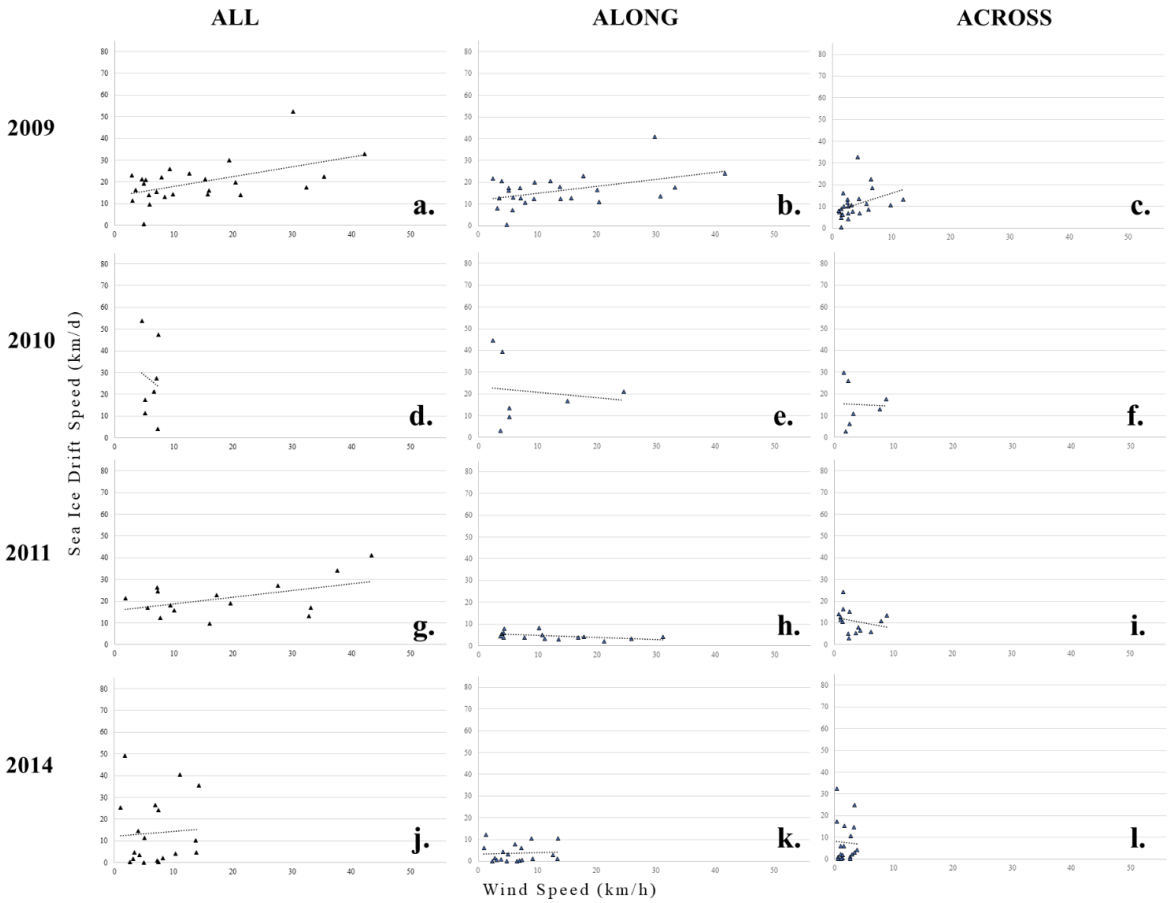

Figure D.1a: regression plots for wind speed (km/h) versus sea ice drift speed (km/d) for Robeson Channel. Correlations by year and along-channel vs. across- channel vs. vector.

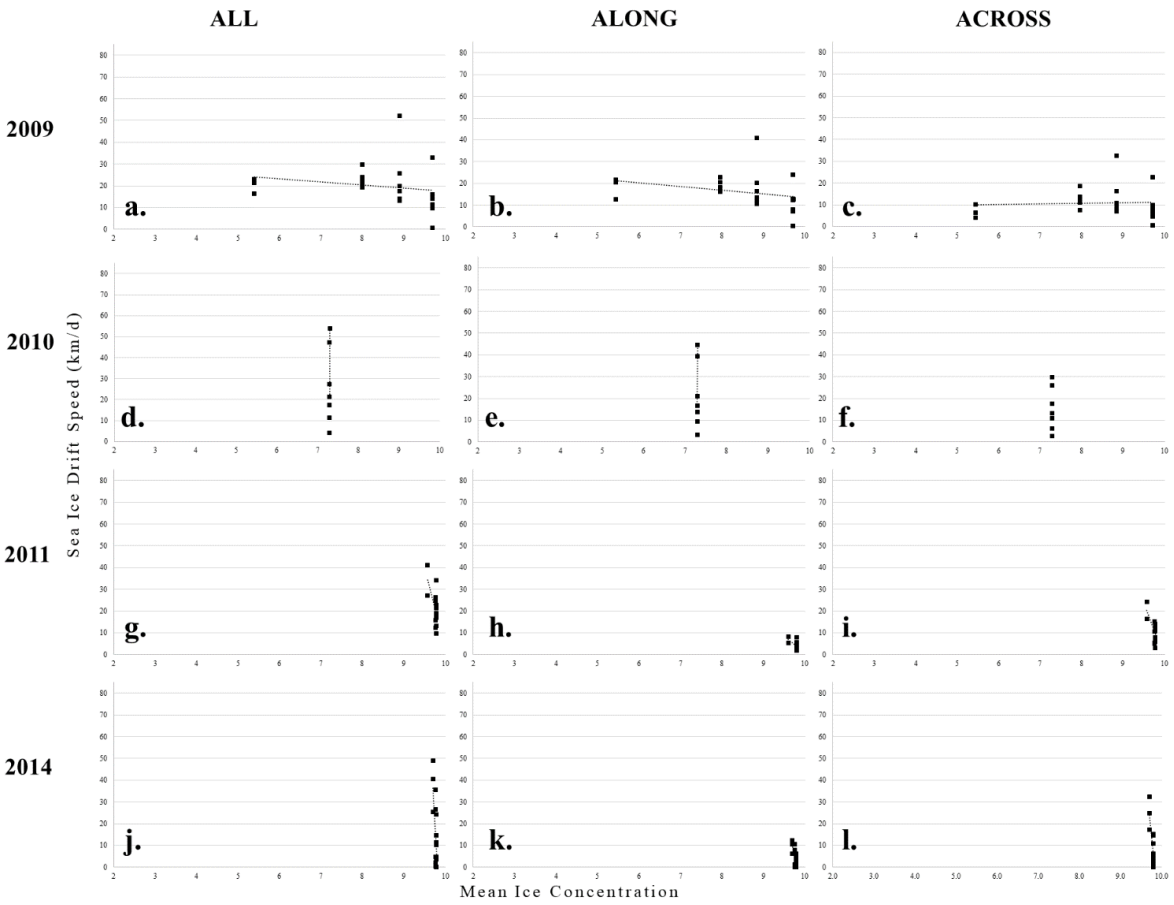

Figure D.1b: regression plots for mean sea ice concentration versus sea ice drift speed (km/d) for Robeson Channel. Correlations by year and along-channel vs. across- channel vs. vector.

D.2 Kennedy Channel

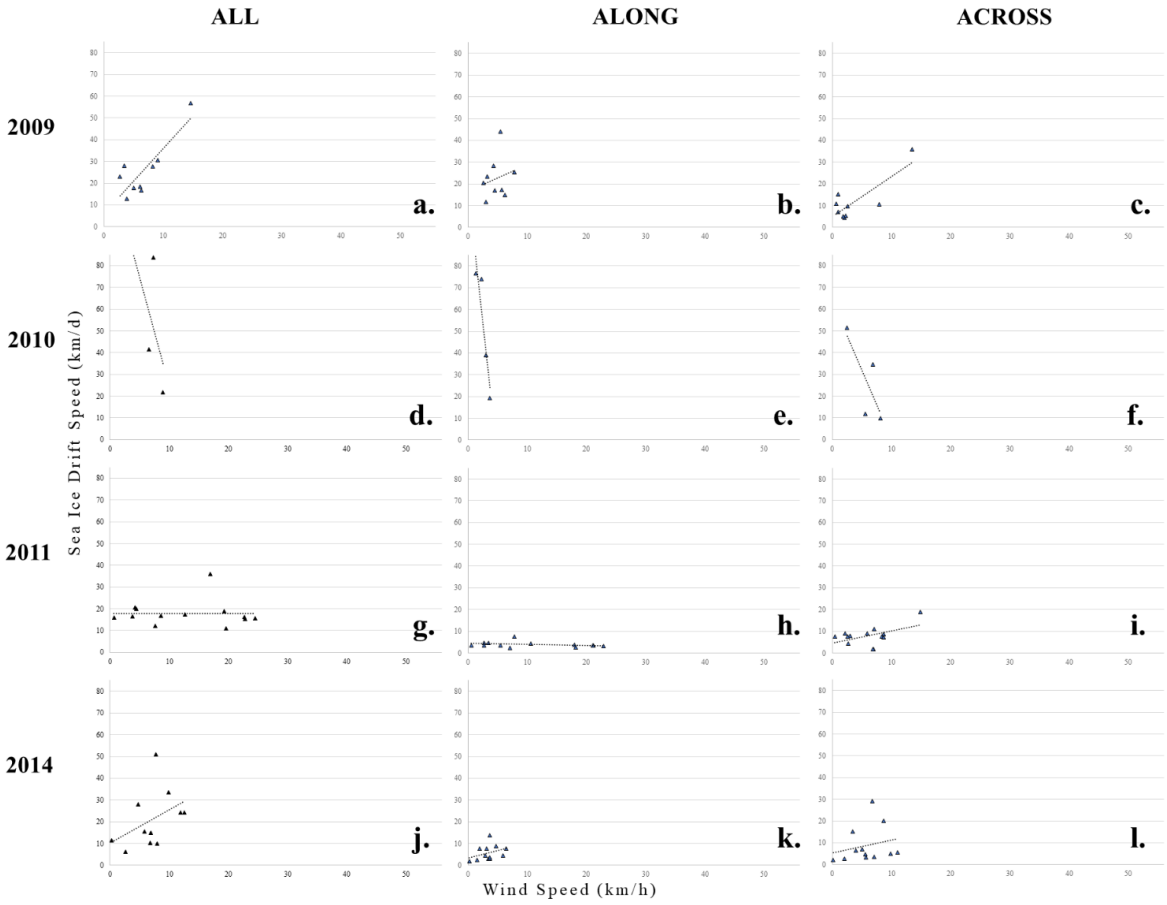

Figure D.2a: regression plots for wind speed (km/h) versus sea ice drift speed (km/d) for Kennedy Channel. Correlations by year and along-channel vs. across- channel vs. vector.

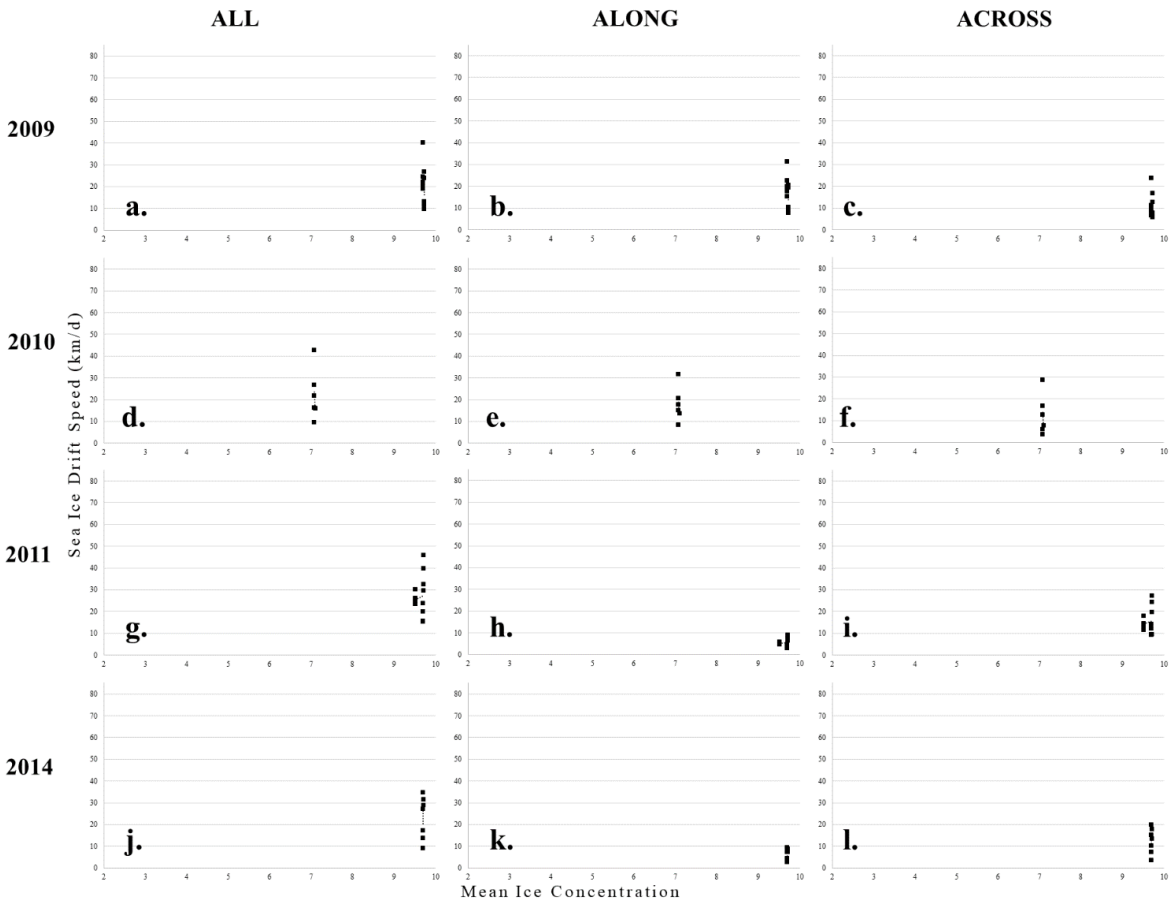

Figure D.2b: regression plots for mean sea ice concentration versus sea ice drift speed (km/d) for Kennedy Channel. Correlations by year and along-channel vs. across- channel vs. vector.

D.3 Kane Basin

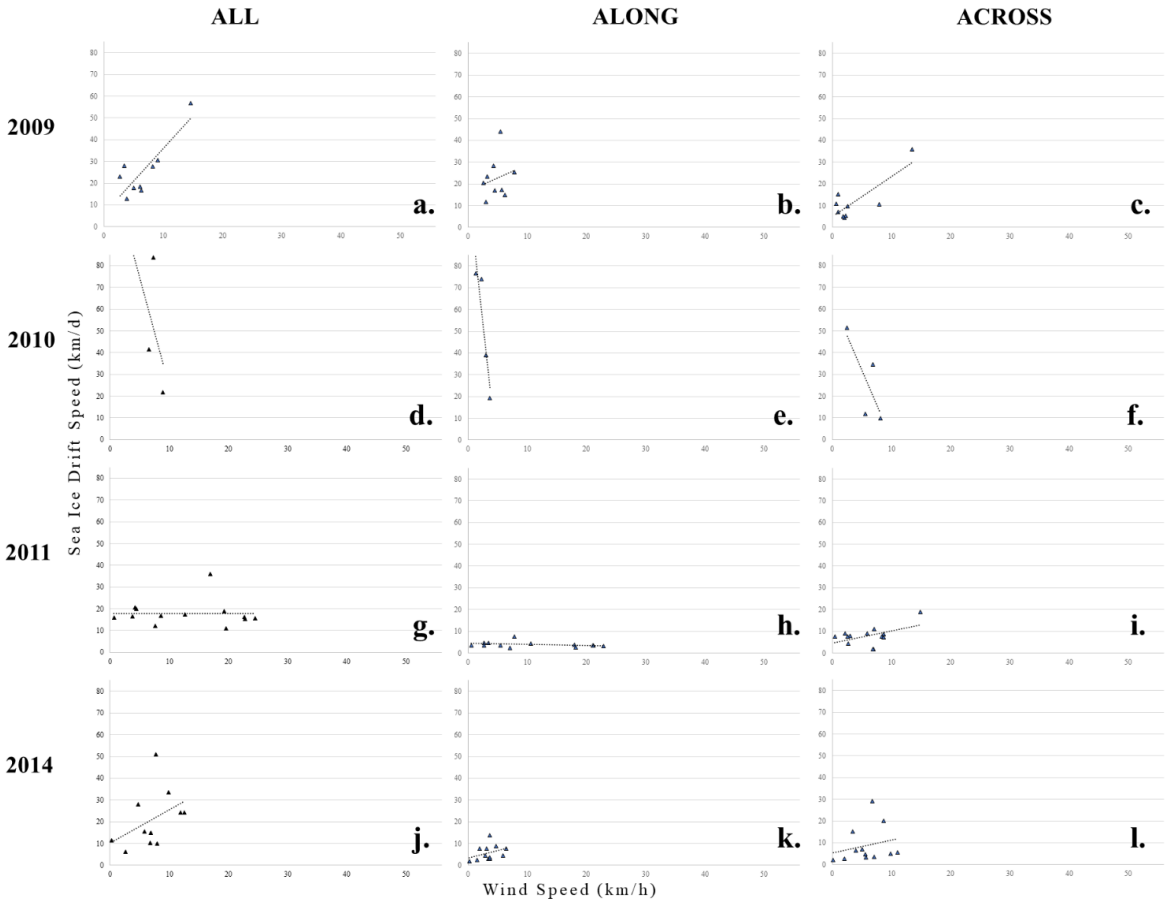

Figure D.3a: regression plots for wind speed (km/h) versus sea ice drift speed (km/d) for Kane Basin. Correlations by year and along-channel vs. across- channel vs. vector.

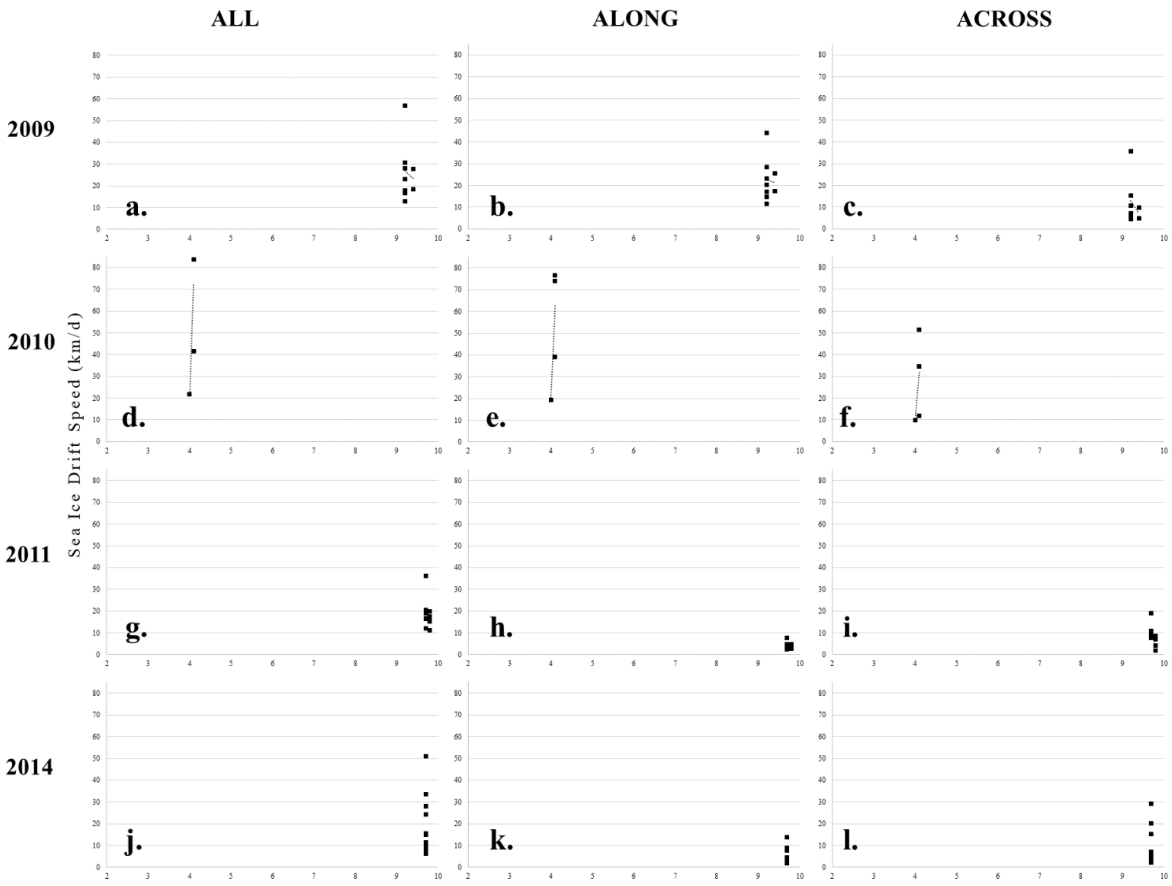

Figure D.3b: regression plots for mean sea ice concentration versus sea ice drift speed (km/d) for Kane Basin. Correlations by year and along-channel vs. across- channel vs. vector.

D.4 Smith Sound

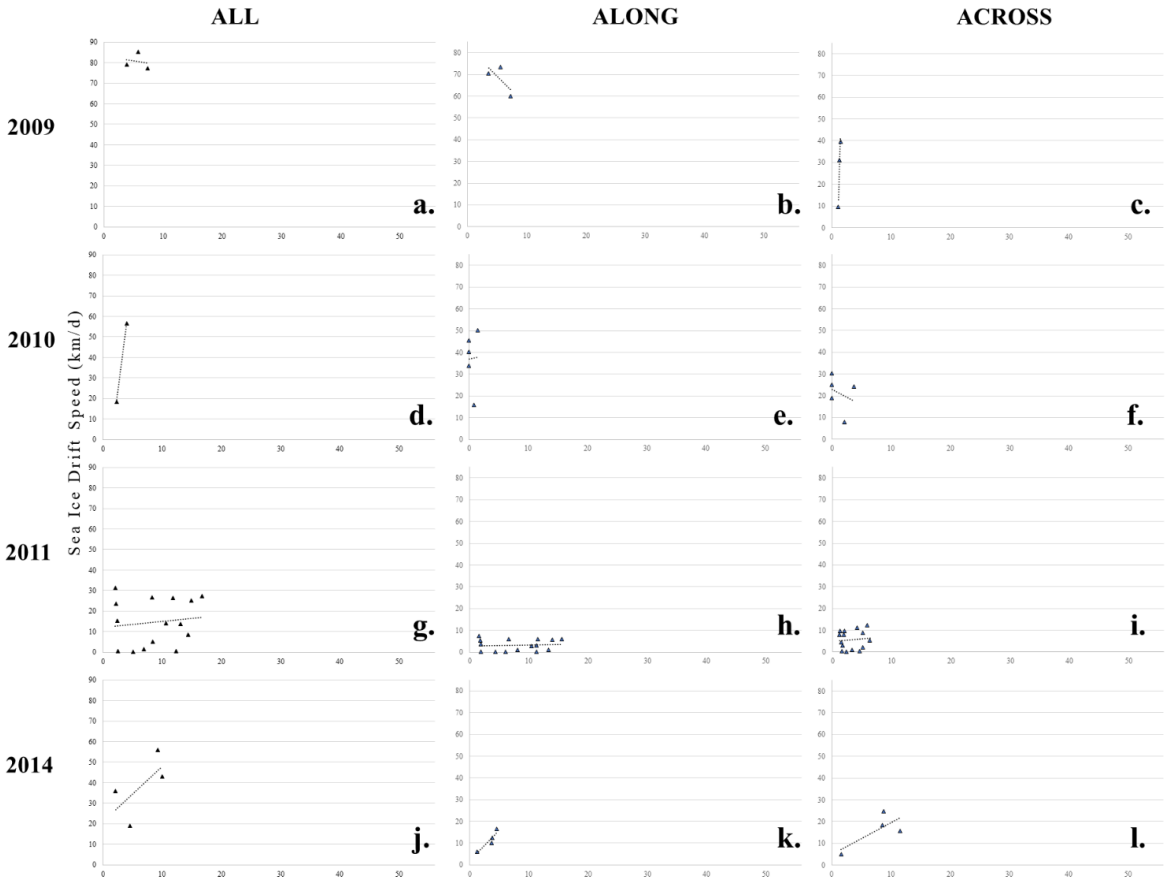

Figure D.4a: regression plots for wind speed (km/h) versus sea ice drift speed (km/d) for Smith Sound. Correlations by year and along-channel vs. across- channel vs. vector.

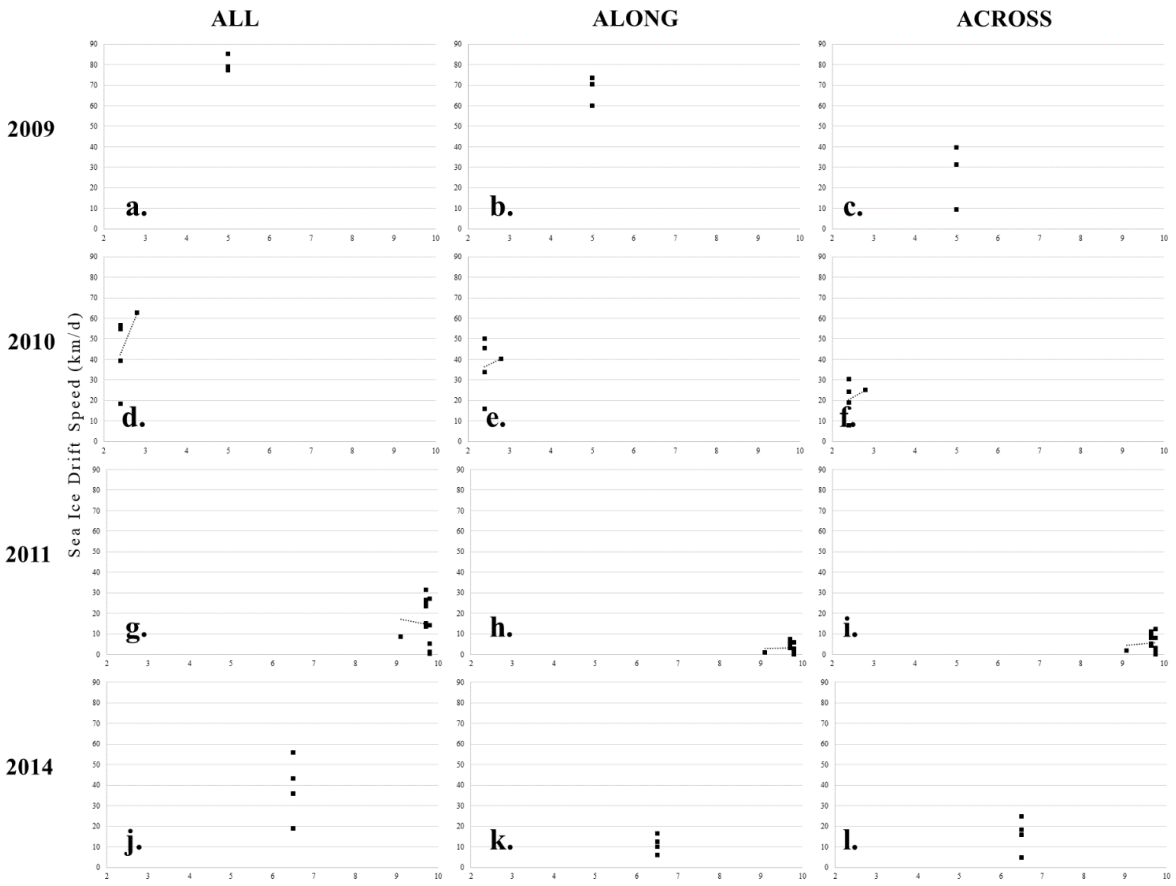

Figure D.4b: regression plots for mean sea ice concentration versus sea ice drift speed (km/d) for Smith Sound. Correlations by year and along-channel vs. across- channel vs. vector.